Improving the understanding of and methods for the detection of fungal wheat pathogens

Emily May Roberts, BSc (Hons)

Thesis submitted to The University of Nottingham for the Degree of Doctor of Philosophy, September 2017





ABSTRACT

Wheat is a staple food for 35% of the world's population providing roughly 20% of its calorific and 25% of its protein intake. *Puccinia triticina, Zymoseptoria tritici* and *Fusarium graminearum* are some of the most economically damaging fungi causing huge wheat yield losses. Problems that arise when trying to manage fungal pathogens include: the ability of fungal species to quickly adapt and overcome resistant cultivars of wheat, the overuse of fungicides leading to a high selection pressure for pathogen resistance and early detection often being dependent upon the experience and skill of the observer. This thesis focuses on developing detection methods which highlight the need for an integrated approach to disease management.

In this study a specific monoclonal antibody, 29.G7.A9, was developed for early detection of *Fusarium graminearum* macroconidia spores. Immunofluorescence demonstrated the ability of this antibody to bind to the native protein in *F. graminearum* spores. The 29.G7.A9 antibody was incorporated into a portable amperometric immunosensor system for spore detection using screen printed electrodes.

A *Z. tritici* population from three farms was analysed for the prevalence and distribution of amino acid alterations in the *CYP51* protein, as well as the presence of inserts in the putative *CYP51* promoter region, resulting in two general potential targets for detecting azole resistance being proposed. A clustering effect was observed with certain variant types showing association to certain geographical locations i.e. farm, field, and areas within a field. For this reason a future sampling plan was suggested with different sampling options in order to optimise the detection of certain variant types that may occur within a population in a specific location.

A method was established to quantitatively characterize the development of *Z. tritici* on wheat plants throughout a complete infection cycle as well as observe differences in disease progression when different doses of a fungicide (epoxiconazole) were applied.

This thesis provides techniques and information for generating further research and contributing new ideas for a more integrated approach for fungal crop pathogen detection research.

ACKNOWLEDGEMENTS

I would like to thank my supervisors Prof. Matthew Dickinson and Prof. Neil Boonham for all their advice and support throughout this project.

I would also like to thank the team at FERA Science Ltd. for all their guidance and in particular Kate Perkins and Catherine Harrison for support and their continual encouragement. Kate Perkins was a great source of knowledge for developing the antibodies and helped with immunisations and following protocols. Catherine Harrison worked with me on the *Zymoseptoria tritici* work as part of an Agri project and carried out all of the analysis of the CYP51 promotor region. Thank you also to Roy Macarthur a statistician at FERA Science Ltd who assisted with the statistics in Chapter 4.

I would also like to thank those that helped me in the early months of the project at the School of Biosciences at The University of Nottingham in particular Kanjana Warawichanee who provided me with tried and tested protocols and techniques for creating recombinant proteins. Thanks must also be extended to Dr Frankie Rawson and Paola Sanjuán Alberte at the School of Pharmacy at The University of Nottingham for giving up their time and sharing their knowledge about sensors.

I gratefully acknowledge the funding received towards my PhD from the Biotechnology and Biological Sciences Research Council (BBSRC).

Lastly I would like to thank my family and friends without whom there is no way I would have kept going. You have all been amazing, listening to my ramblings and so generous with your time. A special thanks to my mum who has always believed in me and provided such humour in frantic times, dad for being the target for most of our humour (!) and also to Billy for everything you do for me.

The University of Nottingham BBSRC Doctoral Training Partnership (DTP) is undertaken in partnership with Rothamsted Research. In Year One there is an initial period of intensive training which takes place over the course of the first six months. This comprises a two-week introductory training programme, 24 weeks of laboratory rotations, followed by a week-long 'Spring School' (conference-style training event for all DTP cohorts) and ending in a science outreach event. The PhD project begins in Month 7. In Years Two to Four training is mainly concentrated in the week long annual Spring School, although additional training and seminars are delivered where required throughout the year. A three month Professional Internship for PhD Students (PIPS) placement is usually taken in Year Three and, as BBSRC specifies, this is not in an area related to the students' PhD research programme. Below is the required submission of the PIP reflection form.

Professional Internships for PhD Students

Reflection Form

Name of Organization

Arthritis Research UK

Details of Placement

Please describe your main activities during the placement (150-200 words)

I worked alongside the Research Liaison and Evaluation team. The role of this team is to act as a single point of contact for anyone within the charity who is seeking information on research funded by Arthritis Research UK. I helped to make sure that news and information emerging from the Research directorate, including the charity's research outputs and successes, were clearly translated and provided in a timely manner to the relevant teams across the charity. I was also involved in evaluating the outputs of awards, and highlighting achievements. Responsibilities included:

- Preparing written material for the fundraising and communication departments, external publications and creative agencies.
- Liaising with researchers for relevant publications, images and arranging meetings.
- Answering basic science questions from the fundraising and communication departments.
- Analysing Researchfish reports for examples of cutting edge science, engagement activities etc. with communication and fundraising potential.

Placement Achievements

Please detail all outcomes from the placement, including any publications, presentations given and reports written etc. (150-200 words)

- Experience in communicating research to lay audiences, both written and verbal.
- Increased understanding of grant funding process, including the involvement of patients in the review of applications.
- Greater understanding of musculoskeletal disorders and the difficulties experienced by the charity's users.
- Initiated a blog series to celebrate British Science Week to engage with the work force and make them aware of the science activities available within that week.
- Writing profiles and reports on Grants that had been awarded or papers that had been published by their researchers for the website and press releases.
- Compiling information and creating a timeline of achievements and testimonials for the charity which was used in their leaflets.
- Helping to organise The Fellows Day event.

Skill development

Has this Placement helped you developed any new skills or enhanced your previous skill set? (100-150 words)

This placement helped me to increase my confidence when constructing written content and helped me to find and develop my writing voice. I was also able to progress my project management skills and the ability to manage multiple projects simultaneously whilst also delivering on deadlines. I had the opportunity to liaise with a variety of professionals, including researchers, doctors, fundraisers and funding bodies which not only built confidence but gave insight into the multidisciplinary team needed for the charity's success. I gained a better understanding of not only the charity sector, but how valuable research can be in influencing changes in policy that can have an impact on the public's lives.

Future Work

Has this Placement influenced your future career aspirations? If so, in what way? (100-200 words)

This placement with Arthritis Research UK It has reinforced my belief that the effective communication of science is crucial to build support which can lead to better funding in research areas. If carried out effectively it opens meaningful debate which in turn affords science a stronger presence in society. It has shown me the possibility of other potential careers involving science outside the research lab. It was also very fulfilling working for a charity and I feel it allowed for more creativity and flexibility as new ideas were met with encouragement allowing for the individual to develop the scope of their role.

CONTENTS

ABSTRACT i

ACKNOWLEDGEMENTS iii

THE NATURE OF THE PHD iv

CONTENTS vii

LIST OF TABLES xi

LIST OF FIGURES xii

ABBREVIATIONS xv

Chapter 1 General Introduction 1

1.1 Wheat production 1

1.2 Wheat fungal diseases relevant to this study 1

1.2.1 *Zymoseptoria tritici* 1

1.2.2 *Puccinia triticina* 4

1.2.3 *Fusarium graminearum* 7

1.3 Problems with control of fungal crop pathogens 10

1.4 Disease management strategies 11

1.4.1 Diagnosis of fungal wheat pathogens 11

1.4.2 Indirect methods 14

1.4.3 Biosensors 15

1.4.4 Identifying targets of interest and phases for detection 17

1.5 Aims and objectives 18

Chapter 2 Developing monoclonal antibodies to fungal spores for incorporation into an immunosensor. 19

2.1 Introduction 19

2.2 Methodology 22

2.2.1 Fungal material 22

2.2.2 Identifying potential antigenic protein targets *of P. triticina* urediniospore to create recombinant proteins for antibody generation. 22

2.2.3 Developing monoclonal antibodies to fungal spores 27

2.3 Results 35

2.3.1 Identifying potential antigenic protein targets *of P. triticina* urediniospores to create recombinant proteins for antibody generation. 35

2.3.2 Developing monoclonal antibodies to fungal spores 39

2.4 Discussion 49

Chapter 3 Amperometric detection of Fusarium graminearum spores via an immunosensor using screen printed electrodes. 51

3.1 Introduction 51

3.2 Methodology 53

3.2.1 Immunoreagents for assays 53

3.2.2 ELISA – secondary antibody optimisation 54

3.2.3 Immunosensor apparatus 55

3.2.4 Characterisation of the Working Electrode 55

3.2.5 Immunosensor assays 55

3.2.6 Data Analysis 55

3.3 Results 56

3.3.1 ELISA – secondary antibody optimisation 56

3.3.2 Characterisation of the Working Electrode 56

3.3.3 The HRP/TMB detection system 59

3.3.4 Main assay experiment 60

3.4 Discussion 63

Chapter 4 The isolation and analysis of distribution of Zymoseptoria tritici CYP51 variants in order to give insight into future sampling and potential targets for detection 65

4.1 Introduction 65
4.2 Methods 67
4.2.1 Sampling protocol 67
4.2.2 Culturing *Zymoseptoria tritici* from leaf samples 68
4.2.3 Storage of cultures for future use 68
4.2.4 DNA extraction 68
4.2.5 PCR 68
4.2.6 Sequencing and analysis 70
4.2.7 Analysis of the *CYP51* promoter region 70
4.2.8 Statistical analysis 70
4.3 Results 71
4.3.1 Overall *Zymoseptoria tritici* collection 71
4.3.2 The geographical distribution of variant types 75
4.3.3 Developing future detection sampling strategies 78
4.4 Discussion 82
Chapter 5 Assessment of life cycle traits of different *Zymoseptoria tritici* CYP51 variants to understand which variants are of most importance for detection. 85
5.1 Introduction 85
5.2 Methodology 86
5.2.1 Experimental design 86
5.2.2 Plant material 86
5.2.3 Fungicide application 87
5.2.4 Inoculation 87
5.2.5 Disease assessment 87
5.3 Results 89
5.3.1 Visual assessments 89

5.3.2 Fungal quantification using real-time PCR 96

5.4 Discussion 99

Chapter 6 General discussion 103

6.1 Main conclusions 103

6.1.1 Specific monoclonal antibody 29.G7.A9 was developed to detect for spores of *Fusarium graminearum*. 103

6.1.2 Production of a recombinant protein of *P. triticina* spores for future antibody development. 103

6.1.3 Development of an amperometric immunosensor system for onsite detection of *Fusarium graminearum* spores using SPEs 104

6.1.4 Potential targets identified for detection of azole resistant *Z. tritici* isolates. 104

6.1.5 A future sampling plan was suggested with different sampling options, in order to optimise the detection of certain variant types that may occur within a population of *Z. tritici* in a specific location 105

6.1.6 Evidence that life cycle traits of *Z. tritici* resistant variants are impacted differently by fungicide use. 105

6.2 Suggestions for future research 105

References 108

LIST OF TABLES

Table 2.1 Primers that were designed for the hypothetical antigenic targets: Protein 1 and Protein 3. 23

Table 2.2 Primers incorporating *Pst*I and *EcoR*I restriction enzyme sites 25

Table 2.3 Details of fungal species used for cross reactivity studies 33

Table 4.1 Components used for the PCR reaction to amplify the CYP51 gene of *Zymoseptoria tritici* 70

Table 4.2 The amino acid alterations corresponding to the different *CYP51* variants of *Z. tritici* found in this study 73

Table 4.3 The insertions found in the *CYP51* putative promoter regions of *Z. tritici* found in this study 74

Table 4.4 The number of times variants were found on each farm location represented as percentage of location sample size 76

Table 4.5 The number of times the 6 most common overall variants were found in each field location represented as percentage of location sample size 77

Table 4.6 The mean prevalence of the 6 most common overall *Z. tritici* variant types represented as percentage of location sample size and the estimated parameters that describe the expected prevalence and variation of different variant types. 79

Table 4.7 Limits of detection (95% probability of detection) for the presence of *Z. tritici* variants when different sampling protocols are employed 81

Table 5.1 Isolates used in this study, showing the SNPs present in the CYP51 gene 86

LIST OF FIGURES

Figure 1.1 Schematic representation of the life cycle of *Zymoseptoria tritici*. 3
Figure 1.2 National foliar disease incidence, main three diseases (mean % samples affected) 4
Figure 1.3 Uredinia of *Puccinia triticina* on flag leaves of wheat. 5
Figure 1.4 National foliar disease incidence, rusts (mean % samples affected). 7
Figure 1.5 wheat showing typical bleaching symptoms of Fusarium head blight. 8
Figure 1.6 Incidence of ear (head blight) Fusarium (mean % samples affected) 10
Figure 1.7 Schematic representation of the different components that can make up a biosensor 15
Figure 2.1 Blue-white selection plate. 24
Figure 2.2 PCR amplification of target sequences using primers designed against cDNA of *P. triticina*. 35
Figure 2.3 Colony PCR utilising M13 primer binding sites inherent in the vector system to detect the insertion of target DNA into pGEM-T vector. 36
Figure 2.4 Restriction digests digested with *Eco*RI and *Pst*1 restriction enzymes. ... 37
Figure 2.5 Colony PCR utilising pBAD primers was performed on potential pBAD-HisB-Target 1 and Target 3 transformants. 38
Figure 2.6 Western blot showing protein expression at various concentrations of L-arabinose. 39
Figure 2.7 Evaluation of tail bleeds from 6 mice via western blot. 40
Figure 2.8 Western blot to evaluate hybridomas' reactivity to *P. triticina* spores.... 42
Figure 2.9 Western blot to evaluate hybridomas' reactivity to *F. graminearum* spores……4
3
Figure 2.10 Western blot to evaluate clones reactivity to *F. graminearum* spores...45
Figure 2.11 Western blot to evaluate clone 29.G7.A9 cross reactivity to a range of fungal antigens.. 46
Figure 2.12 Western blot to evaluate purified monoclonal antibody 29.G7.A9. a.) Purified antibody at different concentrations to detect *F. graminearum*..... 47
Figure 2.13 Western blot of the negative control Nosema purified monoclonal D095 to evaluate cross reactivity to a range of fungal antigens. 48

Figure 2.14 Detection of *F. graminearum* spores in an immunofluorescence assay with monoclonal antibody from cell line 29.G7.A9. Red arrows indicate the spores. 48
Figure 3.1 Redox cycling for the quantification of oxidised TMB. 52
Figure 3.2 Immunoassays with immunoreagents used for ELISA and the immunosensor……5
4
Figure 3.3 ELISA results showing the optimisation of secondary antibody (HRP) for both the negative and positive controls and the AFB antigen assay..... 56
Figure 3.4 The electrochemical behaviour of ferricyanide (1 mM) on the SPE when varying the scan rate. 58
Figure 3.5 A voltammogram of TMB with H_20_2 in the presence of HRP with and without stop solution (H_2SO_4) in the potential range of -0.35 V to 1 V..... 59
Figure 3.6 The colour change (blue to yellow) and oxidation of TMB (ox1) to TMB (ox2) on the SPE when the stop solution (H_2SO_4) is added. 60
Figure 3.7 A voltammogram of the negative control assay, positive control assay, AFB antigen assay and 29.G7.A9 assay without stop solution (H2SO4) in the potential range of -0.35 V to 1 V. 61
Figure 3.8 a.) A voltammogram of the negative control assay, positive control assay, AFB antigen assay and 29.G7.A9 assay with stop solution (H_2SO_4) in the potential range of -0.35 V to 1 V. b.) A comparison of the peak currents (µA) observed by all the aforementioned assays with stop solution (H_2SO_4) in the potential range of --0.35 V to 1 V. 62
Figure 3.9 The correlation of the ELISA absorbance (OD_{450} nm) readings and the peak current (µA) of the negative control assay, positive control assay, AFB antigen assay when stop solution was added (H_2SO_4). 62
Figure 4.1 PCR amplification of target sequences for *Z. tritici*.. 72
Figure 5.1 Typical *Zymoseptoria tritici* lesion development..... 89
Figure 5.2 Life cycle traits of all isolates without fungicide application.. 91
Figure 5.3 Life cycle traits of WT isolate at varying fungicide doses. 92
Figure 5.4 Life cycle traits of isolate type 14 at varying fungicide doses. 94
Figure 5.5 Life cycle traits of isolate type 15 at varying fungicide doses. 95

Figure 5.6 Detected DNA of all isolates at varying fungicide doses. 97
Figure 5.7 The correlation of qPCR % control against % control of the different life cycle traits 98
Figure 5.8 The EC_{50}s calculated from qPCR DNA results 99

ABBREVIATIONS

AFB	American Foul Brood
APS	Ammonium Persulphate
CMV	Cucumber Mosaic Virus
Ct	Cycle Threshold
CV	Cyclic Voltammetry
DMI	Demethylation Inhibitor
DON	Deoxynivalenol
DTBIA	Direct Dot Blot Immunoassay
EST	Expressed Sequence Tag
FAM	6-carboxyfluorescein
FAO	Food and Agriculture Organisation of the United Nations
FCS	Fetal Calf Serum
FHB	Fusarium Head Blight
FITC	Fluorescein isothiocyanate
GC-MS	Gas Chromatography–Mass Spectrometry
HAT	Hypoxanthine-Aminopterin-Thymidine
hCG	Human Chorionic Gonadotropin
HRP	Horseradish Peroxidase
IF	Immunofluorescence
IFA	Immunofluorescence Assays
LAMP	Loop mediated isothermal amplification
LB	Luria-Bertani
LFD	Lateral Flow Device
LFIA	Lateral Flow Immunoassays
MAbs	Monoclonal Antibodies
MBC	Methyl Benzimidazole Carbamates
MGW	Molecular Grade water
MMB	Micro Magnetic Beads
MRFM	Magnetic Resonance Force Microscopy
OD	Optical Density
PAbs	Polyclonal Antibodies
PBS	Phosphate Buffered Saline
PCR	Polymerase Chain Reaction
PDA	Potato Dextrose Agar
PDVF	Polyvinylidene Fluoride
PTA-ELISA	Plate Trapped Antigen ELISA
PVY	Potato Virus Y
QCM	Quartz Crystal Microbalance
QoI	Quinone Outside Inhibiters
qPCR	quantitative Polymerase Chain Reaction
RE	Restriction Enzyme
SCF	Sutton Court Farm
SDHI	Succinate Dehydrogenase Inhibitor
SEM	Scanning Electron Microscope

SNA	Synthetic Nutrient Agar
SPE	Screen Printed Electrode
SPR	Surface Plasmon Resonance
STB	Septoria Tritici Blotch
TBE	Tris/Borate/EDTA
TMB	3,3',5,5'-Tetramethylbenzidine
TWA	Tap Water Agar
VOC	Volatile Organic Compound
WE	Working Electrode
WT	Wild Type

Chapter 1 General Introduction

1.1 Wheat production

Europe is the largest producer of wheat, with 2017's production forecast to reach 253.9 million tonnes (FAO, 2017). Wheat is a staple food for 35% of the world's population and provides more calories and protein in the global diet than any other cereal (Garg et al., 2014), with the Food and Agriculture Organization of the United Nations (FAO) reporting that the average person consumes the grain from 50 wheat plants daily, which provides them with roughly 20% of their calorific and 25% of their protein intake (Uauy, 2017). Wheat is set to remain an important component of human nutrition and increasing its production is therefore a necessity for food security. Animal feed requirements and those of the growing energy sector put added strain on the need to optimise wheat production. Currently, low yields can be mainly attributed to the following factors: adverse climatic conditions, pest and disease outbreaks or political turmoil (Ben-Ari et al., 2016).

1.2 Wheat fungal diseases relevant to this study

1.2.1 *Zymoseptoria tritici*

Zymoseptoria tritici (formerly: Mycosphaerella graminicola) causes Septoria tritici blotch (STB) in both bread *(Triticum aestivum L.)* and durum *(Triticum turgidum ssp. durum L.)* wheat.

1.2.1.1 Appearance

The symptoms of STB develop on the lower leaves as chlorotic flecks and expand into irregular brown lesions. The black fruiting bodies (pycnidia) which can be seen as tiny black spots inside the blotches give the disease its characteristic speckled appearance. When the disease is severe, entire leaves can be covered in disease lesions.

1.2.1.2 Life cycle

The pathogen is heterothallic (two mating types), has high genetic variation and can survive on dead or dying host tissues found in stubble from the previous crop during autumn and winter. Ascospores are produced by strains with opposite mating types, MAT1-1 and MAT1-2 via sexual reproduction (Kema and van Silfhout, 1997). Most

lesions that are formed by the disease are of a single genotype therefore in order for the two mating types to interact lesions must coalesce (Suffert et al., 2011).

It produces many windborne ascospores which consist of 2 cells, and play a major role in distribution (Elbekali et al., 2010). Ascospores are held in asci, formed in fruiting bodies called perithecia, and are usually 48–114 µm in diameter. Each ascus contains 8 ascospores and each perithecia contains on average 26 asci (Eriksen and Munk, 2003). This gives a potential number of 200 ascospores per perithecia.

Twelve hours after infection with these ascospores, at high humidity, spores germinate and are able to penetrate the leaves via the stomata rather than by direct penetration. They switch to hyphal growth upon contact with the leaf. Several studies suggested that the penetration of the stomata is a random process (Shetty et al., 2003). Others report that hyphae respond to an unknown "thigmotropic signal" using surface sensing to navigate their way to the substomatal openings (Duncan and Howard, 2000). Functional characterisation of the protein ZtFus3 (named previously MgFus3) supports this view that stomata recognition is a non-random process. Deletion strains lacking this MAP kinase are unable to recognise the substomatal opening resulting in a failure to infect the plant at all (Cousin et al., 2006).

The infection then develops by invading and colonising the intercellular region between mesophyll cells. A switch from biotrophic to necrotrophic infection occurs and after a long latent period at approximately twelve days post inoculation the host cells start to die and visual necrotic lesions start to appear on the host's leaves (Goodwin et al., 2011). This initial symptomless phase has been associated with the secretion of the effector protein Mg3LysM by *Z. tritici* that competes with defence-inducing chitin receptors of the plant to bind to chitin released from the fungal cell wall (Mentlak et al., 2012). This protein acts as a protection for the fungal cell wall from plant-derived hydrolytic enzymes (Lee et al., 2017).

Fourteen to twenty one days post inoculation, black pycnidia (usually ranging from 60 to 200 µm in size) start to form in the substomatal cavities of the necrotic lesions as a result of asexual reproduction. Under high humidity and rainfall conditions, pycnidiospores are extruded through the stomatal aperture as a spore rich

hydrophobic extracellular matrix known as a cirrus (Goodwin et al., 2011). Pycnidiospores are the secondary inoculum and are dispersed by rain splash to the upper foliage of adjacent plants (Suffert et al., 2011). In the UK, *Z. tritici* completes its cycle from pycnidium formation to pseudothecia in approximately 62- 95 days under field conditions (Hunter et al., 1999).

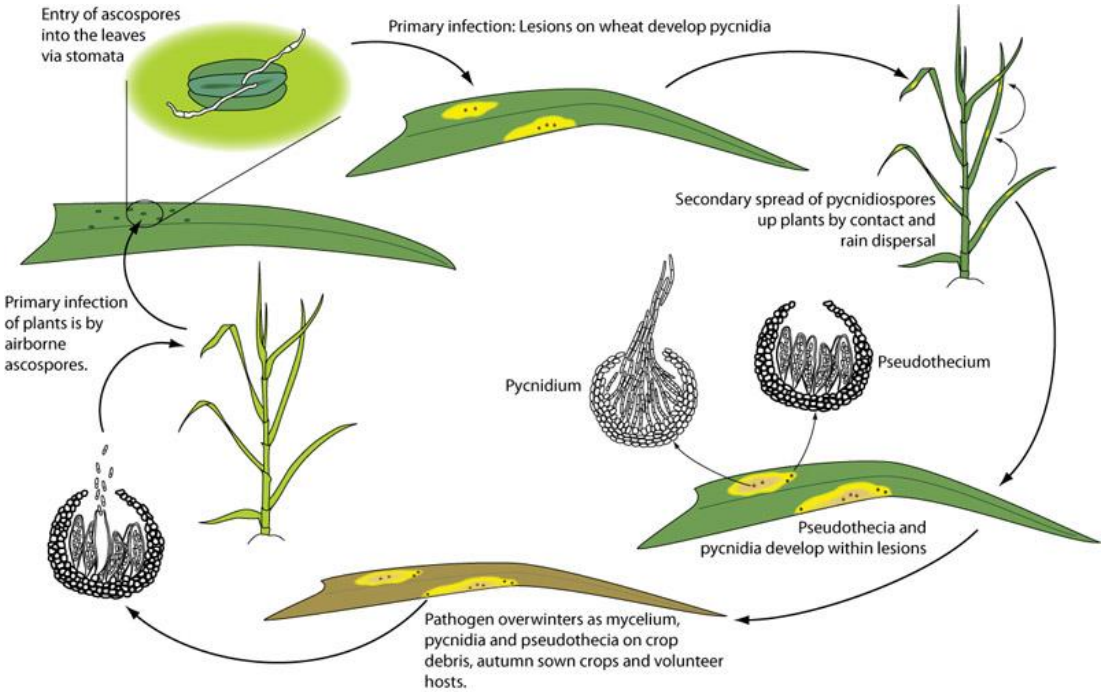


Figure 1.1 Schematic representation of the life cycle of *Zymoseptoria tritici* (APS, 2017).

1.2.1.3 Impact of environmental factors

Farming practices and weather patterns influence Septoria tritici blotch (STB) disease severity. Farmers often use wheat varieties that are only moderately resistant to STB, often resulting in the build-up of inoculum levels and thereby potentially facilitating the emergence of new fungal pathotypes (Fones and Gurr, 2015).

Weather conditions have a great impact on *Z. tritici* spread, as the disease is often transmitted from leaf to leaf via rain splash. The frequency of either very wet days (>10 mm rainfall) or consecutive wet days (three days with at least 1 mm rain) during the early stages of the wheat crop significantly increase the likelihood of outbreaks emerging. However temperatures below −2°C in these early stages of growth actually reduce the risk of STB for winter wheat in the UK (Fones and Gurr, 2015). Therefore

changes in farming practices such as earlier autumn sowing of winter wheat in the UK, in September rather than in November or December, can carry very high risk for STB outbreaks as temperatures are often higher; providing optimum conditions for disease establishment.

1.2.1.4 Losses in wheat yield and cost to industry

Losses due to *Z. tritici* can range from 30–50% during severe epidemics (Eyal, 1987) and with annual losses estimated at around £30 million a year for the UK even with expenditure of £80-90 million on fungicides to control it (Fraaije et al., 2011). A recent 2017 national survey carried out by CropMonitor (2017) found 81% of surveyed crops were affected by *Z. tritici*, an increase of 9% on the previous year's figures (Figure 1.2). The findings showed that *Z. tritici* remained the most common foliar disease, a position it has held since 1990 (CropMonitor, 2017).

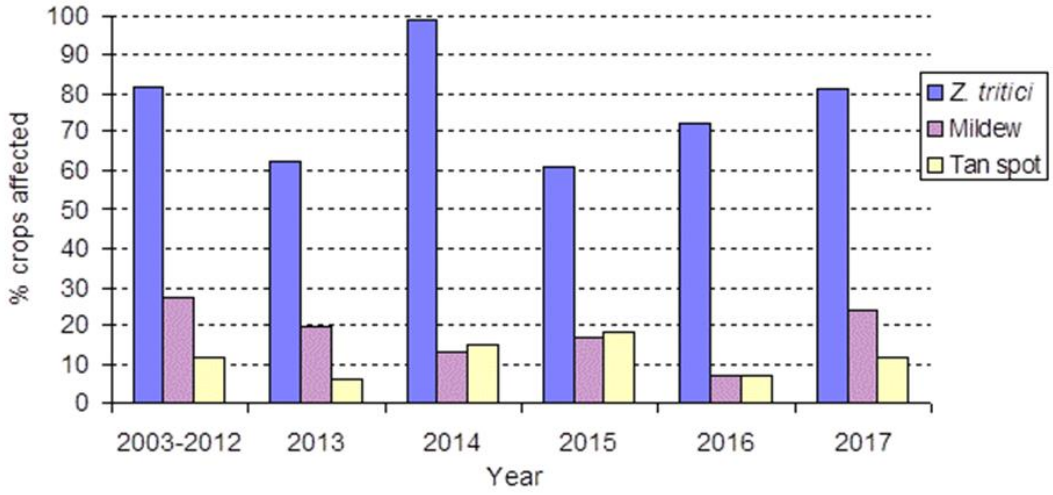


Figure 1.2 National foliar disease incidence, main three diseases (mean % samples affected) (CropMonitor, 2017).

1.2.2 *Puccinia triticina*

The most common rust disease of wheat is leaf rust, caused by *Puccinia triticina* (formerly: *Puccinia recondite* f. sp. *Tritici*) (Bolton et al., 2008).

1.2.2.1 Appearance

Puccinia triticina is well known for its distinct 'rust' like appearance produced by pustules of orange to brown uredinia on the upper surface of leaves (Figure 1.3). They are ovoid shaped and up to 1.5 mm in diameter. Infections cause lower kernel

weights and decreased numbers of kernels per head resulting in yield losses (Roelfs, 1992).



Figure 1.3 Uredinia of *Puccinia triticina* on flag leaves of wheat (Kolmer, 2013).

1.2.2.2 Life cycle

In order to complete the full life cycle the fungus, which is heteroecious, requires a telial/uredinial host, usually wheat, and an alternative pycnial/aecial host *Thalictrum speciosissimum* or *Isopyrum fumaroides*, on which the fungus completes its sexual stage (Elyasi-Gomari, 2010). It has a complex life cycle which includes five different spore types: teliospores, basidiospores, and urediniospores on cereal hosts, and pycniospores and aeciospores on the alternate hosts (Kolmer, 2013).

Uredinia produce urediniospores that are orangey brown and are about 20 µm in diameter with up to eight germ pores scattered in thick, echinulate walls (Bolton et al., 2008). The urediniospores are the asexual infectious propagules and are easily carried long distances by winds leading to epidemics. They have a dikaryotic nuclear condition with the ability of cycling continuously on the cereal hosts. The optimal temperature range for infection is 15-20°C and by 7 to 10 days after infection, new uredinia are formed and the cycle begins again (Wegulo, 2017).

The urediniospore germinate and produce germtubes once they have attached to the leaf surface. The tips of these germtubes differentiate into appressoria which forcibly

enters into the substomatal cavity by turgor pressure. Twenty four hours after germination a haustorial mother cell is then formed adjacent to a plant cell and penetration of the cell wall commences. After invasion of the host plasmalemma a haustorial interface surrounding a mature feeding structure, is eventually produced (Song et al., 2011). This structure is made up of both fungal and host material with the ability to traffic protein and metabolites, some of which are aimed at suppressing host defence responses (Song et al., 2011).

Teliospores, formed under the leaf epidermis, can survive the winter and are important to the disease cycle in areas where alternate hosts of the leaf rust fungus exist (Roelfs, 1992). They are are also produced in the uredinial infections. They germinate and carry out meiosis which produce four haploid basidiospores that are ejected into the air from sterigmata. These are then carried from the telial host by wind short distances to nearby alternative hosts (Kolmer, 2013).

The infection of the alternate host by the basidiospores occur on the upper leaf surface and are of two mating types that form the pycnial structures within which flexous hyphae produce haploid pycniospores. These are often transported by insects to other pycnial infections where combinations of pycniospores and flexuous hyphae of opposite mating type result in plasmogamy; the fusion of two genetically distinct cells that restores the dikaryotic nuclear condition. This then develops into a dikaryotic aecium on the underside of the leaf surface and within these are chains of aeciospores (Kolmer, 2013). When these have reached maturity, the aeciospores are released and wind dispersed to infect their cereal host. Uredinial infections then follow, which can then cycle continuously or develop into teliospores, therefore completing the life cycle.

1.2.2.3 Losses in wheat yield and cost to industry

Of the biotrophic fungi that infect wheat, rusts are some of the most economically damaging with the United States alone having economic losses of $350 million due to *P. triticina* between 2000 and 2004 and *P. striiformis* being reported to cause annual yield losses of 5.47 million tonnes of wheat, equivalent to $979 million (Singh et al., 2016). In Australia, losses attributed to *Puccinia triticina* are calculated at AU$ 12 million (Figueroa et al., 2017).

In a UK 2017 survey carried out by CropMonitor (2017), the incidence of *Puccinia triticina* was much higher than previous years, with 11% of crops affected which was the highest incidence of brown rust in the survey since 2012, when 17% crops were affected. Within crops, 0.09% (flag) and 0.05% (leaf 2) mean leaf areas were recorded which was the highest severity of *Puccinia triticina* since 2007 when 0.27% and 1.14% mean leaf areas were recorded respectively (Figure 1.4).

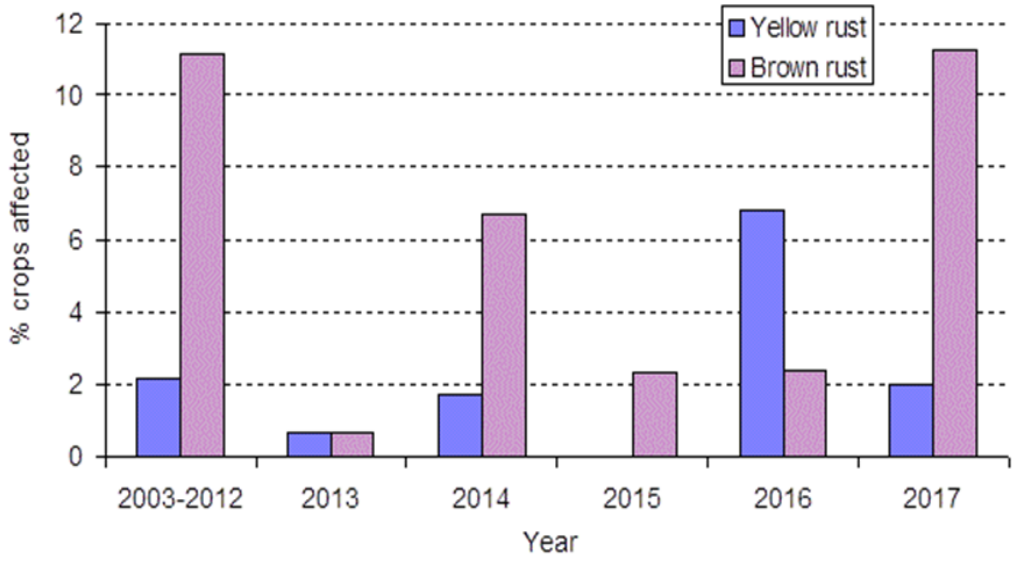


Figure 1.4 National foliar disease incidence, rusts (mean % samples affected) (CropMonitor, 2017).

1.2.3 *Fusarium graminearum*

Fusarium graminearum is one of the causal agents of Fusarium head blight (FHB). It bleaches the head of wheat and also produces several mycotoxins, including deoxynivalenol (DON) and zearalenone which contaminate cereal products and can be harmful to humans, animals, and plants (Yang et al., 2013). DON especially causes feed refusal or poor weight gain in animals and has been linked to immunological and birth defect problems in humans (Desjardins, 2006).

1.2.3.1 Appearance

The fungus damages wheat by causing 'whitened' or bleached heads. The first symptoms of Fusarium head blight occur shortly after flowering. Diseased spikelets appear premature, bleached or whitened in colour as the pathogen grows and spreads within the head (Figure 1.5). If the environment is warm and moist, light pink/salmon coloured spores (sporodochia) may appear on glumes of individual

spikelets. Later in the season, black spherical bodies known as perithecia may appear on the surface of affected spikelets (Schmaile and Munkvold, 2009).



Figure 1.5 wheat showing typical bleaching symptoms of Fusarium head blight (Goswami and Kistler, 2004).

1.2.3.2 Life cycle

F. graminearum overwinters as saprophytic mycelia in soil and on infested crop residues. During warm damp conditions the mycelium on these crop residues produce both macroconidia (asexual spores) and ascospores (sexual spores produced in perithecia).

The asexual macroconidia spores are produced on the surface of infected plants or on crop residue during damp periods. They are produced in mucus like masses borne on sporodochia (cushion-shaped hyphal structures) (Trail, 2009) and are dispersed usually short distances by rain splash.

F. graminearum is homothallic, meaning that it does not need a sexually distinct partner to develop sexual spores (ascospores). The two nuclei of the binucleate cells are genetically identical (Trail, 2009). In spring mature perithecia formed on the surface of crop debris contain asci; tubular sacs containing the ascospores. This coincides with the flowering of cereal crops. The mucus like ascospores are forcibly

discharged from perithecia into the air and dispersed by wind, rain or insects to host plants (Trail, 2009). The airborne ascospores are the primary inoculum of the disease, which is considered to be a monocyclic disease, they land on the plant via natural openings. Once it has entered the plant it colonises the tissue and causes the characteristic 'bleaching' symptoms.

Initially does not penetrate directly through the epidermis instead hyphae develop on the exterior surfaces of glumes. The *F. graminearum* grows towards the stomata and is then is able to invades its hosts by secreting cell-wall degrading enzymes (Kikot et al., 2009). Other points of entry have been suggested such as via partially or fully exposed anthers, openings between the lemma and palea of the spikelet during and through the base of the wheat glumes where the epidermis and parenchyma are have thin walls (Bushnell et al., 2003). Once inside the *F. graminearum* is able to easily colonise the plant and has a short-term biotrophic relationship with its host before switching to the necrotrophic phase (Trail, 2009). This is process is aided by mycotoxin biosynthesis. Following infection of wheat florets it expresses the genes for DON biosynthesis which triggers tissue necrosis in the wheat (Desjardins, 2006). The pathogen is then able to spread via the vascular tissues of the spikelet disrupting the xylem and phloem tissues in the infected rachis rendering them unable to function effectively leading to preamature death of the spikelet. Whilst colonisation of developing seeds is accompanied by DON accumulation which results in shrivelled grain referred to as tombstones (Trail, 2009).

1.2.3.3 Losses in wheat yield and cost to industry

Fusarium head blight (FHB) is a major necrotrophic fungal disease worldwide. The United States alone reported to have losses of $7.67 billion to the disease in wheat and barley between 1993 and 2001 (McMullen et al., 2012) and losses in Canada have ranged from $50 million to $300 million annually since the early 1990s (Alberta Ag-Info Centre, 2002).

In a UK 2017 survey carried out by CropMonitor (2017) found the incidence of FHB symptoms was lower than last year, with 76% samples and 16% ears affected compared with 84% of samples and 21% ears affected in 2016. Although lower than

last year, it is the second highest incidence since 2012, when 96% samples were affected (Figure 1.6).

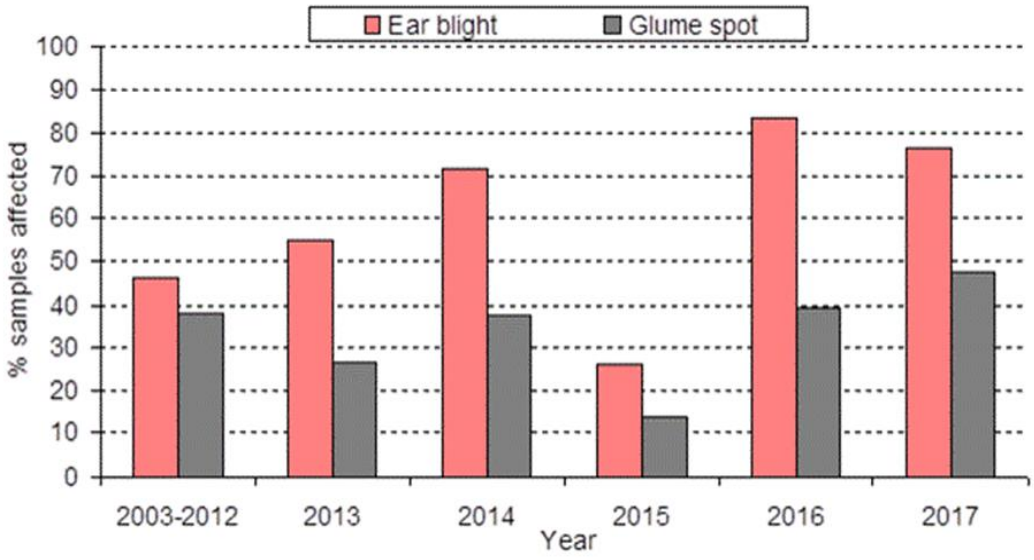


Figure 1.6 Incidence of ear (head blight) Fusarium (mean % samples affected) (CropMonitor, 2017).

1.3 Problems with control of fungal crop pathogens

There are several problems that arise when trying to manage fungal pathogens. Although wheat cultivars have been developed by plant breeding that are less susceptible to certain fungal pathogens, this is time consuming and often fungal species are quick to adapt and overcome the resistance. By 2010 all the commercially available wheat cultivars were susceptible or only partially resistant to *Z. tritici* (Cools et al., 2010). The overuse of fungicides, with several applications a year, some of which are prophylactic in nature may also cause problems. This overuse can lead to a high selection pressure for pathogen resistance. For example, *Z. tritici* has gained resistance to azole fungicides due to point mutations in the *CYP51* gene (34 to date), which greatly reduces the affinity between azoles and the 14α-demethylase enzyme (Cools et al., 2010). Qualitative findings depend on the experience and skill of the observer. For example the subtle differences between pathogens such as yellow rust *P. striiformis* and brown rust *P. triticina* especially in the seedling stage of infected wheat plants are hard to distinguish between (Gao et al., 2013). Disease control is more difficult and more costly the later the disease is detected. Risk predicted through early warning systems, e.g. RustMapper- developed by the CIMMYT GIS unit

in 2010 by using “Google Earth”, rely on the assumption of accurate identification of pathogens (CIMMYT, 2010).

1.4 Disease management strategies

Before disease management strategies are put in place it is imperative that a robust identification system is developed for the diagnosis of plant fungal infections. This is a holistic approach that takes into account not only how to detect the pathogen but also where/when to detect and for what purposes one needs to detect. To execute this, knowledge needs to be gathered on the fungal population in its entirety, particular traits of interest and the prevalence of these traits as well as a better understanding of life cycle components that give insight into the optimum stage of development to detect the disease in order to make interventions.

1.4.1 Diagnosis of fungal wheat pathogens

Identification of fungal pathogens traditionally involves interpreting the visual symptoms, isolating pathogens into culture and identification using morphological characteristics. Often fungal pathogens display similar symptoms in the field, which can result in the inability to distinguish between different species and therefore can lead to misdiagnosis. This process is often reliant on the skills and judgement of specialist personnel and variation between individuals causes problems with repeatability. Although plating and culturing gives a more accurate diagnosis, it is time consuming, taking, in some cases, weeks to confirm which species are present (McCartney et al., 2003). Therefore novel diagnostic techniques have been developed, although these are usually still lab based and use nucleic acid based methods such as polymerase chain reaction (PCR) or immunology based methods such as enzyme linked immunosorbent assay (ELISA).

1.4.1.1 Nucleic acid diagnostic methods

Nucleic acid based diagnostic methods typically consist of a sample extraction, followed by a PCR amplification step and then a product analysis step. The techniques are highly specific, can be used for species that are hard to culture and alleviates the need to isolate them (Lievens and Thomma, 2005). Many assays using a form of PCR

have been developed for fungal pathogens. A PCR assay was developed for the detection *of P. striiformis* by Lihua et al. (2008) which was able to detect *Pst*-infected wheat leaves just 2 days after inoculation. Guo et al. (2006) developed a successful real-time PCR assay for the pre-symptomatic and accurate detection of *Z. tritici*. Using real-time PCR, otherwise known as quantitative polymerase chain reaction (qPCR), is also quantitative and estimates of the amount of pathogen can be estimated by monitoring the cycle threshold (Ct) value measured at early exponential stages of PCR reactions and requires no post amplification processing therefore reducing analysis time (Schaad and Frederick, 2002). Zheng et al. (2013) also developed a real-time PCR assay for the detection of wheat powdery mildew, caused by the fungal pathogen *Blumeria graminis* f. sp. *tritici* which, it has been suggested could, help to estimate the initial inoculum potentials of epidemics in the field. Although rapid compared to culturing, it can still take a number of days and although in-field assays have been developed, still multiple steps are required and trained personnel are needed to complete the process.

Another nucleic acid diagnostic method currently popular is the loop-mediated isothermal amplification method (LAMP) which has many advantages over conventional PCR. A technique developed by Notomi et al. (2000), allows for the amplification of nucleic acid in isothermic conditions (60-65°C). These temperatures make it possible to carry out the diagnosis in the field with small portable devices such as a GENIE machine (OptiGene). Su et al. (2016) developed a LAMP assay for the detection of *Sporisorium scitamineum,* the causal agent of smut a fungal disease with widespread prevalence in sugarcane. It was shown to be very accurate, with 100 times higher sensitivity with certain targets compared to a conventional PCR assay. Huang et al. (2011) also found the technique to be highly sensitive when developing an assay for *P. striiformis,* which could be used to detect as little as 2 pg/µl template DNA and could be used to achieve detection from leaves as early as 24 hours after inoculation.

1.4.1.2 Immunology diagnostic methods

Immunoassays have also been used widely for plant pathogen detection. Assays have been developed around the concept of antigen-antibody bindings and are reliant on

the availability of suitable antisera or antibodies. Polyclonal antisera (PAbs), Monoclonal antibodies (MAbs) and phage-displayed recombinant antibodies can be developed to detect specific species. These can then be incorporated in various assays based on ELISA. Simple ELISA techniques are popular for plant disease diagnostics (Eibel et al., 2005, Kutilek et al., 2001, Lu et al., 1994, Olsson and Hetberg, 1997). Other immunoassays that are based on the use of antibodies for detection include direct immunofluorescence Assays (IFA), lateral flow immunoassays (LFIA), dipstick immunoassays and other membrane based techniques such as tissue print ELISA, direct dot blot immunoassay (DTBIA) or western blotting (Khater et al., 2017).

IFA involves fixing the antigen onto a microscope slide, after which a pathogen specific antibody labelled with a suitable fluorochrome (fluorescein isothiocyanate, FITC) is then applied and analysis is carried out using an epifluorescent microscope. Gao et al. (2013) successfully used this technique using a monoclonal antibody (LPT-2) that they had developed against the urediniospores of *P. triticina* combined with a secondary antibody, goat anti-mouse conjugated PE-cy3. IFA must be carried out in a laboratory because an epifluorescent microscope is needed which has the correct excitation and emission filters and often only a few samples can be processed daily.

Dipstick assays have been documented for a while (Cahill and Hardham, 1994, Priestley et al., 1994) however lateral flow immunoassays are the preferred commercial immunoassay and have several advantages over other techniques as they can be used for on-site diagnostics, are user friendly, robust, and inexpensive. The technology has been used for clinical diagnostics for a while, e.g. in the home pregnancy test, which detects the glycoprotein hormone, human Chorionic Gonadotrophin (hCG) in urine of pregnant women. LFIA involve the unidirectional flow of particles coated with analyte-specific antibody along a nitrocellulose membrane. Braun-Kiewnick et al. (2011) produced a lateral flow immunoassay for *Erwina amylovora* which was highly specific and had a low detection limit, 5.7cfu ml^{-1} which is the typical concentrations of the pathogen in an infected plant. It reduced the diagnosis time from 2 days in the lab to less than 15 minutes. This method is also used by FERA Plant Health and Seed Inspectorate for the detection of *Phytophthora ramorum* and *Phytophthora kernoviae,* which proved a successful component in the

management of these diseases. Other lateral flow immunoassays have been effective for on-site detection of pathogens (Lane et al., 2007, Danks and Barker, 2000) as well as important compounds produced by fungi such as mycotoxins (Zheng et al., 2006). Although techniques such as tissue print-ELISA and lateral flow devices have been used for on-site detection their sensitivity is relatively low and therefore only usually used for the confirmation of plant diseases after visual symptoms appear instead of pre-symptomatic detection (Fang and Ramasamy, 2015). Immunological-based detection methods are not as specific and sensitive compared to the nucleic acid-based detection methods, but are often faster, more robust, simpler to perform and more economical (Ray et al., 2017).

1.4.2 Indirect methods

Indirect methods usually rely on analysing the plant's physiological response to a pathogen by detecting metabolites produced by the plant and the overall impact on the plant. They usually fall into two distinct categories; spectroscopic and imaging techniques (stress-based disease detection techniques) and volatile organic compound (VOC) detection techniques (biomarker-based detection techniques) (Ray et al., 2017).

VOCs released from diseased plants can be analysed by gas chromatography combined with mass spectroscopy (GC–MS) and many studies have successfully been able to detect plant pathogens using this technique (Jansen et al., 2009). Becker et al. (2014) identified changes in a set of volatile compounds that were emitted from corn, between plants infected with *Fusarium* and those that were uninfected and several other studies have analysed VOCs of diseased crops including carrots (Vikram et al., 2006) and potatoes (Lui et al., 2005). Spectroscopic and imaging techniques have also been explored in many studies to detect diseased plants (Chaerle et al., 2004, Narvankar et al., 2009, Bürling et al., 2011, Al Masri et al., 2016). Using some techniques colour differences between infected and uninfected areas have to be distinct, however this distinction is not always clear with some diseases such as powdery mildew infection on sweet cherry leaves (Olmstead et al., 2001). Many researchers are also currently working on developing unmanned aerial vehicles (i.e. drones) or ground vehicles for imaging of crop canopies (Prashar et al., 2013).

1.4.3 Biosensors

A biosensor consists of a biological receptor element such as antibodies, DNA probe or phage amongst others, which is either integrated or intimately associated with a physiochemical transducer (Khater et al., 2017, Turner et al., 1987) (Figure 1.7). It produces either a discrete or continuous digital electronic signal proportional to the interaction of the biomolecules (the sample). There are several different types of biosensors which include optical, volatile, electrochemical and mass based. They are becoming of increasing interest due to their ability to deliver sensitive specific detection of plant diseases on site (Ray et al., 2017). There is often no need for sample preparation and due to the digital display, results are clear, quantifiable and non-subjective, thus skilled operators are not essential.

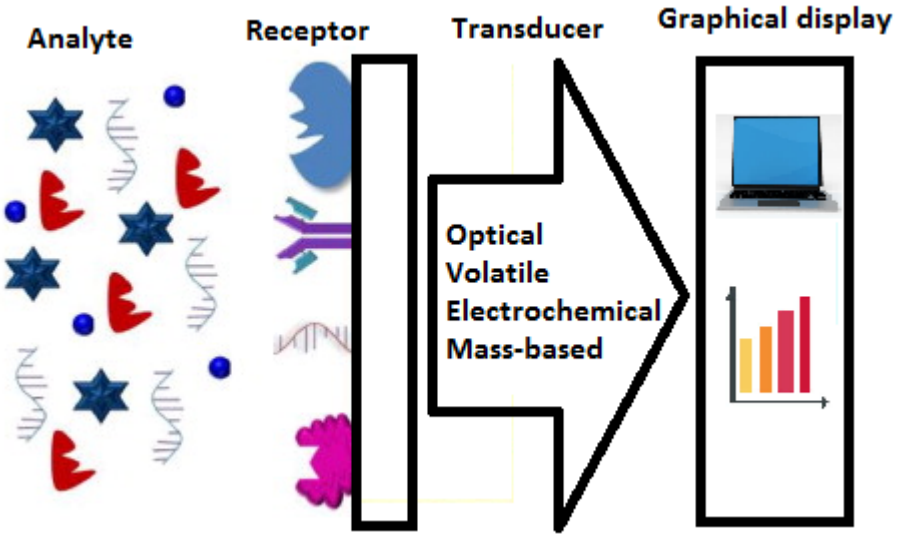


Figure 1.7 Schematic representation of the different components that can make up a biosensor

1.4.3.1 Optical biosensors

Optical biosensors consists of a light source, optical transmission medium, immobilised biological recognition element and an optical detection system (Ray et al., 2017). There are three different types of optical biosensor: fluorescence, chemiluminescence and surface plasmon resonance (SPR). Surface plasmon resonance (SPR) sensors are a popular choice for pathogen detection, due to their speed, high specificity and sensitivity. They also allow for real time analysis and are label free. This system has been used by Skottrup et al. (2007b) for the detection of

urediniospores of *P. striiformis* using monoclonal antibodies as the receptor and Zezza et al. (2006) for the detection of *F. culmorum* using a DNA receptor. *P. striiformis* was also detected by Bravo et al. (2004) using another form of optical biosensor which utilises a hyperspectral imaging platform; the sensor was able to discriminate diseased from healthy crop with an error of approximately 10%.

1.4.3.2 Volatile biosensors

Volatile biosensors have detectors that sense different specific gasses and are able to perform real-time analyses of gas concentrations released from diseased plants (Ray et al., 2017). Markom et al. (2009) developed a volatile biosensor utilising a commercially available electronic nose, Cyranose 320, which was able to detect basal stem rot disease caused by *Ganoderma boninense* in oil palm. Another volatile sensor was developed by Ghaffari et al. (2011) which measured volatiles released from diseased tomato plants and was able to detect those infected with powdery mildrew (*Oidium neolycopersici)*.

1.4.3.3 Electrochemical biosensor

Electrochemical biosensors usually consist of an electrochemical transducer combined with a biological recognition element which converts a binding event into an electrical signal. There are usually four types; amperometric, potentiometric, impedimetric and conductimetric. Amperometric detection can be used in conjunction with screen-printed electrodes and usually incorporates enzyme labelled components. Sharma et al. (2017) used an amperometric immunosensor for the detection of Capsicum chlorosis virus in bell peppers and found it to be 800-1000 times more sensitive than the equivalent direct antigen coated ELISA for the detection of the virus. Impedimetric biosensors have also been developed to detect plant viruses (Jarocka et al., 2013, Jarocka et al., 2011) and some fungal pathogens such as *Penicillium sclerotigenum* in infected yams (Silva et al., 2013) and Asian rust on soybean leaf extracts (Mendes et al., 2009). Potentiometric sensors sense the variation in protons (usually a pH change) and have currently been developed for the detection of aflatoxin B_1, a mycotoxin produced by *Aspergillus flavus* (Li et al., 2016).

1.4.3.4 Mass based biosensors

Mass based biosensors as the name suggests detect small changes in mass with piezoelectric sensors being the most commonly used (Cooper and Singleton, 2007). This change in mass can be due to an interaction between two entities, e.g. an antibody and an antigen and systems usually utilise Quartz crystal microbalance (QCM). When changes in the mass occur it causes alterations in resonance frequency (Heitmann et al., 2007). Wong et al. (2002) used this method to create an immunoassay which distinguished between *Salmonella* spp. from other related serogroups (*S. paratyphi, S. typhimurium, S. enteritidis*) with detection limits of 10^4 cells ml^{-1} even when the sample included 10^8 cells ml^{-1} of other strains of *Salmonella* and *E. coli*. Piezoelectric immunosensors are a cost effective option for pathogen detection, and incorporating QCM allows for the direct detection of analytes and lessens the need for labelled secondary antibodies. They can also be used for investigating biomolecular interactions between antigen and antibody instead of simply detecting the quantity in a sample (Zhang et al., 2002).

1.4.4 Identifying targets of interest and phases for detection

Effective methods and procedures for disease assessment and sampling are crucial at every stage of the disease, whether that is providing a direct forecast of imminent disease risk i.e. air sampling for potential pathogens, the pre-symptomatic stage or when visible signs of the disease are present and a prognosis needed to limit further spread. Information gained from air sampling has been used in previous studies to ascertain if it is possible to separate susceptible crops from potential pathogen sources (Maldonado-Ramirez et al., 2005) and to help make decisions about when precisely to apply fungicides (Brachaczek et al., 2016, Cao et al., 2016).

Although diagnostic techniques have been advancing in recent years, many of the afore mentioned techniques only focus on identification at a species level and little has been carried out to go beyond this and detect for specific traits that might be of particular interest for the end user such as avirulance/virulance profiles or fungicide sensitivity. For example, resistance of *Z. tritici* to certain fungicides has been linked to mutations in the *CYP51* gene which encodes the sterol 14α-demethylase (Cools et al., 2010). By screening populations of *Z. tritici* to ascertain which mutations are

prevalent and which are particularly resistant to fungicides, potential targets for detection can be identified. This would not only inform the end user of potential problematic variants found in their fields, but would also lead to effective fungicide use, economising on ineffective spraying, improvement in yield, decreased losses, prevention of build-up of resistance thus prolonging the life of active chemicals. The *CYP51* gene in *Fusarium* could also be a potential source for different detection targets as it has been linked to being a reliable marker for differentiating between different mycotoxin producing *Fusarium* species (Fernández-Ortuño et al., 2010). As well as these specific traits, life cycle components of different variants of a species must also be studied as they may give insight into why one variant is more prevalent than another.

1.5 Aims and objectives

This study aims to highlight what needs to be considered when developing an effective in-field specific disease detection system. The study focused on the following main areas:

- To create antibodies that are able to detect spores of *Puccinia triticina* and *Fusarium graminearum*.
- To illustrate how these antibodies could be incorporated into a transportable immunosensor system for onsite detection.
- To isolate and analyse the distribution of *Z. tritici CYP51* variants in order to give insight into future sampling strategies and potential targets for detection.
- To assess the life cycle traits of fungicide resistant *Z. tritici CYP51* variants to understand which variants are of most importance for detection.

Chapter 2 Developing monoclonal antibodies to fungal spores for incorporation into an immunosensor.

2.1 Introduction

Both of the wheat pathogens, leaf rust (causal agent; *Puccinia triticina)* and fusarium head blight (causal agent; *Fusarium graminearum)* are of increasing concern in the UK. With the emergence of new races of *P.triticina* able to overcome previously deployed resistance genes, for example *Lr14a* and *Lr72* genes in wheat (Soleiman et al., 2016), and it now being more common and wide spread globally than either stem rust (*P. graminis f. sp. tritici*) or stripe rust (*P. striiformis f. sp. tritici*), the need for early detection of *P. triticina* has never been more important. In north-western Europe fusarium is also of great concern especially those species able to produce deoxynivalenol (DON) toxin, such as *F. graminearum*, against which no wheat variety is fully resistant (West et al., 2017). These mycotoxins are not only a problem for human and animal health but have also been shown to disrupt quality of products in other industries for example brewing where it can cause over foaming of bottled beer (Denschlag et al., 2012).

Both *P. triticina* and *F. graminearum* infection can be sporadic and are dependent on many factors. By detecting the inoculum before infection events happen, the timely application of fungicides can be used to prevent significant losses in crops. Air sampling to detect spores is useful to monitor changes in pathogen populations in order to forecast imminent disease risk.

Spore traps are currently used to determine the presence or absence of plant pathogens by sampling air. However these samples generally have to be examined in a lab, usually by microscopy observation by trained technicians or undergo lab diagnostics to identify the presence of any spores of pathogens.

Visual identification is only possible for identification of large or visually characteristic spores and added to this air samples have a range of other particulates such as pollen, dust etc., which combine to make the identification process even more difficult (West

et al., 2017). DNA can be extracted from this mixture of particles and then tested in the lab using PCR or qPCR to detect specific target pathogens (Gao et al., 2016, Duvivier et al., 2016). Although the latter technique allows for more specific identification, such as the different genotypes of a species, by sending it off to a lab, identification time, risks with possible contamination of the collected samples and delays in decision make this an unattractive option.

Using loop-mediated isothermal amplification (LAMP) is a good way to overcome most of the above problems as it can be performed in isothermal conditions, potential detection can be carried out in the field and assays have already been established for *F. graminearum* (Denschlag et al., 2012, Niessen and Vogel, 2010). However, multiplexing with LAMP is often difficult and so the method would not be suited if a number of different pathogens had to be detected at the same time, as is the case with analysis of air samples.

Other methods have been investigated for identification of diseased crops. These include optical sensing using techniques such as fluorescence-imaging, which has been used to detect levels of *P. triticina* (Bürling et al., 2010, Römer et al., 2011) and thermal imaging making it possible to detect and map fusarium infection (West et al., 2017). These methods usually rely on identifying different responses in plants. Therefore it can only be used once the pathogen is in the crop and so could only be used as an additional decision tool. As this technology is also relatively new, improvements are needed in establishing an appropriate measurement system and subsequent algorithms for disease pattern recognition.

By integrating existing spore traps with immunosensors able to detect different spores, difficulties could be minimised. Antibodies are robust and once a monoclonal cell line is established a constant and renewable antibody source is generated with batches being identical, eliminating batch variability associated with polyclonal antibodies. Different antibodies can be produced for different antigens and the time taken to screen cell lines can potentially be reduced by immunising mice with recombinant proteins made from target sequences, pre-selected using bioinformatics for unique regions of the pathogen.

Rowe and Dinh (2012) have proposed such an idea using Magnetic Resonance Force Microscopy (MRFM) techniques for use in the rapid identification of the collected sample; however, they used a DON antibody which was not totally specific to *F. graminearum* spores. Other antibodies have been produced by other groups for the identification of *F. graminearum.* However, again these were only developed against DON and not the spore itself, so would not be of use at this early stage of detection (Ji et al., 2008, Lee et al., 2013, Sanders et al., 2014). An antibody was also developed by Gao et al. (2013) for the detection of *P. triticina* spores. However, although having a good level of detection, the antibody also showed cross reactivity to *P. striiformis f.sp.tritici* and *P. graminis f.sp.tritici*. A monoclonal antibody was also developed by Skottrup et al. (2007a) for the detection of *P. striiformis* to be incorporated into an immunosensor. This also showed reactivity towards *P. triticina*, so therefore was not specific. Hill et al. (2006) have produced the best *Fusarium*-specific monoclonal antibodies to date using IF8 cell lines; no cross-reactions with other ascomycota species were observed. However, these were not specific to one particular *Fusarium* species and no limit of detection was established.

This work aims to create specific antibodies that could be used to detect spores of *Fusarium graminearum* and *Puccinia triticina* when incorporated into an immunosensor for in-field detection. Two approaches are proposed to gain greater specificity: using whole spores as antigens and using recombinant proteins created from spore cDNA.

2.2 Methodology

2.2.1 Fungal material

2.2.1.1 Puccinia triticina

Puccinia triticina urediniospores were from current stocks at The University of Nottingham, isolate WBRS-97-3. Wheat was inoculated with the *P. triticina* urediniospores in order to replenish as needed. Fourteen day old wheat plants were inoculated by dusting the leaves with spores mixed with talc 1:20. Inoculation was carried out late afternoon in a cool glass house (<15°C) under high humidity, this was achieved by putting the plants in a propagator, misting and filling the tray with 2 cm of water. After 24 h the plants were removed from the propagator to a warmer glasshouse. After two weeks, spores were collected by shaking the leaf to dislodge the spores before being collected in Eppendorf tubes to be stored at -80°C.

2.2.1.2 Fusarium graminearum

The *Fusarium graminearum* FC974 isolate was provided by FERA Science Ltd. from current stocks. Spore numbers were maintained by routinely culturing on SNA (Synthetic Nutrient Agar) (distilled water, 500 mL. purified agar or Bacto agar, 10 g. potassium phosphate, 0.50 g. potassium nitrate, 0.50 g. magnesium sulfate, 0.50 g. potassium chloride, 0.25 g. Glucose, 0.10 g. Sucrose, 0.10 g. Streptomycin, 0.10 g). Plates were incubated at room temperature and left on a lab window sill for 2 weeks. Spores were collected by washing plates with sterile water and stored at -20°C.

2.2.2 Identifying potential antigenic protein targets *of P. triticina* urediniospore to create recombinant proteins for antibody generation.

2.2.2.1 Identify potential antigenic protein targets

Potential antigenic proteins of *P. triticina* urediniospores were identified using EST databases from previous work carried out by Xu et al. (2011) and another database from Hu et al. (2007). Potential protein targets were then subjected to a Blast search to help classify function and similarities to other fungi which may cause a problem if using them for antibody production due to potential cross reactivity. A potential target was identified, one from Xu et al. (2011)database known as clone FL_JHHR_P002_F10g1aT3a.f1 (Protein 1) and another identified with the accession number EC400170.1 (Protein 3).

2.2.2.2 RNA Extraction

RNA was purified from *P. triticina* spores using the Qiagen RNeasy Plant Mini Kit. An on-column DNase treatment step was used to eliminate contaminant DNA, and RNA was quantified using a Nanodrop.

2.2.2.3 Reverse transcription and PCR

Reverse transcription reactions were performed on total RNA utilising oligo dT primers to provide total cDNA. A SuperScript Reverse Transcriptase kit was used from Thermo Fisher Scientific. cDNA was used instead of the DNA for an entire gene, as it does not include DNA which interrupts the coding sequence of the protein (e.g., introns). A PCR was then performed on the cDNA templates using primers that were designed for the hypothetical antigenic target using Primer3 software (Version 0.4.0) (Table 2.1). Cycling conditions were 94°C for 2 min followed by 30 cycles of 94°C for 1 min, 53°C for 1 min and 72°C for 1 min and a final extension step of 72°C for 10 min. PCR products were separated on 1.2 % agarose gels in TBE (90 mM Tris/borate/EDTA) buffer containing a final concentration of 0.2µg/mL ethidium bromide and visualized under UV light.

Table 2.1 Primers that were designed for the hypothetical antigenic targets: Protein 1 and Protein 3.

Primer name	T_m	GC%	Sequence 5'-3'	Product size (bp)
Protein 1-F	68.85	58.33	CCCAAGCAACGTGTGTAGGTGGAC	323
Protein 1-R	65.01	54.55	GCGCGTGTGGAGACAACAATAC	
Protein 3-F	71.90	60.00	TTAGCAGCTCCGGCAGGGTATGAGC	610
Protein 3-R	69.76	52.17	GGCATGATGGGCATGAGATTTGC	

2.2.2.4 pGEM-T easy vector system

Adenine residues are commonly added to PCR products by *Taq* polymerase, pGEM T Easy vectors (Promega) contain a thymidine overhang at each end of the cloning site, which allows for easy binding to the adenine tail of the PCR product. The pGEM T Easy vector was also chosen as it has the β lactamase enzyme gene which causes bacterial ampicillin resistance; this allows for selection of *E.coli* which have the plasmid and therefore are successful recombinants. Purified PCR products were ligated into the pGEM-T easy vector system (Promega) following the manufacturer's instructions and cloned into JM109-High Efficiency Competent *E.coli* cells. Selection was performed on LB media (1% NaCl, 0.5% Yeast Extract, 1% tryptone, 1.5% agar) supplemented with 100 mM ampicillin, 100 mM IPTG and 50 mg/ml X-Gal. Plasmids which contained an insert were identified because they were unable to metabolise X-gal due to the *LacZ* gene not functioning properly, so the colonies would remain white instead of producing a blue product on the agar (Figure 2.1). Transformant colonies were analysed by PCR using primers M13For and M13Rev to confirm the presence of the desired insert. Cloned products were purified using a Qiaquick PCR Purification kit (Qiagen) before being sent for sequencing.

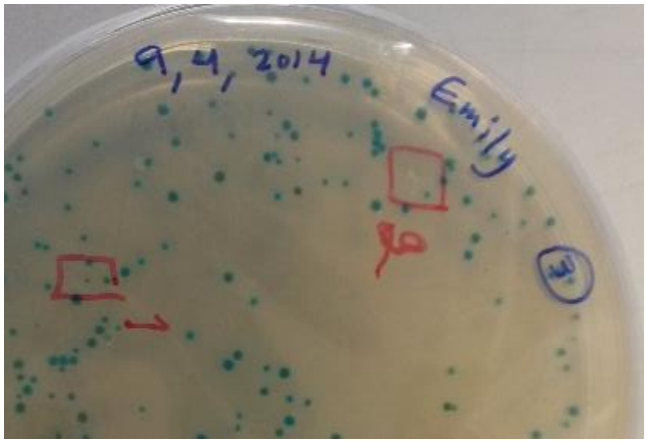


Figure 2.1 Blue-white selection plate. White colonies indicate the plasmid contains an insert as the colonies are unable to metabolise X-gal. Blue colonies without the insert preserve this ability and metabolise X-gal, thus appearing blue.

2.2.2.5 pBAD-HisB expression vector

After the correct target gene was confirmed by sequencing, digests were performed to liberate the cloned insert from the plasmid DNA. By engineering two different restriction enzyme (RE) sites into the primers the insert can be incorporated into the

expression plasmid in its desired orientation. New primers, incorporating PstI and EcoRI restriction enzyme sites, were designed and a PCR was then carried out on the previously identified successful transformants (Table 2.2). PCR products were purified using a Sigma-Aldrich Gen elute PCR clean up kit following the manufacturer's protocol and DNA was quantified using a Nanodrop. Molecular cloning of the desired insert was done using the pBAD-HisB expression vector. PCR products and the pBAD-HisB vector were digested by EcoRI, PstI and using Buffer H following Promega protocols. These digest reactions were run on a 0.8% agarose gels in TBE. Gels were visualised under UV light and desired bands were excised with a scalpel, weighed and extracted using a Qiagen QIAquick Gel Extraction Kit and DNA was quantified using a nanodrop. Ligation reactions were then performed with a ratio of 1:3 DNA product to linearised pBAD-HisB vector, using T4 DNA ligase and buffer following the New England Biolabs protocol. Products were incubated overnight at 4°C.

After successful ligation, 5 µl of the ligation reaction was transformed into TOP10 E. coli by heat shock, cells were plated on LB agar plates supplemented with ampicillin and incubated overnight at 37°C. Clone inserts were amplified from transformant colonies by PCR using pBad forward and pBad reverse primers, and sequencing was performed by Eurofins to confirm the insert was in frame.

Table 2.2 Primers incorporating *Pst*I and *EcoR*I restriction enzyme sites

Primer name	Sequence 5'-3'
F1 -PST I	CTGCAGCTATGCAAGCAACGTGTGTAGGTGGAC
R1- EcoRI	AGCACCGAATTCTTAGGCGTCATCGAGCTTGGA
F3 -PST I	CTGCAGCTATGCATGATGGGCATGAGATTTGC
R3- EcoRI	ATCACCGAATTCTTAATGAGCTCGATCCTTGATTGG

2.2.2.6 Protein Expression

LB medium (2ml) containing 50 µg ml-1 ampicillin was inoculated with a single recombinant E. coli colony. These were grown overnight at 37°C with shaking (225–250 rpm) to an OD600 = 1–2. The next day, 10 ml of LB containing 50 µg ml-1 ampicillin was added to 5 flasks and inoculated with 0.1 ml of the overnight culture and these were incubated at 37°C with vigorous shaking to an OD600 = 0.5. Once the OD reading had been reached 1 ml aliquot of cells from each tube was removed and the cell pellet stored at –20°C as the zero time point. L-arabinose was added to the five 10 ml cultures to give final concentrations of: 0.2%, 0.02%, 0.002%, 0.0002% and 0.00002%. These were incubated at 37°C as before for 4 hours after which 1 ml samples were taken and stored at –20°C.

2.2.2.6.1 SDS-PAGE and Western Blotting

SDS–PAGE was carried out using Mini-PROTEAN® TGX™ Precast Gels from Biorad. Each sample pellet was re-suspended in 100µl of 1X SDS-PAGE sample buffer and boiled for 5 min following the pBAD-HisB vector user manual, before being loaded into the gel. Electrophoresis was carried out at 100V for 50 min using the running buffer (25mM Tris base, 0.2M Glycine, 4mM sodium dodecyl sulphate (SDS) in de-ionized water).

After SDS-PAGE proteins were transferred onto Polyvinylidene fluoride (PVDF) membrane in Transfer Buffer (0.2M Glycine, 25mM Tris base, 2.5% v/v Methanol) at 350mA for 60 min. The membrane was soaked in methanol for 20 s then Transfer Buffer for a minimum of 30 min. The membrane was blocked by incubation for 1 h at room temperature in Tris Buffered Saline + 0.5%v/v Tween 20 (TBS-T) containing 5% w/v Marvel milk powder which was filtered prior to use through lens tissue. The membrane was washed three times in TBS-T (1 x 15 min and 2 x 5 min) changing TBS-T after each wash. The membrane was then incubated with Anti-Xpress-HRP (horseradish peroxidase-conjugated) diluted 1:5000 in TBS-T containing 1% w/v Marvel milk powder for 1 h. The blots were developed using a chemiluminescence detection system (GE Healthcare UK Ltd) following the manufacturers' protocol.

Results were visualised on autoradiography film which was developed and fixed following manufacturers protocols (Kodak).

2.2.3 Developing monoclonal antibodies to fungal spores

2.2.3.1 Antigen Preparation

Spores of both *F. graminearum* and *P. triticina* were counted using a haemocytometer using standard procedure and suspensions (2 ml containing $5x10^5$ spores ml^{-1}) were made by suspending the sporesin phosphate buffered saline (PBS).

2.2.3.2 Immunisation

Two antigens were used for immunisations: i) *F. graminearum* ($5x10^5$ spores ml^{-1}) ii) *P. triticina* ($5x10^5$ spores ml^{-1}). Each immunisation was performed on three 6-week old female BALB/c mice. Initial immunisations were carried out subcutaneously with 100 µl of the antigen suspension which had been mixed 1:1 with Freunds complete adjuvant.

Following this, three further immunisations of 100 µl were carried out at two week intervals intraperitoneally with the antigen suspension mixed 1:1 with incomplete Freunds adjuvant. Blood samples (100 µl) were taken two weeks after the final immunisations and the serum analysed by western blotting for an immune response. From these results the mice showing the best immune response were boosted intraperitoneally four days before fusion, with 100 µl of immunogen in PBS.

2.2.3.3 Fusion

After analysis of tail bleeds via western blot the selected mouse's spleen was dissected and cells were recovered by Kate Perkins (lab technicianat Fera Science Ltd). Splenocytes and myeloma cells were first prepared for counting by adding 80 µl of Hanks' Balanced Salt Solution (HBSS) (Invitrogen), 10 µl trypan blue stain and 10 µl of cell suspension into a well of a 96 well plate. This was mixed thoroughly counted using a haemocytometer using standard procedure. Cell viability was calculated as the number of viable cells divided by the total number of cells within the grids on the hemacytometer. If the cells took up trypan blue stain, they were considered non-viable. Splenocytes were then washed in HBSSand fused with myeloma cell line SP02/0-AG14 at a ratio of 3:1. The fusion was carried out by the addition of 1 ml of

50% polyethylene glycol over 1 min, followed by the addition of 6 ml of RPMI 1640 medium (RPMI 1640, Invitrogen), over 4 min and a further 40 ml of RPMI 1640, before centrifugation at 17,900 x g for 5 min. The cell pellet was resuspended into RPMI 1640 growth medium containing 20% fetal calf serum (FCS) and supplemented with hypoxanthine, aminopterin, thymidine (HAT) and MRC-5 conditioned medium. The resulting cell suspension was pipetted into 50 X 96-well cell culture plates at 100 µl / well (potentially giving 4,800 wells of antibody cell lines) and incubated at 37°C in an atmosphere containing 5% CO_2.

HAT is used to select against unfused myelomas. The aminopterin found in the medium blocks the de novo DNA nucleotide synthesis pathway, those cells with the enzyme called HGPRT are able to use the salvage pathway as an alternative means to replicate. Unfused myelomas do not have this enzyme and so die. Hybridomas have a functioning Hypoxanthine-guanine phosphoribosyltransferase (HGPRT) enzyme from the spleen cells resulting in the ability to replicate in the medium. Myeloma cells were observed under a microscope to determine their viability. Healthy viable cells were considered to be round and bulbous. When all unfused myeloma cells were no longer viable, aminopterin was omittedfrom the growth medium. 2% HT supplement replaced the HAT supplement containing the aminopterin. . The cells were fed on day 3 by adding 100 µl of growth medium to all wells and on days 6 and 10 by removing 100 µl of cell culture supernatant and adding 100 µl of fresh growth medium. Supernatants were screened with an activity test 12 days after fusion for antibodies that recognised IgG antibodies. Selected hybridoma cell lines were grown on and further tested using western blotting for specific spore antigen detection.

2.2.3.4 Cloning

Fusion wells contain a mixed population of hybrids but only one of these may be producing the antibody of interest. It is important to isolate the useful hybridoma cell lines as soon as possible after screening the fusion. If cloning is not carried out at this stage the potentially useful cell line may be overgrown by non-secreting variants. Cloning is achieved by serial dilution of the cell population to isolate single cells in separate culture wells. Any cell line resulting from an isolated hybridoma cell

will contain identical cells all producing a single identical monoclonal antibody. The hybrid cells from the selected wells were diluted to 5 cells ml^{-1} and plated out on a 96-well plate at 100 µl/ well; therefore, half the wells should contain one cell and half no cells. After approximately 12 days the single cells have multiplied to fill the well and produce monoclonal antibodies for screening. Clones were tested in the same way as hybridomas were and screened with an activity test for antibodies that recognised IgG antibodies. Selected active clones were grown on and further tested via western blotting for specific spore antigen detection and cross reactivity testing with other fungal spores and mycelia.

2.2.3.5 Weaning

Weaning was carried out by gradually removing the concentration of MRC-5 and HT in the medium when cells were fed so that the supplements were no longer present. This process is vital before purification as these impurities can interfere in the antibody purification procedure. It was also ensured that cells were observed under a microscope at each feed to check cells were still growing and healthy in the supplement-reduced medium. Healthy viable cells were considered to be round and bulbous and wells where the medium had turned pink (due to the phenol red ph indicator in the medium) were also an indication of good growth. The FCS concentration was also gradually reduced until the percentage of supplement was 10%. Once the cells were growing well in this medium, they were bulked up by growing them in increasingly larger flasks until 1 litre of the desired cell line culture was achieved before purification.

2.2.3.6 Purification

One litre of the desired cell line culture medium was purified using HiTrap Protein G columns (GE Healthcare Life Sciences) connected to a peristaltic pump. The pump was adjusted to 4ml/minute and left for approximately 3 hours. Purified mAbs were identified using the Coomassie protein assay (Pierce). After the highest concentrations were identified these were pooled and 1% sodium azide was added. The purified antibody concentration was then quantified by spectrophotometry before being stored at -20°C. The purified antibody was then tested using western

blotting for specific spore antigen detection and cross reactivity testing with other fungal spores and mycelia to confirm specificity.

2.2.3.7 Screening

2.2.3.7.1 ELISA activity testing-IgG specific

Plates were coated with rabbit anti-mouse antibody diluted (1/32000) in coating buffer (15nM Na_2CO_3, 35 mM $NaHCO_3$, pH9.6), 100 µl per well and incubated at 4°C overnight. Plates were then washed 3 times with PBST (20 mM sodium phosphate, 150 mM sodium chloride pH 7.4) and blocked by adding 200 µl of blocking buffer (PBST containing 1 % BSA) to each well. Plates were then incubated at 33°C for 1 h. Plates were then washed 3 times as before. The samples were diluted 1:2 in dilution buffer (PBST containing 0.2 % BSA), and 100 µl of this was added to the plate, incubated at 33°C for 1 h and then washed. The media was used as a negative control diluted 1:2 in dilution buffer and two positive controls were used: mouse tail bleed and IgG specific antibody raised in a mouse. Rabbit anti-mouse alkaline phosphatase was applied diluted 1:4,000 dilution buffer, incubated at 33°C for 1 h and washed prior to the addition of 1 mg ml^{-1} p-Nitrophenyl Phosphate. The plates were kept in the dark for 30 min to 1 h, and colour change was determined by spectrophotometry at 405 nm in a Thermomax Microplate reader with SOFT Max Pro software. Positive wells with high ODs were carried forward and negative wells discarded.

2.2.3.7.2 SDS- PAGE and western blotting

2.2.3.7.2.1 Protein extraction

Spore suspension (1ml containing $5x10^5$ spores ml^{-1}) was centrifuged for 1 min at 20,000 x g. The supernatant was removed and 400 µl SDS sample buffer (100mM Tris-HCl pH 6.8, 4% β-mercaptoethanol, 4% SDS) was added. The sample was homogenized by adding glass beads and using a mini-beadbeater for 3 min. Samples were then heated for 10 min at 96°C, centrifuged for 10 min at 20,000 x g and supernatant transferred to a clean tube, protease inhibitor was added and stored at -20 °C.

2.2.3.7.2.2 SDS-PAGE

All SDS-PAGE and electrophoretic transfer of proteins to membranes were carried out using the mini-protean system (Biorad). Proteins were separated on 10%

resolving gels with 4% stacking gels as follows, 10% resolving gel (33% ProtoGel, 25% Resolving Buffer (Geneflow), 1% ammonium persulphate (APS), 0.1% N,N,N',N'-Tetramethylethylene diamine (TEMED) in MGW), and 4% stacking gel (13% ProtoGel, 25% Stacking buffer (Geneflow), 0.7% APS, 0.1% TEMED) in MGW). Prior to addition of samples the wells were rinsed with running buffer (25 mM Tris-base, 0.2 M Glycine, 4 mM sodium dodecyl sulphate (SDS) in de-ionized water), using a syringe and needle to remove any un-polymerised acrylamide. Total protein extractions were added to 4 x Loading buffer (1 M Tris-HCl pH 6.8, 4% β- mercaptoethanol, 1 M SDS, 0.1 M bromophenol blue, 40% glycerol in MGW) at a ratio of 3:1, and heated for 10 min at 96°C then centrifuged at 20,000 x g for 3 min prior to loading on the gel alongside a PageRuler™ Plus Pre-stained Protein ladder (Fermentas). Gels were run at 200 v for 40 min or until dye had reached the end of the resolving gel.

2.2.3.7.2.3 Coomassie

To check for successful protein extraction, gels were developed by Coomassie stain, prior to western blot. Gels were put in a weighing boat and covered with Coomassie blue stain (Coomassie stain Brilliant Blue R250 0.25 g, Glacial acetic acid 10%, 45% MetOH, 45% dH_2O) and shaken for 20 min. The Coomassie stain was then removed and the gel was soaked in Destainer (Glacial acetic acid 10%, 40% MetOH, 50% dH_20,) whilst shaken until the gel was clear and stained bands were showing.

2.2.3.7.2.4 Western blot

Proteins were transferred to Polyvinylidene fluoride (PVDF) membrane in transfer buffer (0.2 M Glycine, 25 mM Tris base, 2.5% MetOHl) at 350 mA for 1 h. The membrane was soaked in methanol for 20 s then Transfer Buffer for a minimum of 30 min. The membrane was blocked by incubation for 1 h at room temperature in Tris Buffered Saline + 0.5% Tween 20 (TBS-T) containing 5% Marvel milk powder which was filtered prior to use through lens tissue. The membrane was washed three times in TBS-T (1 x 15 min and 2 x 5 min) changing TBS-T after each wash. The membrane was incubated with primary antibody (either cell culture supernatant diluted between 1 in 2 or purified monoclonal antibodies at a concentration of 1 in 4000 in TBS-T containing 1% Marvel milk powder, overnight at 4°C with gentle shaking. Negative controls were either supernatant or purified antibody DO95 both

raised to the bee pathogen *Noseam apis*. Membranes were washed as above. The membrane was then incubated with rabbit anti- mouse IgG conjugated to HRP diluted 1 in 8000 in TBS-T containing 1% w/v Marvel milk powder. The blots were developed using a chemiluminescence detection system (GE Healthcare UK Ltd.) following manufacturers' protocol. Results were visualized on autoradiography film which was developed and fixed following manufacturer's protocols (Kodak).

2.2.3.7.3 Cross reactivity testing

Cross reactivity testing was carried out using western blot using the same method previously described. Eighteen different samples were used (Table 2.3) these were grown on either standard Potato Dextrose Agar (PDA) (70139 Sigma-Aldrich) supplemented with ampicillin (250 µg/ml) for mycelia growth, orSNA (recipe as before)) for spore production. Plates were incubated in a growth room between 25 and 30°C for 2 weeks. Both *P. triticina* and *P. striiformis* were grown by methods described previously.

Table 2.3 Details of fungal species used for cross reactivity studies

I.D	Name
107	*Fusarium solani*
107s	*Fusarium solani (spore)*
95	*Fusarium avenaceum*
95s	*Fusarium avenaceum (spore)*
97	*Fusarium oxysporum*
97s	*Fusarium oxysporum (spore)*
98	*Fusarium culmorum*
322	*Fusarium poae*
325	*Alternaria alternata*
Yel	*Puccinia striiformis (spore)*
Brown	*Puccinia triticina (spore)*
Sep	*Septoria tritici (spore)*
T.Ros	*Trichothecium roseum*
655	*Septoria nodorum (spore)*
1794	*Hymenula cerealis*
1968	*Rhizoctonia solani*
2726	*Aspergillus niger*
3805	*Cladosporium cladosporioides*

2.2.3.8 Immunofluorescence assay

A spore suspension of *F. graminearum* (500 µl containing $5x10^5$ spores ml^{-1}) was spun down, re-suspended in Loading Buffer (as before) and added to an Eppendorf and kept at 33°C overnight. This was then centrifuged at 20,000 x g and the supernatant was removed. The cells were then washed 3 times with PBST and centrifuged as before. This was then treated with the monoclonal antibody produced in this chapter (29.G7.A9) at a concentration of 1/1000 and incubated at 33°C for 1 h. This was then

centrifuged and washed again as before and then treated with Anti-Mouse IgG (whole molecule)–FITC at a concentration of 1/250. This was incubated as before and centrifuged and washed. The mixture was mounted on a microscope slide using glycerol buffer and examined with a fluoroscope. This procedure was repeated with a Nosema monoclonal antibody DO95, and PBS buffer as negative controls.

2.3 Results

2.3.1 Identifying potential antigenic protein targets *of P. triticina* urediniospores to create recombinant proteins for antibody generation.

2.3.1.1 Target Sequence Selection

A potential target was identified, one from the Syngenta database known as clone FL_JHHR_P002_F10g1aT3a.f1 (Target 1) and another identified with the accession number EC400170.1 (Target 3). BLAST searches revealed no significant homology between the sequences, but both had similarity to hypothetical proteins of *Puccinia graminis* f. sp*. tritici* otherwise known as stem rust. This was considered to be beneficial as the antibody, although maybe not specific to one rust, could potentially be used to detect both types of rust. A target region for both Target 1 and 3 was selected. The lengths of the sequences were 323 bp for Target 1 and 610 bp for Target 3.

2.3.1.2 Amplification Target DNA and Ligation into pGEM-T vector

A fluorescent band of DNA was observed between the 500 and 750 bp marker for Target 3 and between the 250 and 500 bp marker for Target 1 (Figure 2.2), these correlated with the approximate sizes of 323 bp for Target 1 and 610bp for Target 3.

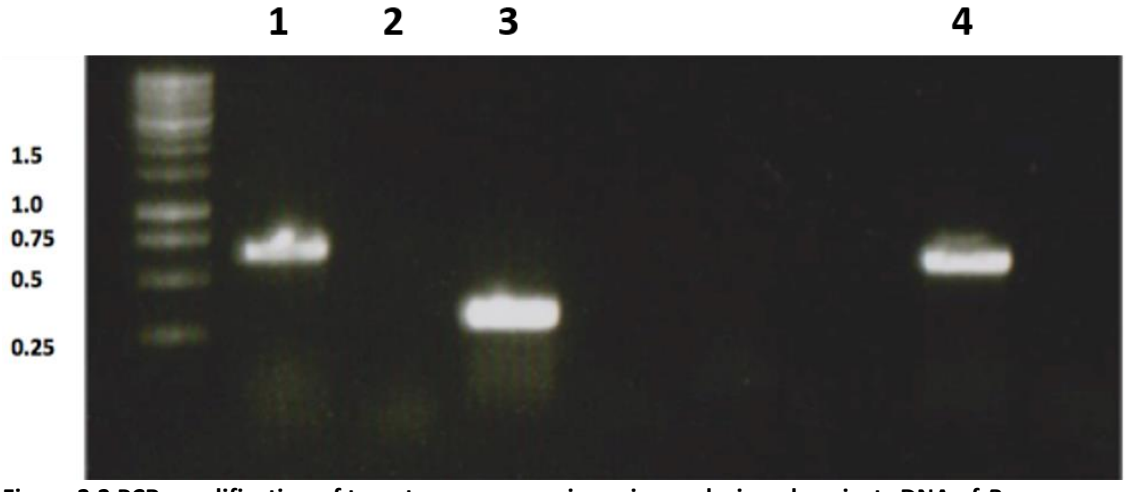


Figure 2.2 PCR amplification of target sequences using primers designed against cDNA of *P. triticina*. 1; positive control, 2; negative control, 3; Target 1, 4; Target 3.

Following PCR the products were ligated into pGEM T Easy vectors. They were then transformed into *E.coli*, grown on selection plates to select for the presence of the

pGEM vector. A confirmation colony PCR was carried out using the M13 primers specific to the plasmid to confirm that the inserts were in the plasmid (Figure 2.3) and, both targets were shown to be present.

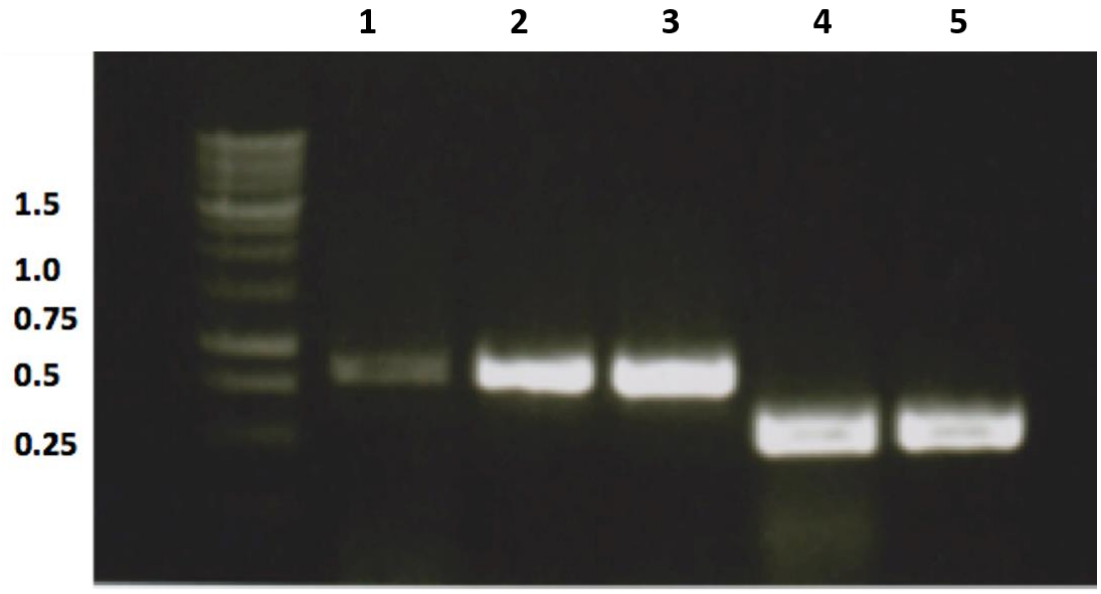


Figure 2.3 Colony PCR utilising M13 primer binding sites inherent in the vector system to detect the insertion of target DNA into pGEM-T vector. 1-3; Target 3, 4-5; Target 1.

2.3.1.3 pBAD-HisB expression vector – ligation and transformation

Restriction digests were performed on the PCR products and pBAD-HisB expression vector using the appropriate restriction enzymes' for each construct. The digested samples were then run on a gel (Figure 2.4) and both targets were shown to be present and were the size expected and the linear cut plasmid also had a single band of the expected size as opposed to the two bands present in the circular uncut sample of the plasmid. These bands were excised from the gel and ligation was carried out using the linearised pBAD-HisB expression vector.

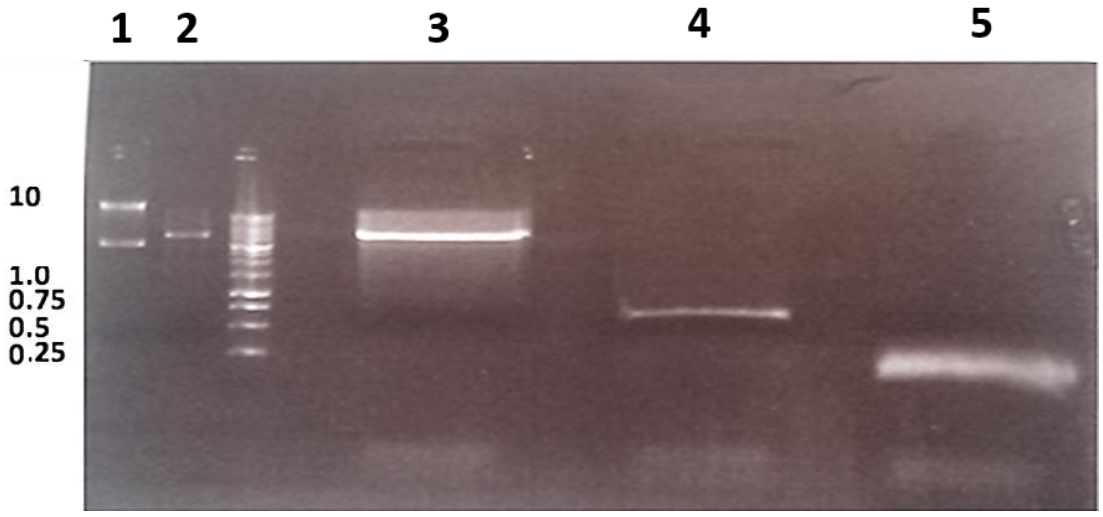


Figure 2.4 Restriction digests digested with *Eco*RI and *Pst*1 restriction enzymes. 1; circular uncut pBad-HisB vector control, 2; cut linear pBad-HisB vector control, 3; pBad-HisB vector, 4; Target 3, 5; Target 1.

The ligated samples were then transformed into competent Top10 *E. coli*. A confirmation colony PCR was carried out (Figure 2.5). Of the 9 white colonies that were analysed on the gel, two positive colonies were found. Sample 7 (Target 3) and sample 13 (Target 1), shown in Figure 2.5, were selected to grow up further and were sent off for sequencing to confirm that the plasmid contained the expected target fragment.

Sequence results confirmed that sample 7 did contain Target 3 and was in the right reading frame. However, the sequencing results for Sample 13 contained a base substitution resulting in a stop codon, transformation using this insert would have resulted in expression of a truncated protein, and therefore Target 1 was not carried forward to the expression experiments.

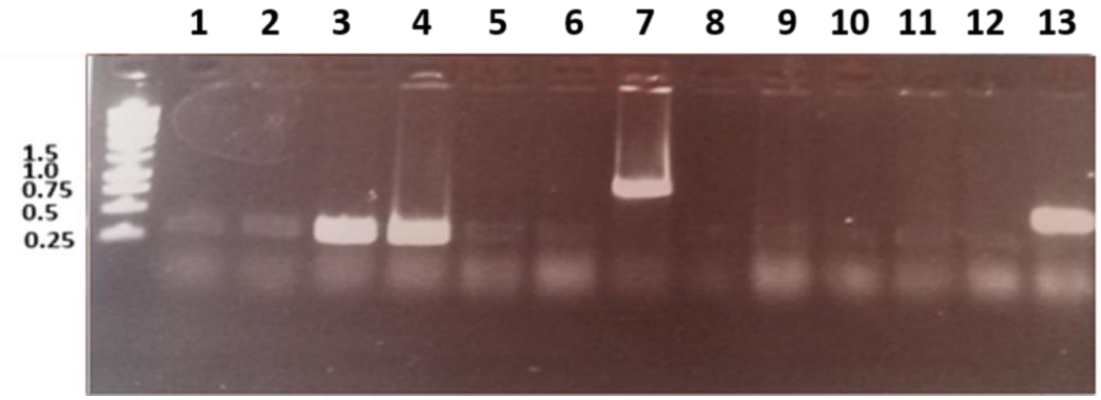


Figure 2.5 Colony PCR utilising pBAD primers was performed on potential pBAD-HisB-Target 1 and Target 3 transformants. 1-2; Negative control Pbad Z, 3-4; pBAD-HisB vector, 5-8; potential pBAD-HisB-Target 3, 9-13; potential pBAD-HisB-Target 1.

2.3.1.4 pBAD-HisB expression vector – Expression experiment.

A single recombinant colony from sample 7 in Figure 2.5, was grown up and an expression experiment was carried out using L-arabinose to give 5 flasks with final concentrations of: 0.2%, 0.02%, 0.002%, 0.0002% and 0.00002% L-arabinose. These were inoculated with the recombinant colony. Results were obtained using SDS-PAGE and visualisation by western blot (Figure 2.6). The molecular weights of Target-3 in the pBAD-HisB expression vector were calculated to be 29.62 kDa, and the induced protein bands, which can be seen in Figure 2.6 in samples 1-4, correspond to the expected size of 29.62 kDa. The best level of induced expression was seen at a L-arabinose concentration of 0.02%, although expression was seen at all concentrations of L-arabinose except 0.00002%.

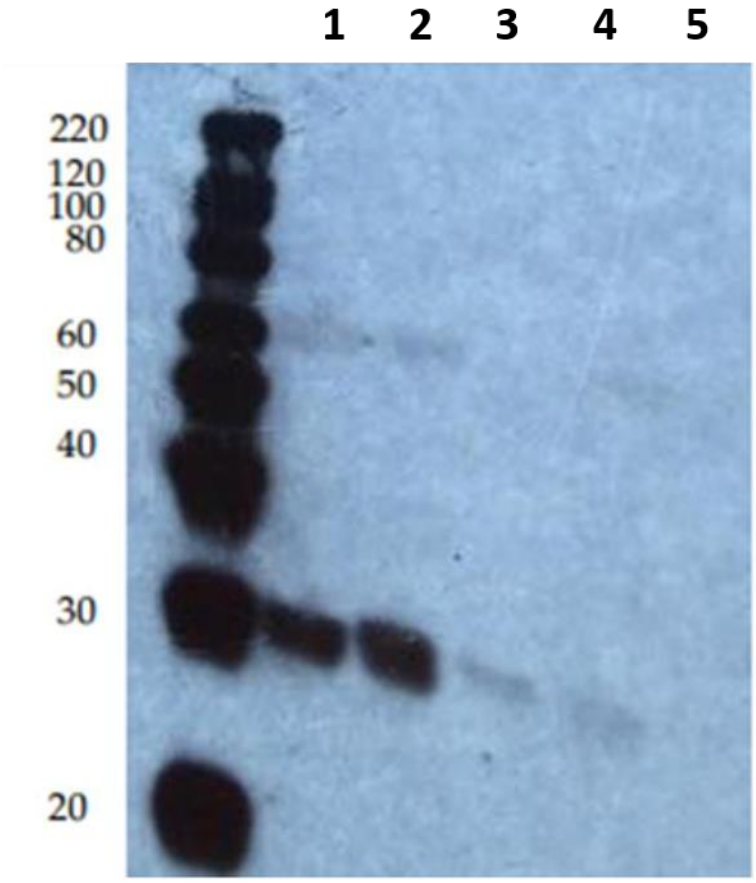


Figure 2.6 Western blot showing protein expression at various concentrations of L-arabinose. 1-5; 0.2%, 0.02%, 0.002%, 0.0002% and 0.00002% L-arabinose respectively

Following confirmation from the small scale inductions that a protein of the expected approximate molecular weight was expressed, large scale inductions would have been carried out and the protein would have been purified using a His-Bind chromatography on a soluble column. However ethics approval was not obtained for this work as mice had already been immunised with *P. triticina* spores. Work was paused at this point until the outcome of the spore immunisations was known. .

2.3.2 Developing monoclonal antibodies to fungal spores

2.3.2.1 Mouse selection

In order to ensure a good immune response for mAb development, six mice were immunised, three with *P. triticina* spores (called 323.1/.2/.3) and three with *F. graminearum* spores (called 324.1/.2/.3). To assess the immune response of each mouse to the desired spores, western blots were carried out using the tail bleed from each mouse (Figure 2.7). Tail bleeds 323.3 and 324.3 were chosen for mAb production

as they appeared to have the greatest response to the appropriate antigen. Tail bleed 323.3 showed a clear strong band at 100 kDa and 324.3 showed a strong immune response from 250-55 kDa with two additional bands at approximately 45 kDa and 20 kDa.

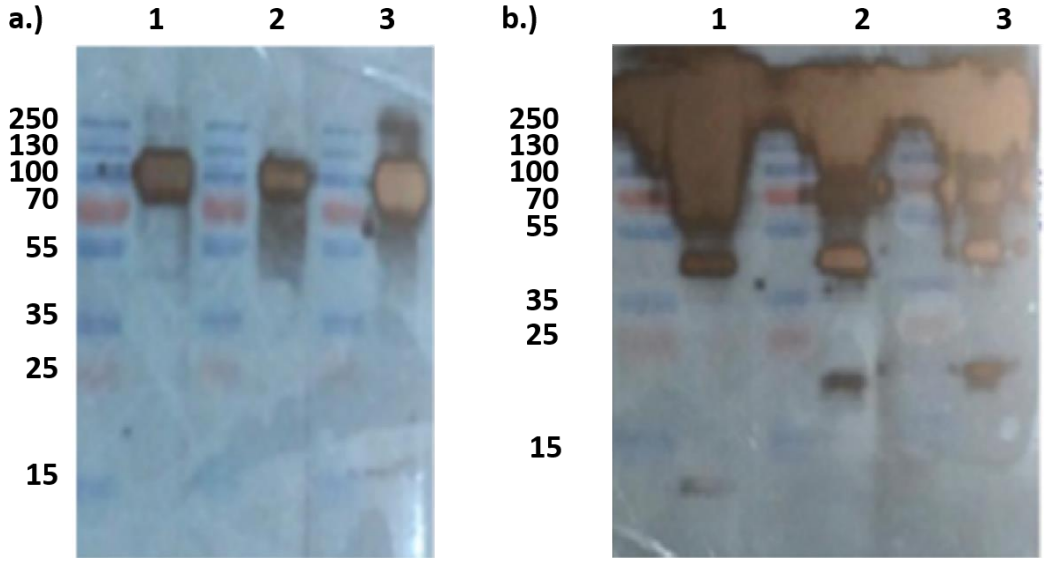


Figure 2.7 Evaluation of tail bleeds from 6 mice via western blot. a.) *P. triticina*, 1; tail bleed 323.1, 2; tail bleed 323.2, 3; tail bleed 323.3. b.) *F. graminearum*, 1; tail bleed 324.1, 2; tail bleed 324.2, 3; tail bleed 324.3.

2.3.2.2 Fusion

Fusion was carried out using the spleen cells from the chosen mice. A total of 1.1x 10^8 spleen cells were recovered from the mouse chosen for *F. graminearum* and 1.72x10^8 from the mouse chosen for *P. triticina*. These were fused at a ratio of 3:1, spleen cells to myeloma cells (SPO2/0-Ag14). It was observed that the *P. triticina* mouse's spleen was much smaller than that of the mouse immunised with *F. graminearum.* SPO2/0-Ag14 myeloma cells were found to have approximately 86% viability.

2.3.2.3 Activity testing hybridomas

After fusion the 4800 hybridomas were analysed for active cell lines using ELISA with an IgG antibody. Thirty four *P. triticina* cell lines showed reactivity towards the IgG antibody and 71 for *F. graminearum*. These hybridoma continued to be fed and the others were discarded. Cells were also assessed visually under a microscope for viability. Of the 34 *P. triticina* cell lines only 15 showed strong viability with strongly

dividing cells; however, all 71 cells for *F. graminearum* grew well during the feeding schedule and showed strong viability.

2.3.2.4 Western specificity hybridomas

The selected cell lines for each antigen were tested using western blots to identify cell lines with reactivity towards the specific spore antigen of interest. Plate trapped antigen ELISA (PTA- ELISA) with spores could not be carried out as preliminary tests showed problems with spores binding to the plate surface; therefore, a western blot analysis approach was taken.

2.3.2.4.1 *P. triticina* hybrids

Of the 15 *P. triticina* hybrids none showed any strong reactivity towards *P. triticina* spores (Figure 2.8). A faint band was observed from some of the hybrids at approximately 60 kDa; however, this was also observed on the negative control (growth media) and was not as dominant as the band observed for the positive control (tail bleed). Hybrid 2.B11 seemed to have significant reactivity; however, after further testing this was only due to nonspecific binding with the ladder.

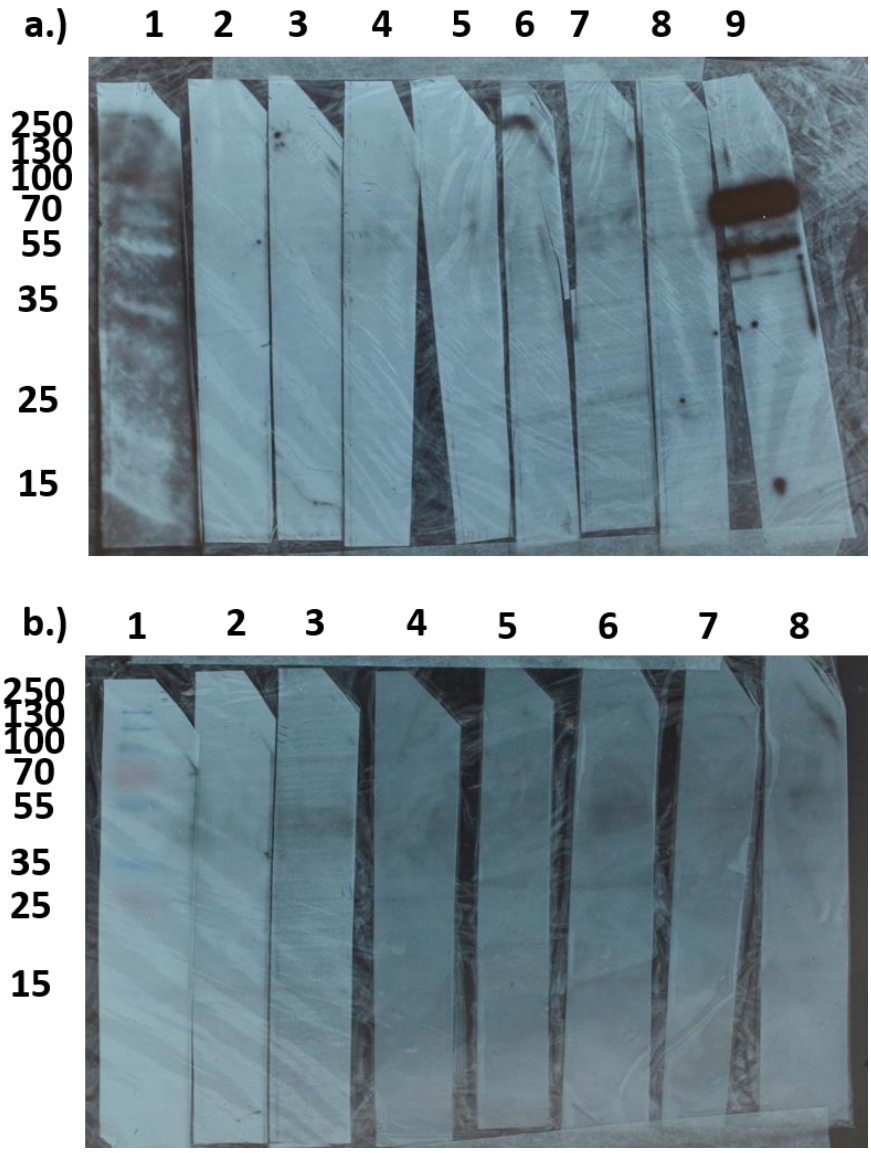


Figure 2.8 Western blot to evaluate hybridomas' reactivity to *P. triticina* spores. a.) 1-9; cell line 2.B11, 3.A5, 5.C7, 5.D12, 14.C6, 23.A8, 24.E1, 26.F5 and positive control – tail bleed. b.) 1-8; cell line 30.B8, 32.H4, 33.C4, 34.G5, 41.G6, 48.C6, 48.F10 and negative control

2.3.2.4.2 Fusarium hybrids

Of the 71 hybridomas that were screened against *F. graminearum* spores, 10 were found to have reactions with varying specificities (these are indicated by the red circles in Figure 2.9). Cell lines; 15.E5, 29.G7, 30:C8 and 43.F12 showed clear defined bands. Cell lines 28.B10, 31.G9, 38.E5, 43.F11, 44.C11 and 47.A10 did not show clear bands but did display some potential reactivity that was not present on the negative controls. Therefore all 10 of these cell lines were chosen to be taken forward and cloned.

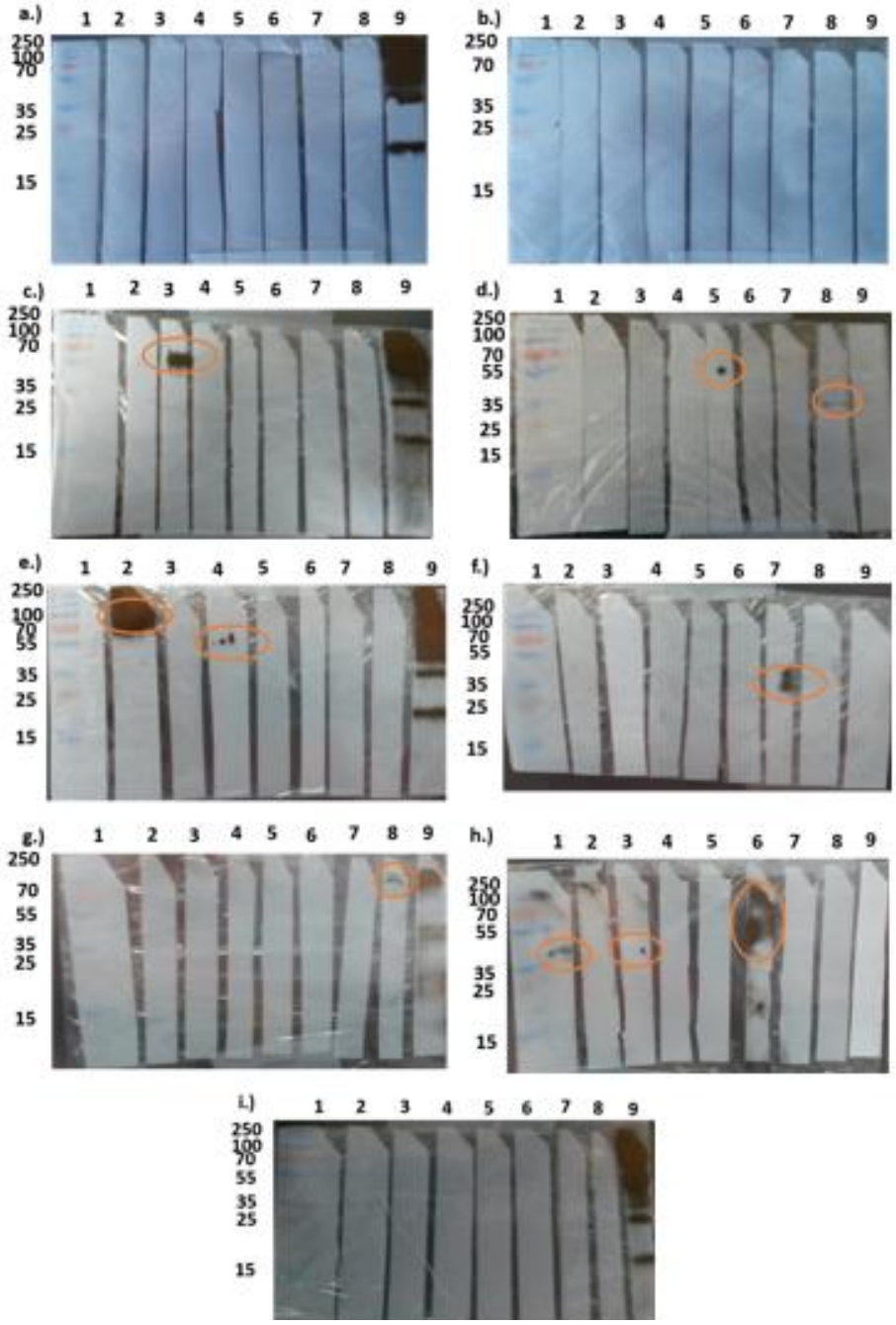
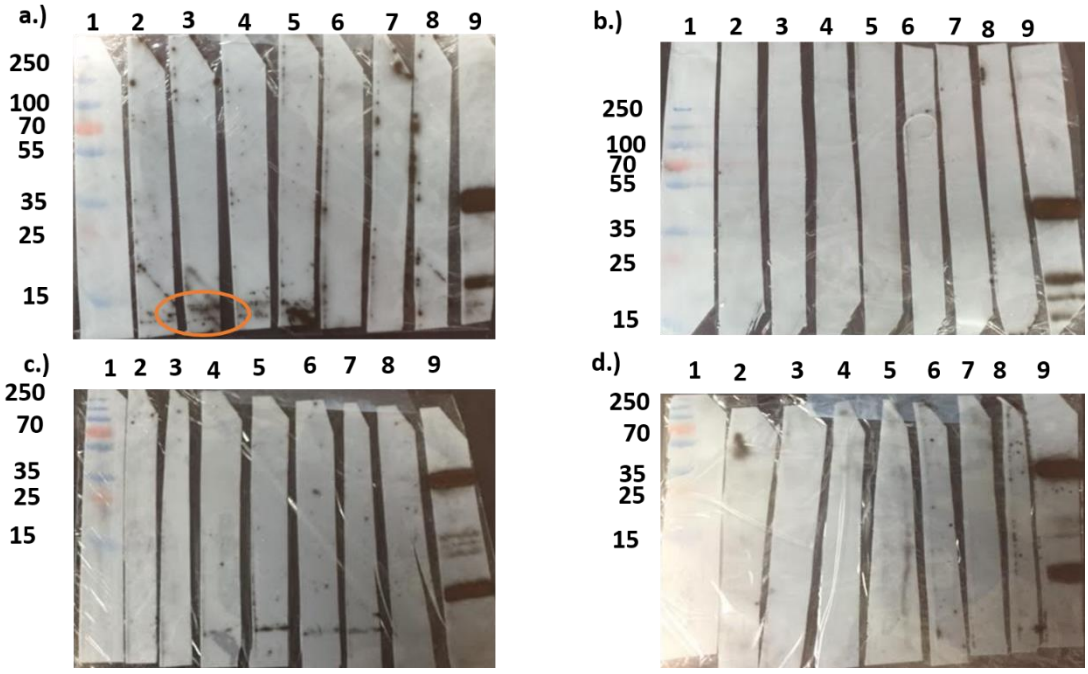


Figure 2.9 Western blot to evaluate hybridomas' reactivity to *F. graminearum* spores. a.) 1-9; cell line 3.C2, 4.A4, 5.D12, 6.C10, 6.H8, 7.C8, 7.E1, 8.D1 and positive control b.) 1-9; cell line 9.B11, 9.C11, 9.H11, 10.B11, 10.D8, 10.D10, 12.D8, 14.A8 and negative control c.) 1-9; cell line 14.F1, 14.G1, 15.E5, 17.A3, 18.A6, 18.C6, 21.B9, 22.B6 and positive control d.) 1-9; cell line 22.F11, 25.A11, 26.F10, 28.A6, 28.B10, 28.C11, 29.D4, 29.G7 negative control e.) 1-9; cell line 29.H12, 30.C12, 30.D1, 31.G9, 32.A12, 33.H10, 35.F7, 35.H11 and positive control f.) 1-9; cell line 36.E10, 38.A12, 38.B12, 38.C12, 38.D3, 38.D12, 38.E5, 39.A10 and negative control g.) 1-9; cell line 39.C3, 39.H6, 40.D8, 40.E1, 41.F10, 42.F3, 43.D9, 43.F11 and positive control h.) 1-9 cell line 43.F12, 44.B2, 44.C11, 45.E7, 46.H5, 47.A10, 47.C2, 47.E2 and negative control i.) 1-9; cell line 47.E12, 49.E10, 50.D3, 50.D9, 50.E7, 50.E10, 50.G11, negative control and positive control. All negative controls are growth media and positive controls are the tail bleed. Red circles depict reactive responses of interest.

2.3.2.5 Cloning and specificity of clones

Activity tests were carried out as before to indicate which clones were active (data not shown). Cells were also observed under a microscope to ascertain which lines were growing the best. After this was carried out 79 clones were chosen to test for a reaction towards *F. graminearum* spores (Figure 2.10). Four clones were chosen to take forward (indicated by red circles in Figure 2.10). These were chosen based on trying to take forward clones from different cell lines and differing specificity profiles. It was clear at this stage that clones from cell line 29.G7 showed the most promise, with all but one of the clones showing a strong reaction with a clear defined band at 45 kDa. The most promising cell line before cloning appeared to be 15.E5; however, the clear band at approximately 60 kDa was no longer present, and only reactivity at approximately 10 kDa was observed.



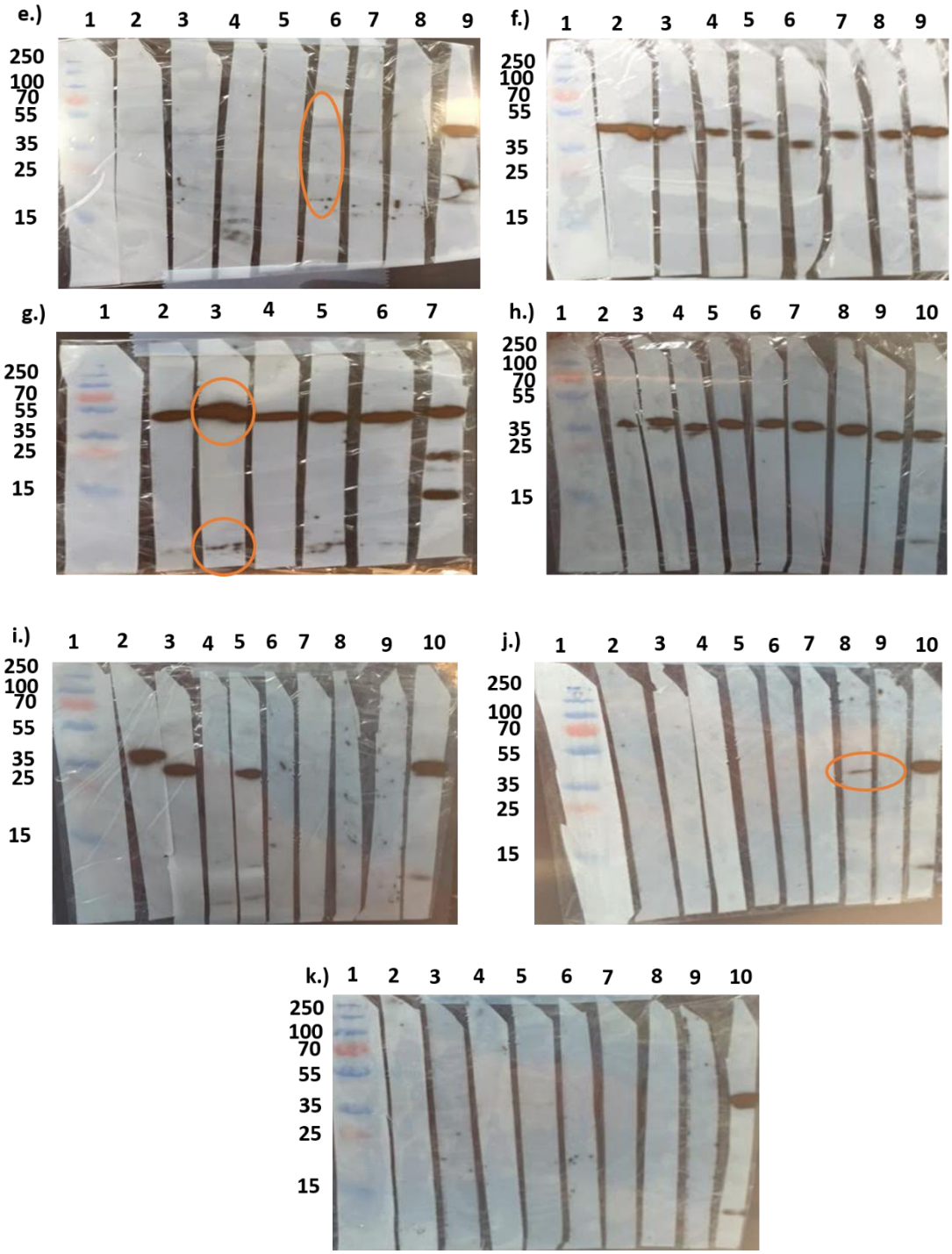


Figure 2.10 Western blot to evaluate clones reactivity to *F. graminearum* spores. a.) 1; negative control, 2-3; clones of 15.E5, 4-7; clones of 47.A10, 8; clones of 31.G9, 9; positive control. b.) 1; negative control, 2-8; clones of 31.G9, 9; positive control. c.) 1; negative control, 2-8; clones of 28.B10, 9; positive control. d.) 1; negative control, 2-8; clones of 28.B10, 9; positive control. e.) 1; negative control, 2; clones of 31.G9, 3-8; 28.B10, 9; positive control. f.) 1; negative control, 2-8; clones of 29.G7, 9; positive control. g.) 1; negative control, 2-6; clones of 29.G7, 7; positive control. h.) 1; negative control, 2-9; clones of 29.G7, 10; positive control. i.) 1; negative control, 2-5; clones of 29.G7, 6-9; 43.F11, 10; positive control. j.) 1; negative control, 2-5; clones of 43.F11, 6-9; clones of 44.C11, 10; positive control. k.) 1; negative control, 2-9; clones of 44.C11, 10; positive control. All negative controls are growth media and positive controls are the tail bleed. Red circles depict reactive responses of interest.

2.3.2.5.1 Clones- cross reactivity

The 4 clones carried forward were tested for cross reactivity towards 18 different antigens (Antigens shown in Table 2.3). These included other species of Fusarium as well as different fungal species. All clones displayed cross reactivity towards *Aspergillus niger* (655) and *Trichothecium roseum* (T.ros), however this was also observed with the negative control (Nosema antibody supernatant). Both 44.C11.G7 and 28.B10.C12 also showed cross reactivity towards *P. triticina* and *P. striiformis* f.sp. *tritici*. Clone 15.E5.G12 showed cross reactivity to some other Fusarium species and also did not show any significant reaction this time to F. *graminearum (data not shown).* For these reasons clone 29.G7.A9 (Figure 2.11) was chosen to be purified.

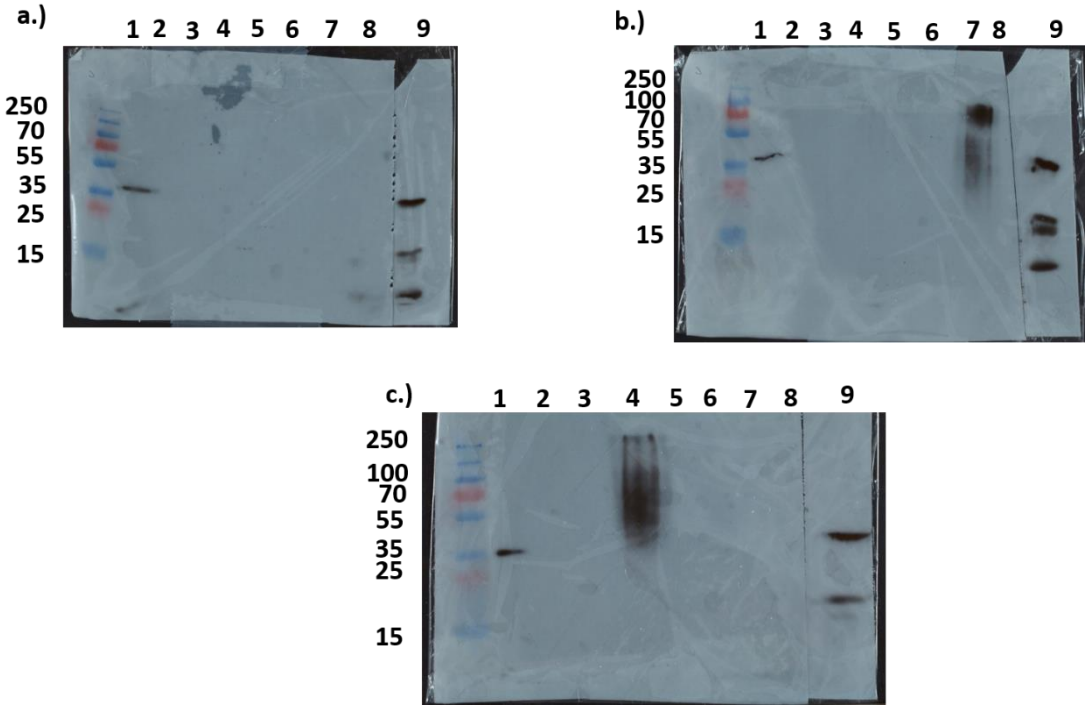


Figure 2.11 Western blot to evaluate clone 29.G7.A9 cross reactivity to a range of fungal antigens. a.) 1; F.g, 2; 107, 3; 107s, 4; 95, 5; 95s, 6; 97, 7; 97s, 8; 98, 9; positive control. b.) 1; F.g, 2; 322, 3; 325, 4; Yel, 5; Brown, 6; Sep, 7; T.ros, 8; 655, 9; positive control. c.) 1; F.g, 2; 1794, 3; 1968, 4; 2726, 5; 3805, 6; blank, 7; blank, 8; blank, 9; positive control. All positive controls were tail bleed.

2.3.2.6 Purification – purified antibody specificity and cross reactivity

Clone 29.G7.A9 was purified and the monoclonal antibody diluted to a concentration of 2.1 mg/ml. A serial dilution was carried out to ascertain the best concentration at which to apply the purified monoclonal (Figure 2.12a). Even at a concentration of 1/1000 the antibody still showed a clear distinct band visible at approximately 35 kDa.

A cross reactivity test was carried out as before using the purified monoclonal and it showed cross reactivity with *T.roseum;* although, these proteins appear to be bigger, with multiple bands (40-70 kDa) compared to the protein band found with the *F. graminearum* sample (30 kDa). No other cross reactivity was detected with any of the other antigens (Figure 2.12c). The negative control (purified Nosema monoclonal DO95) also showed cross reactivity with proteins of sizes ranging from 15-25 kDa in *T. roseum* and proteins of sizes 15 kDa in *Septoria tritici* the antibody also binds to proteins in the ladder (Figure 2.13).

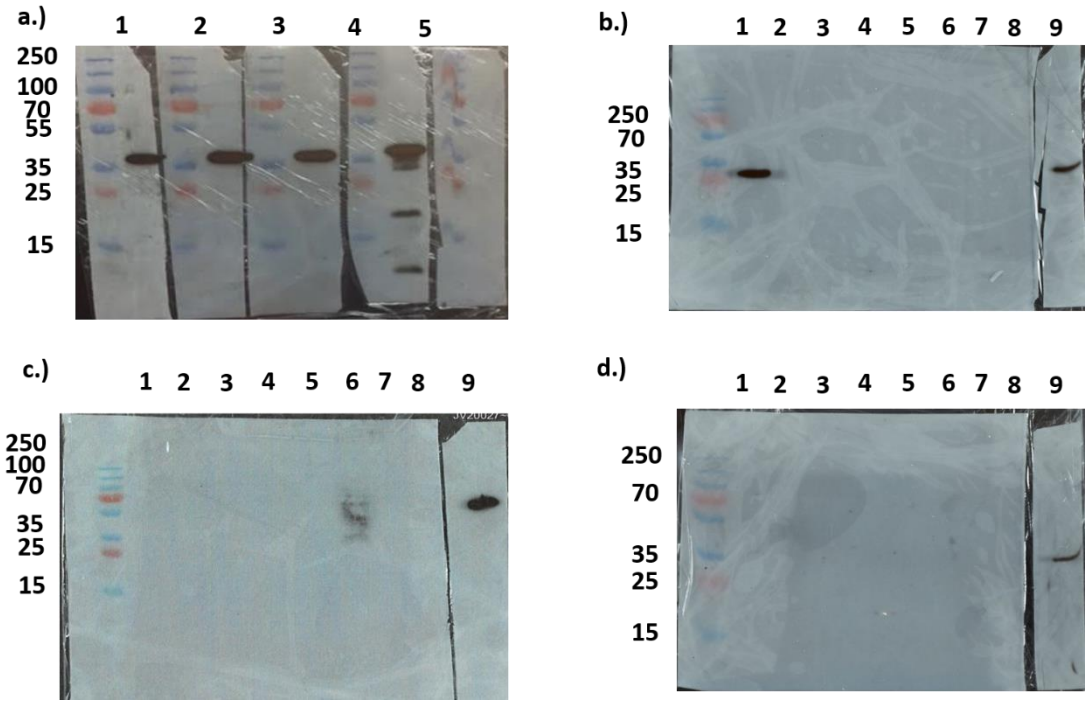


Figure 2.12 Western blot to evaluate purified monoclonal antibody 29.G7.A9. a.) Purified antibody at different concentrations to detect *F. graminearum*. 1; 1/1000, 2; 1/500, 3; 1/250, 4; positive control, 5; negative control. b.) cross reactivity a range of fungal antigens. 1; F.g, 2; 107, 3; 107s, 4; 95, 5; 95s, 6; 97, 7; 97s, 8; 98, 9; positive control. c.) cross reactivity a range of fungal antigens 1; 322, 2; 325, 3; Yel, 4; Brown, 5; Sep, 6; T.ros, 7; 655, 8; 1794, 9; positive control. d.) 1; 1968, 2; 2726, 3; 3805, 4; blank, 5; blank, 6; blank, 7; blank, 8; blank, 9; positive control. All positive controls were tail bleed.

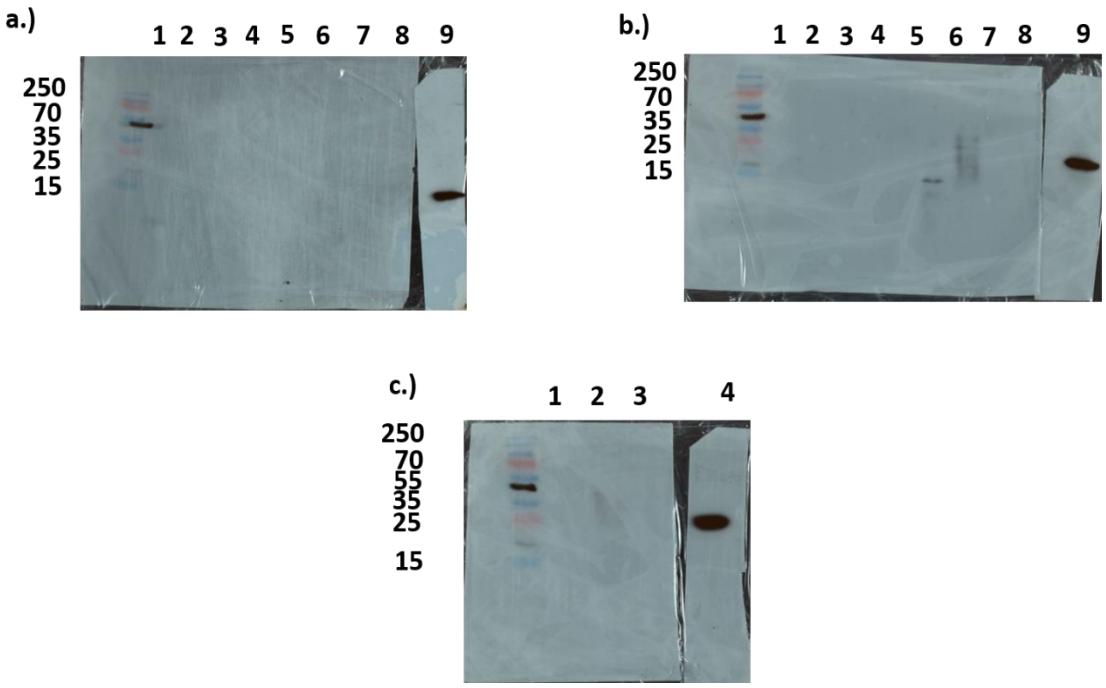


Figure 2.13 Western blot of the negative control Nosema purified monoclonal D095 to evaluate cross reactivity to a range of fungal antigens. a.) 1; F.g, 2; 107, 3; 107s, 4; 95, 5; 95s, 6; 97, 7; 97s, 8; 98, 9; positive control. b.) 1; 322, 2; 325, 3; Yel, 4; Brown, 5; Sep, 6; T.ros, 7; 655, 8; 1794, 9; positive control. c.) 1; 1968, 2; 2726, 3; 3805, 4; positive control. All positive controls were tail bleed.

2.3.2.7 Immunofluorescence assay

In a crude immunoassay the monoclonal antibody from 29.G7.A9 showed specific binding identified by a green fluorescent signal with F. *graminearum* spores, as indicted by the red arrows in Figure 2.14. This fluorescence was not observed when using negative control Nosema antibody DO95 or with just PBS (data not shown).

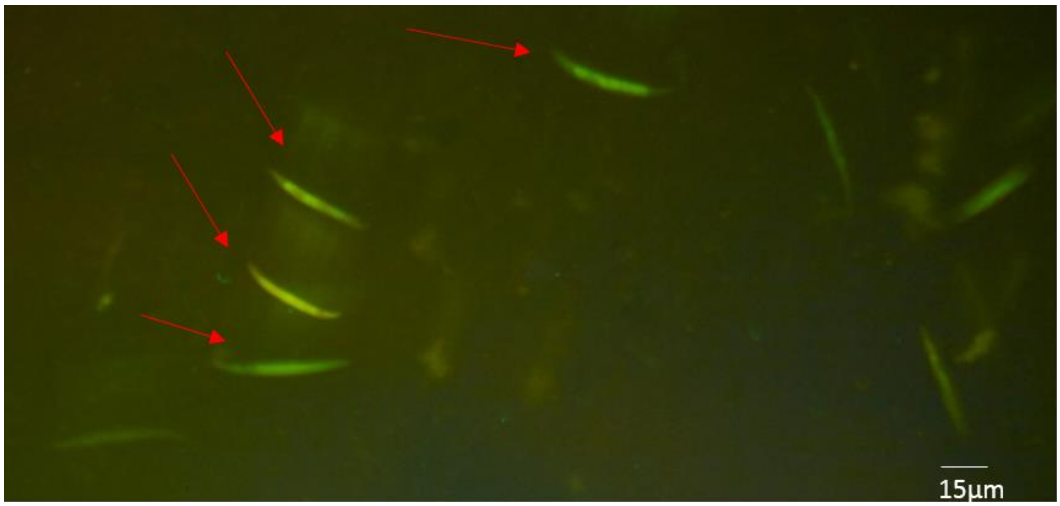


Figure 2.14 Detection of *F. graminearum* spores in an immunofluorescence assay with monoclonal antibody from cell line 29.G7.A9. Red arrows indicate the spores.

2.4 Discussion

In this chapter a monoclonal antibody has been generated for the detection *of F. graminearum.* This monoclonal was shown to be specific to *F. graminearum,* not cross reacting with other pathogens except *T. roseum.* However the negative control antibody DO95 raised to the honey bee pathogen *Nosema apis* also showed reactivity towards *T. roseum* and this may be indicating a property of the antigen, perhaps binding IgG antibodies in a non-specific fashion. In addition on the PVDF membrane the pigmentation from the extracted *T. roseum* could be seen, indicating potential overloading of the proteins onto the gel or presence of contaminating compounds which may exacerbate the cross reaction with IgG antibodies. The reaction towards *T. roseum* may be due to the pathogens ability to produce mycotoxins such as rosetoxins which have obvious similarities to the properties of *F. graminearum*. Further tests using epitope mapping by mass spectrometry to identify the antigen would have to be carried out to ascertain if this was truly a cross reaction (Yu et al., 1998). Although a plant pathogen, *T. roseum* does not infect wheat; therefore, the antibodies if they do cross react could still be used for diagnosing *F. graminearum* in known diseased samples of wheat.

Although western blotting gives clear negative and positive results with the facility to show sizes of proteins, ELISA could have been used. Several other labs were able to adhere spores to the ELISA plate surface (Banks et al., 1996, Skottrup et al., 2007a), however it proved unsuccessful for this work. Several attempts were made to adhere spores to the surface of ELISA plates, changing plate surfaces and using different pH buffers to help with binding. However, a repeatable reliable method was unfortunately not established. This could have cut down screening time and tests could have been carried out to see if the antigen protein was continuous or discontinuous and therefore if the antibody was able to recognise it in its native structure without extraction. This could for example be the reason why the hybrids for *P. triticina* were not showing a reaction as they had instead developed reactivity towards a protein that consisted of residues from different parts of the sequence, brought together by the folding of the protein to its native structure. This could have

been tested if the ELISA method was available. However, the immunofluorescent assay results are an indication that the antibody that was developed for *F. graminearum* was able to bind to the protein in its native form, showing that there is not a need for an extraction procedure when using this antibody. If time had permitted further immunofluorescent study with spores from other fungi would have been undertaken to demonstrate the specific nature of the antibody.

Unfortunately, the recombinant protein that was produced for *P. triticina* spores was unable to be used due to ethics approval not being granted as previously explained. However, had this been used for immunisation, screening may have been reduced and a more in depth analysis of epitopes could have been carried out. Also by knowing the exact protein that is being detected, competitive binding assays could have been developed later on to ascertain the analyte concentration present in the sample (Darain et al., 2003). However by not knowing the exact protein an enzyme-conjugated analyte cannot currently be produced.

Although concentrations of spores were counted before extraction and BCA methods were used to quantify protein in all cross reactivity samples, the amount of protein present after extraction could have been variable. Although this was analysed by staining gels using Coomasie and protein was found to be present in all samples the concentration of protein may not have been exact after extraction. This makes the level of detection difficult to ascertain using western blot analysis and again ELISA based methods without the need for extraction could have been more accurate when it came to cross reactivity analysis.

The monoclonal antibody produced within this work will go forward to be used as a bio-receptor component of an immunosensor in a later chapter. The recombinant protein that was shown to have good expression could also now be purified and used for antibody development now that it is confirmed that the mice immunised with *P. triticina* spores were unsuccessful in producing a suitable cell line.

Chapter 3 Amperometric detection of Fusarium graminearum spores via an immunosensor using screen printed electrodes.

3.1 Introduction

Immunoassays are extensively used for the detection of target analytes using highly specific antibodies which have been raised to detect specific antigens. Enzyme Linked Immunosorbent Assays (ELISA) is the method which is employed the most and a number of immunosensors have been developed incorporating the classic ELISA format with amperometric, photometric and chromatographic detection methods (Giesen et al., 2010, Fei et al., 2016, Matsuda et al., 2015).

Amperometric immunosensors rely on measuring electrochemically active products which are produced via redox-enzymes. These enzymes are usually conjugated to either the antigen or antibody and substances are either consumed or released when a specific binding event has occurred causing an electric current signal to be amplified (Darain et al., 2003).

Horseradish peroxidase (HRP) is widely used as the enzyme of choice in most studies and has been used in various amperometric immunosensors developed to detect plant pathogens. Zhao et al. (2014) used it successfully in an electrochemical sandwich immunosensor for the detection of *Pantoea stewartii* subsp. *stewartii*-NCPPB 449 (PSS). Jiao et al. (2000) also used HRP when developing an immunosensor for the detection of *Cucumber mosaic virus* (CMV) and found that using the immunosensor improved the limit of detection of the CMV by 5-fold when compared to traditional ELISA/spectrophotometric detection. The enzyme was also used by Fernández-Baldo et al. (2010) for the detection of *B. cinerea* using a competitive immunoassay. The study used micro magnetic beads (MMBs) with carbon-based screen-printed electrodes (SPCEs) for the quantification of *B. cinerea* in apple, grape and pear tissues managing to produce a rapid detection method (40 min).

The most commonly used chromogen for HRP is 3,3',5,5'-Tetramethylbenzidine (TMB) in the presence of H_2O_2. It has been extensively used in ELISA kits and comparative studies have been carried out to evaluate its use in immunoassays (Volpe et al., 1998, Fanjul-Bolado et al., 2005). A stop solution is also usually used

(H_2SO_4) to stop the reaction and convert the TMB solution into its electrochemically active form (yellow) (Mistry et al., 2016).

During this reaction, the TMB is oxidized in two steps from TMB (colourless) to TMB(ox1) (blue) to TMB(ox2) (yellow) (Figure 3.1). Both products, TMB (ox1) and TMB (ox2), can be detected via amperometric detection due to the electron transfers or by spectrophotometric detection (λmax = 650 nm (blue), λmax = 450 nm (yellow)) (Lee et al., 2012).

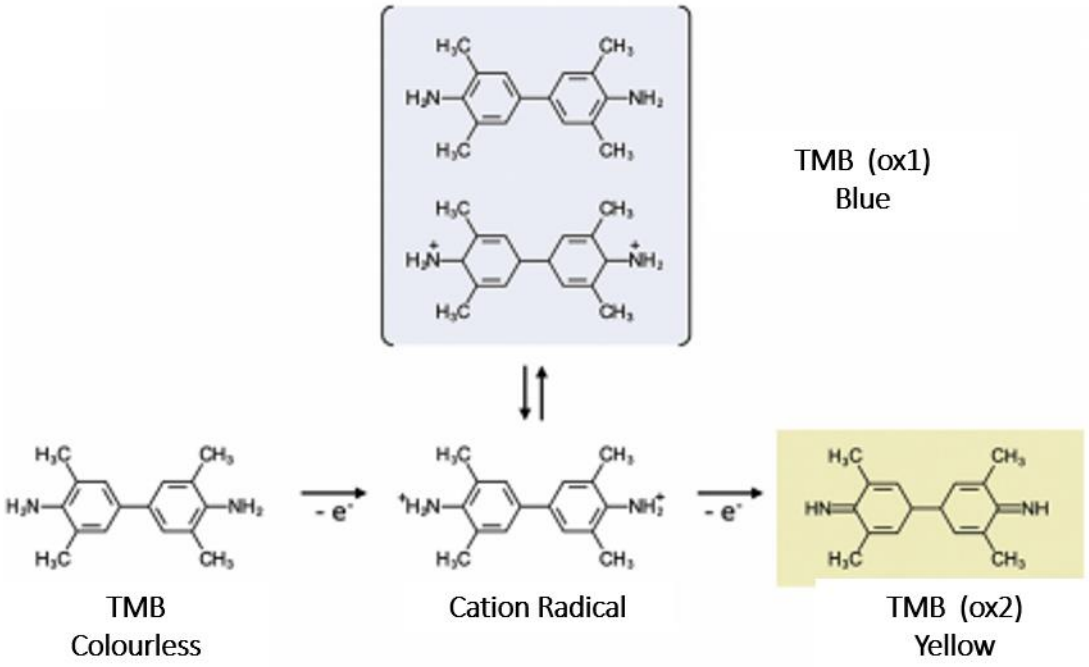


Figure 3.1 Redox cycling for the quantification of oxidised TMB adapted from Lee et al. (2017).

Of late, numerous immunosensors have been developed using screen-printed electrodes (SPEs) (Parkash et al., 2014, Darain et al., 2003, Rastogi et al., 2009, Mistry et al., 2016). SPEs have many advantages over other systems as they are reliable, simple and portable allowing for on-site detection and can be mass produced cheaply making them commercially attractive.

In Chapter 2, the monoclonal antibody 29.G7.A9 was developed and shown to be specific to *Fusarium graminearum* spores. This chapter details studies aiming to

incorporate this antibody into a hand held immunosensor system for onsite detection of *Fusarium graminearum* spores using SPEs and the HRP/TMB detection system.

3.2 Methodology

3.2.1 Immunoreagents for assays

American Foul Brood (AFB) mouse antibody and Potato Virus Y (PVY) rabbit antibody were both developed at FERA Science Ltd. and donated from their stocks. The American Foul Brood antigen sample was also from stocks at FERA Science Ltd and *Fusarium graminearum* spores were used from those collected in Chapter 2.

3.2.1.1 The Positive control assay

The positive control consisted of American Foul Brood (AFB) mouse antibody, with a rabbit anti-mouse conjugated HRP antibody (Figure 3.2a).

3.2.1.2 The Negative control assay

The negative control consisted of Potato Virus Y (PVY) rabbit antibody, with a rabbit anti-mouse conjugated HRP antibody (Figure 3.2a).

3.2.1.3 The AFB antigen assay (positive control)

American Foul Brood antigen with the AFB mouse antibody, with a rabbit anti-mouse conjugated HRP antibody (Figure 3.2b).

3.2.1.4 The 29.G7.A9 assay (Fusarium graminearum)

Fusarium graminearum spores ($5x10^5$ spores ml^{-1}) with the 29.G7.A9 mouse antibody, with a rabbit anti-mouse conjugated HRP antibody (Figure 3.2b).

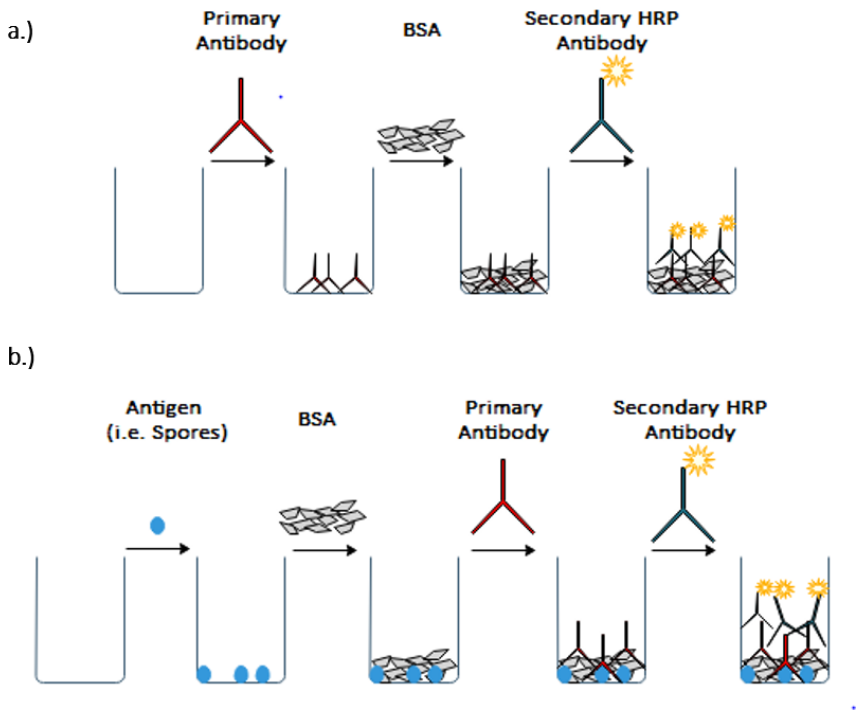


Figure 3.2 Immunoassays with immunoreagents used for ELISA and the immunosensor. a.) Assay developed for positive and negative controls b.) Assay developed for the detection of AFB and *Fusarium graminearum* spores.

3.2.2 ELISA – secondary antibody optimisation

Plates were either coated with primary antibody (PYV or AFB) (1/4000) or with AFB antigen (1/10) in coating buffer (15 nM Na_2CO_3, 35 mM $NaHCO_3$, pH 9.6), 200 µl per well and incubated at 4°C overnight. Plates were then washed 3 times with PBST (20 mM sodium phosphate, 150 mM sodium chloride pH 7.4) and blocked by adding 200 µl of blocking buffer (PBST containing 1 % BSA) to each well. Plates were then incubated at 33°C for 1 h. Plates were then washed 3 times as before. The secondary antibody (100 µl) was then applied (Rabbit anti-mouse HRP) at varying concentrations ranging from 1/4000- 1/6400 in dilution buffer (PBST containing 0.2 % BSA) (except in the case of AFB which first had the primary AFB antibody applied 1/4000 like the other samples and then the secondary antibody). The plates were incubated at 33°C for 1 h and then washed prior to the addition of 100 µl 3,3',5,5'-Tetramethylbenzidine (TMB) + H_2O_2 solution (1:1) (Fisher Scientific). Plates were then left for 5 min and 100 µl of stop solution (2 M H_2SO_4) was added before the colour change was determined by spectrophotometry at 450 nm in a Thermomax Microplate reader with SOFT Max Pro software.

3.2.3 Immunosensor apparatus

Cyclic voltammetry and amperometric detection was carried out using a hand held PalmSense 2 (Palm Instruments, Houten, the Netherlands). PalmSense software was also used on a Lenovo laptop to capture results. Surface printed electrodes (SPE) consisted of a working electrode made from carbon graphite paste and a reference electrode from Ag/AgCL with a 2 mm working electrode surface area (Alvatek Ltd, Gloucestershire).

3.2.4 Characterisation of the Working Electrode

Cyclic voltammetry (CV) analysis was used to characterise the working electrode surface and understand the system before immunosensor assays were carried out. Fifty microlitres of 1 mM $Fe(CN)_6^{3-}$ in PBS (pH 7, 0.1 M KCl) was pipetted onto the SPE. The electrochemical behaviour of ferricyanide (1 mM) on the SPE was studied by varying the scan rate, 0.01 V s^{-1}, 0.05 V s^{-1}, 0.1 V s^{-1}, 0.2 V s^{-1} and 0.5 V s^{-1} with a sweep potential of -0.5 V to 1 V.

3.2.5 Immunosensor assays

The assays were carried out the same way as the ELISA except only 25 µl of each solution was used at every step. Each component was pipetted onto the working electrode and washing was performed by pipetting 30 µl of PBS up and down to flood the working electrode surface. Each component was left to adhere for 10 mins on the working electrode, until dry, before washing steps then took place. Forty microlitres of TMB + H_2O_2 solution (1:1) was added for detection followed by 40 µl of stop solution (2 M H_2SO_4), these were applied to the whole SPE so all electrodes were covered. Amperometric detection was carried out at a scan rate of 0.5 V s^{-1} with a sweep potential of -0.5 V to 1 V.

3.2.6 Data Analysis

Experiments were performed in triplicate and the average used. Analysis of all data including performing T tests and linear regressions were carried out using Prism 7.

3.3 Results

3.3.1 ELISA – secondary antibody optimisation

A preliminary ELISA was carried out to ascertain the appropriate concentrations of secondary (conjugate HRP) antibody that was needed (Figure 3.3). The primary antibodies for all samples used were adjusted to a concentration of 1/4000. This was already shown to be effective when using western blotting for the *Fusarium graminearum* spores as reported in Chapter 1 when an ELISA could not be carried out as the spores were unable to adhere to the plate and therefore was omitted from this initial ELISA. From looking at the results in Figure 3.3 a secondary antibody concentration of 1/8000 was selected where the negative control had a very low OD_{450} and both the AFB antigen assay and positive control assay had similar high OD_{450}. After this concentration, OD_{450} values for both the AFB antigen assay and the positive control assay decreased.

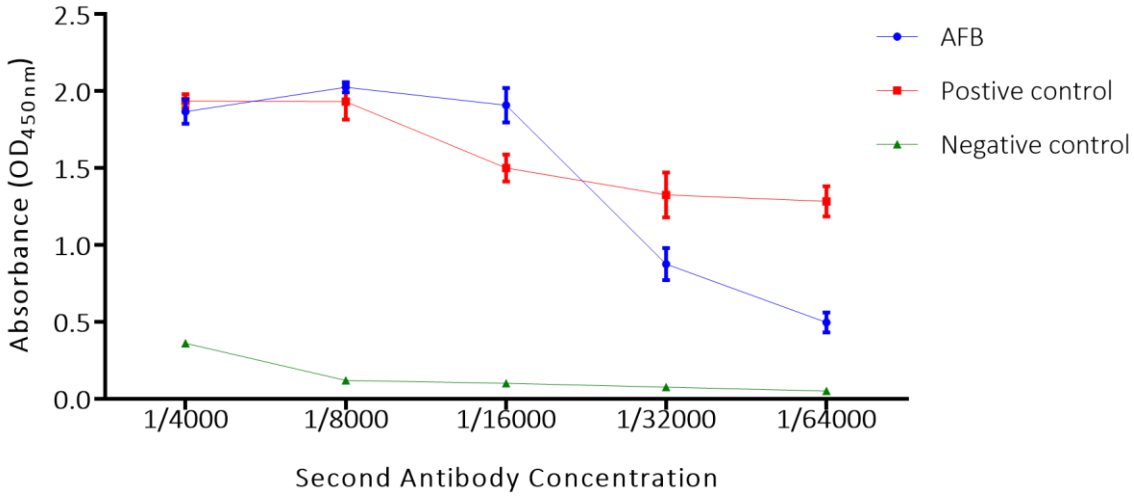


Figure 3.3 ELISA results showing the optimisation of secondary antibody (HRP) for both the negative and positive controls and the AFB antigen assay

3.3.2 Characterisation of the Working Electrode

Cyclic voltammetry (CV) analysis was used to characterise the working electrode surface using cyclic voltammograms of 1 mM $Fe(CN)_6^{3-}$ in PBS (pH 7, 0.1 M KCl). The electrochemical behaviour of ferricyanide (1 mM) on the SPE was studied by varying the scan rate 0.01 V s^{-1}, 0.05 V s^{-1}, 0.1 V s^{-1}, 0.2 V s^{-1} and 0.5 V s^{-1}. Figure 3.4 shows

that the working electrode performs well with peak to peak separation ($\Delta E_p = E_{pa} - E_{pc}$) and at 0.01 V s^{-1} was found to be 0.18 V, which indicates that the electrochemical reaction is quasi-reversible as the $\Delta E_p > 0.0592$ V. The oxidation/reduction peaks were more defined when lower scan rates were used.

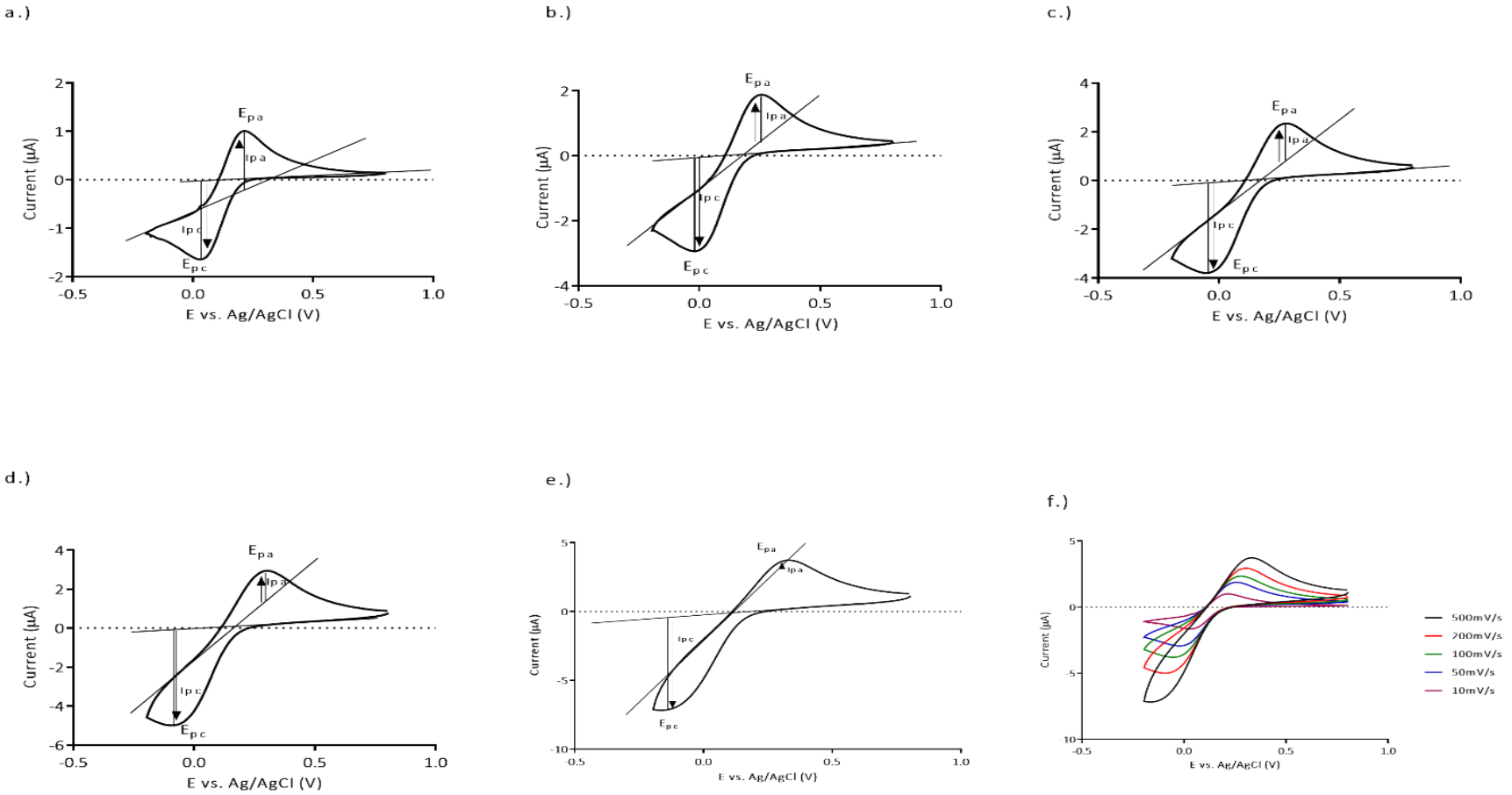


Figure 3.4 The electrochemical behaviour of ferricyanide (1 mM) on the SPE when varying the scan rate. a.) 0.01 V s^{-1}. b.) 0.05 V s^{-1} c.) 0.1 V s^{-1}. d.) 0.2 V s^{-1} e.) 0.5 V s^{-1}. f.) All scan rates.

3.3.3 The HRP/TMB detection system

HRP catalyses the TMB reaction from TMB to TMB (ox1). This enzymatic reaction can be detected by amperometric detection of the reduction in current generated by TMB (ox1) at the working electrode. Figure 3.5 shows the voltammogram of TMB with H_20_2 in the presence of HRP (indicated in red) in the potential range of -0.35 V to 1 V. Two electron redox behaviours were observed with oxidation peaks at 0.2 V and 0.35 V. This is the expected voltammogram profile for this reaction, showing the formation of radical cation intermediates during the electrochemical oxidation (Volpe et al., 1998). When the stop solution H_2SO_4 was added (indicated in green, Figure 3.5) to the reaction, a peak was seen at 0.45 V. This again is typical of this reaction and has been observed by others such as Lee et al. (2012) and Fanjul-Bolado et al. (2005). The oxidation of TMB by HRP produces a blue product, TMB (ox1), which turns yellow after the addition of H_2SO_4 to form the two electron oxidation product (diamine), TMB (ox2). This change in colour was not only observed in ELISA experiments carried out in this study but also on the SPE during these experiments (Figure 3.6).

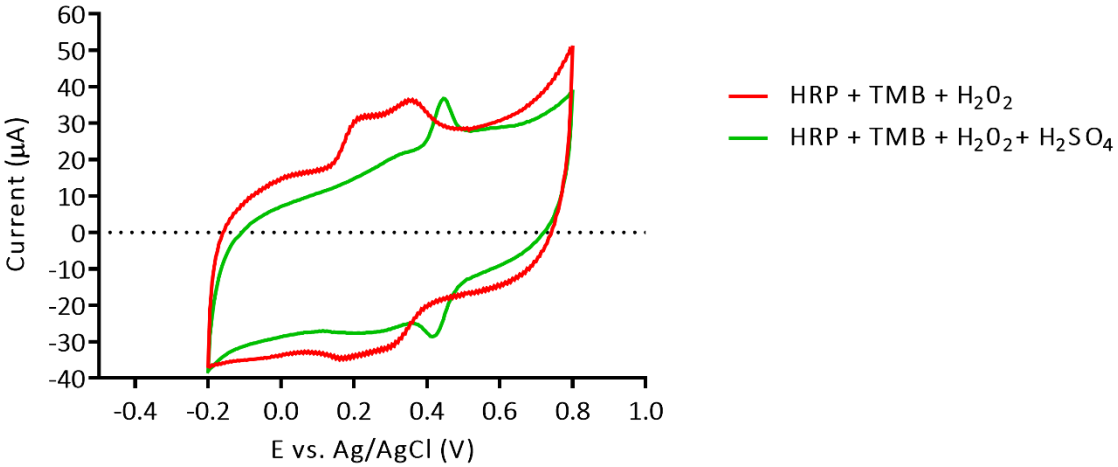


Figure 3.5 A voltammogram of TMB with H_20_2 in the presence of HRP with and without stop solution (H_2SO_4) in the potential range of -0.35 V to 1 V.

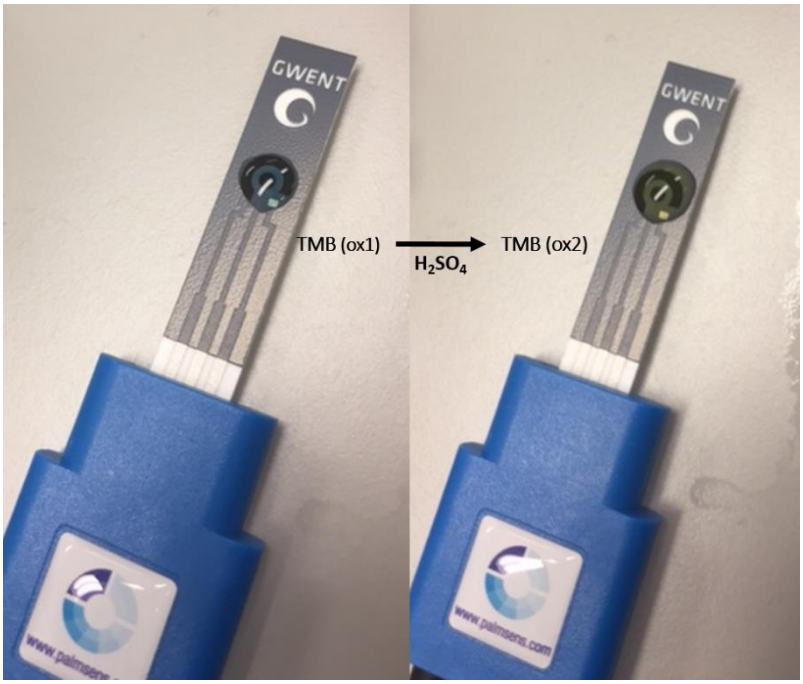


Figure 3.6 The colour change (blue to yellow) and oxidation of TMB (ox1) to TMB (ox2) on the SPE when the stop solution (H_2SO_4) is added.

3.3.4 Main assay experiment

Two electron redox behaviours were observed for all samples with oxidation peaks at approximately 0.25 V and 0.45 V which is typical of TMB (Figure 3.7). A decrease in oxidation potential of the AFB antigen assay, positive control assay and by the 29.G7.A9 assay compared to the negative control was observed. This would suggest that the sensor is able to differentiate between the positive and negative ELISA reactions. As stated previously the addition of HRP to the TMB substrate solution results in the conversion of TMB to TMB (ox1). Therefore a decrease in the oxidation potential and current is seen with the addition of HRP (Rastogi et al., 2009, Volpe et al., 1998). If the HRP conjugated secondary antibody has bound to the primary antibody and there is a positive sample then the TMB is then oxidised and this decrease in the oxidation potential and current is the result (Figure 3.7).

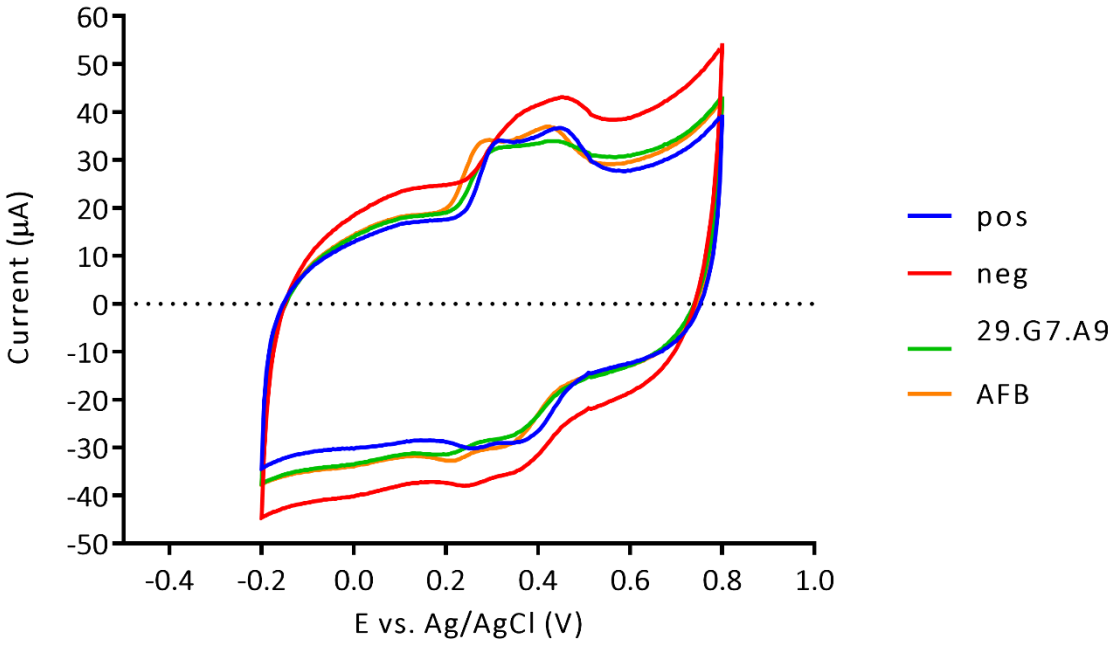


Figure 3.7 A voltammogram of the negative control assay, positive control assay, AFB antigen assay and 29.G7.A9 assay without stop solution (H_2SO_4) in the potential range of -0.35 V to 1 V.

The decrease in the oxidation potential and current of the positive samples compared to that of the negative sample was also observed with the addition of H_2SO_4 with a clear peak seen at 0.52 V (Figure 3.8a). Figure 3.8b shows the peak current for all the samples. There is a significant difference between the AFB antigen assay and 29.G7.A9 assay compared to that of the negative control assay (P= 0.004 and P=0.0035 respectively). Although not significantly different (P=0.0710), the positive control assay showed a reduction in peak current compared to that of the negative control assay but was not as low as the AFB and 29.G7.A9 assays.

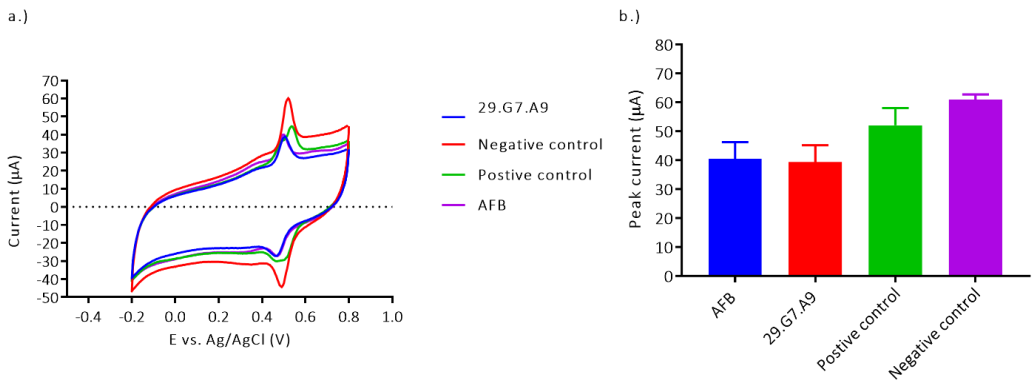


Figure 3.8 a.) A voltammogram of the negative control assay, positive control assay, AFB antigen assay and 29.G7.A9 assay with stop solution (H_2SO_4) in the potential range of -0.35 V to 1 V. b.) A comparison of the peak currents (µA) observed by all the aforementioned assays with stop solution (H_2SO_4) in the potential range of --0.35 V to 1 V.

3.3.4.1 ELISA vs Peak currents

Although a correlation was observed between peak currents and the OD_{450} readings of the corresponding ELISA sample, this was not a strong correlation (Figure 3.9). More samples would be required to ascertain if there was a direct correlation between these two measurements but the two cluster of samples in Figure 3.9 suggests that there is.

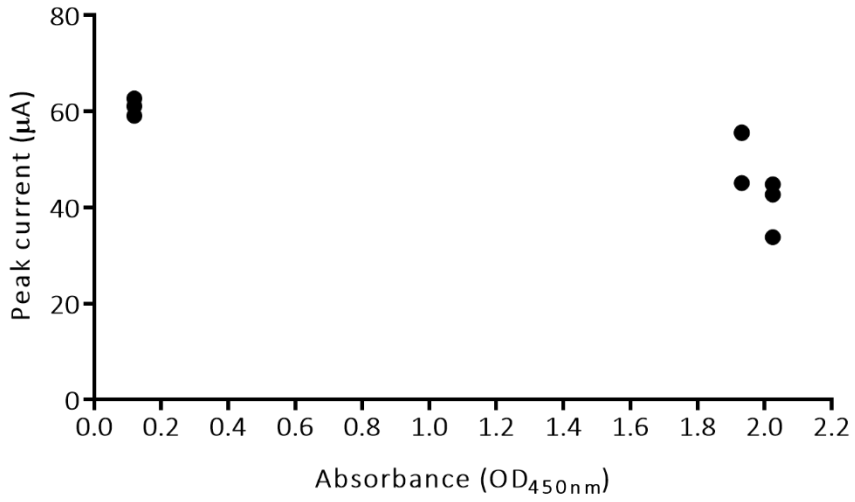


Figure 3.9 The correlation of the ELISA absorbance (OD_{450} nm) readings and the peak current (µA) of the negative control assay, positive control assay, AFB antigen assay when stop solution was added (H_2SO_4).

3.4 Discussion

This study provides early results for a potentially effective, simple approach for the detection of *Fusarium graminearum* spores using an amperometric immunosensor based on SPEs. Differences in peak current were observed between positive and negative control assays, however, as mentioned previously, the positive control assay although showing a reduction in peak current compared to that of the negative assay, was not as low as the AFB antigen and 29.G7.A9 assays. The same was observed when looking at the OD_{450} readings for the same samples via ELISA suggesting that the ELISA needs to be optimised further before application on the SPE. Another reason for this may be due to the SPE having more modification with the AFB antigen and 29.G7.A9 assays, with more immunoreagents needed, compared to that of the positive control assay. This has been shown to have an effect on the peak current with a decrease in peak current occurring when SPEs have more immunoreagents immobilised on them (Parkash et al., 2014). Visualisation of SPEs via scanning electron microscopy (SEM) would provide additional evidence of the immobilisation of certain immunoreagents and could help to confirm this. However, in order to enhance its performance and make this immunosensor system more robust and reliable, future experiments are needed to investigate the optimisation of various parameters of the assay such as: optimum concentration of the antibodies, the sensitivity of the assay (antigen concentration), washing frequencies and incubation times.

This amperometric immunosensor system proposed in this study has the potential to be used out of the lab in a field-based setting operated by non-specialists. LAMP could also be used for in field detection as it only requires isothermic conditions (60-65°C) for nucleic acid amplification. However LAMP requires a form of extraction process before samples can be analysed, unlike the amperometric immunosensor system in this study where the antigen is directly immobilised on the bare WE surface without the need for surface modification of the SPE. Samples from the field could potentially be used directly on the SPE. The system is rapid with less than an hour needed to produce quantifiable results. It is also portable and so has the potential to be used onsite as part of a mobile detection kit with the immunoassay components stored in a cool box. The low cost of the SPEs (less than £5 each), means it is feasible

for multiple SPEs to be prepared with differing detection antibodies in order to detect a range of spores present in a sample from a spore trap. This allows for more flexibility with testing requirements and shows advantages over Lateral flow devices (LFDs) as they are usually only manufactured with one antibody and therefore not for high-throughput screening. Although interpretation of results at this time requires specialist knowledge, with optimisation of experiments a definitive threshold of peak current for a positive sample could be established.

Chapter 4 The isolation and analysis of distribution of Zymoseptoria tritici CYP51 variants in order to give insight into future sampling and potential targets for detection

4.1 Introduction

Septoria tritici blotch, caused by the fungus *Zymoseptoria tritici* (previously *Mycosphaerella graminicola* (Quaedvlieg et al., 2011)), is a major foliar disease of wheat *(Triticum aestivum)* in Europe and was recently identified as the most yield-reducing disease in European countries with intensive wheat production (Jørgensen et al., 2014). Mild winter temperatures combined with high rainfall provides the optimum conditions for rapid spread and development of the disease. While resistance of wheat cultivars to *Z. tritici* has increased over the last two decades (Brown et al., 2015), the control of the disease is still heavily reliant on fungicides. With severe epidemics of *Z. tritici* causing losses of up to 50% of yields, approximately 70% of all annual fungicide usage in the EU is attributed to its control (Fones and Gurr, 2015).

Systemic fungicides, such as the methyl benzimidazole carbamates (MBCs), strobilurins (QoIs) and sterol demethylation inhibitors (DMIs) have dominated the cereal fungicide market for the past 50 years due to their efficacy and ease in application. *Z. tritici* populations have, however, quickly overcome and adapted to these fungicides. MBC resistance has now been reported in over 90 plant pathogens in the field (Hawkins and Fraaije, 2016). This is usually attributed to a mutation in the beta-tubulin target which first emerged in the mid 1980's. Resistance to the quinone outside inhibitors (QoIs; strobilurins) was first reported in 2002, due to a mutation in the mitochondrial cytochrome *b* target (Hawkins and Fraaije, 2016). This is now widespread in *Z. tritici* populations in Western Europe, consequentially QoIs are no longer recommended for *Z. tritici* control.

DMIs, mostly consisting of the azoles (triazole and imidazole), inhibit fungal growth by interfering with the biosynthesis of ergosterol, the predominant sterol in fungal membranes by the interaction of the azole ring with the heme iron of the cytochrome *P450* sterol 14α-demethylase (*CYP51*)(Cools et al., 2010).

Erosion of azole efficacy has been recorded, with higher doses now being required to achieve effective disease control. Three major mechanisms of resistance to DMIs have been reported (Cools and Fraaije, 2013):

- Mutations in the *CYP51* azole target protein resulting in decreased affinity to fungicide.
- Over-expression of the target *CYP51* gene most frequently caused by insertions in the promoter regions.
- Enhanced active azole efflux caused by the over-expression of genes encoding membrane transporters.

The use of Succinate Dehydrogenase Inhibitor fungicides (SDHI) has increased since 2010, however the Fungicide Resistance Action Group UK (FRAG-UK)considers that the SDHI fungicides are at a medium/high risk of resistance development in cereal pathogens ;;;;;;(FRAG-UK,2016). This could potentially be a problem for the UK as in 2015, Teagasc found isolates of *Z. tritici* in the Republic of Ireland with reduced sensitivity to the SDHI group of fungicides (Teagasc, 2017). Some of these isolates had a mutation (C-H152R) in the SDHI target site that had not previously been detected in field isolates. In 2016 a *Z. tritici* isolate was detected in the UK which showed resistance to a full dose of SDHI, and this also carried the same mutation (C-H152R)(FRAG-UK, 2016).

As resistance towards SDHIs continues, it can be surmised that the importance of DMIs will remain high in the future. The past 10–15 years has seen an increasing number of mutations emerging in the *CYP51* protein (Cools and Fraaije, 2013). These mutations and deletions occur in combinations, creating diverse *CYP51* variants with different mutation profiles which impact on particular DMIs in various ways (Wieczorek et al., 2015). The more recent *Z. tritici CYP51* variants have up to eight amino acid alterations compared to the wild type (Cools and Fraaije, 2013).

It is estimated that it takes $256 million and nine years of research and development to bring a new active ingredient to market (ECPA, 2013). It is therefore important to survey the rapidly evolving populations of field *Z. tritici* isolates in order to better understand the distribution and number of *Z. tritici CYP51* variants. Using this

knowledge and that derived from literature to ascertain those isolates which are the most prevalent and resistant to azoles, detection methods for identified potential key target isolates can be developed.

The aim of this research was to:

- Isolate a collection of *Z. tritici* strains from infected leaves, derived from the UK.
- Analyse the collection for *CYP51* variants.
- Analyse the number and distribution of these variants between geographical locations in order to produce a suggested sampling plan for effective detection in a total *Z. tritici* population.
- Identify potential key *CYP51* components that are present in *Z. tritici* variants that are of concern for azole resistance.

4.2 Methods

4.2.1 Sampling protocol

Three fields on three farms (Dorset: located in Salisbury, Sutton Court Farm (SCF): located in Ludlow and Thompson: located in Louth) were included in this study. Each farm was selected as it had 3 adjacent fields to sample of the same wheat variety. Sampling was carried out in April 2015 when wheat were at growth stage 31-33 (Fungicide Timing 1 (T1)). Samples were collected by staff at Agrii under the guidance of Francesca Salinari (R&D Projects Co-ordinator at Agrii). Two different types of sampling were carried out: 'normal' and 'intensive'. The 'normal' sampling consisted of taking 3 plants from 20 locations per field in a 'W' pattern to give good coverage across the whole of the field. The 'intense' sampling consisted of taking 60 plants at diagonal-opposite corners of the field i.e. two corner-points. Personnel were told to choose plants that appeared to be infected with *Z. tritici*.

To ensure that there is no statistical bias on the results, samples were tested in a randomised order. Each sample was given a 'SEPT' number to uniquely identify the sample through the culturing/analysis stages of the study.

4.2.2 Culturing *Zymoseptoria tritici* from leaf samples

Three samples were taken from each plant consisting of one from an inner leaf and two from outer leaves. Approximately 3 cm pieces of leaf were dissected and rehydrated in water for 1 minute. The diseased leaf sections were then put into 0.6% NaOCl solution (Fisher Chemical) for 30 seconds to surface sterilise the leaf and then rinsed in sterile distilled water and blotted with sterile filter paper to get rid of excess moisture. These were then placed onto a tap water agar plate (TWA) with the pycnidia uppermost and incubated for 48 hours at 17-20°C with a near UV light source. After incubation a single cirrus was picked off (1 from each leaf) using a sterile needle under a microscope and placed onto a PDA + 1% streptomycin plate. These were incubated for 5-7 days at 17-20°C with a near UV light source. After initial incubation, samples were sub-cultured a total of 3 times on PDA + 1% streptomycin and incubated under the same conditions as before to ensure a pure culture was achieved.

4.2.3 Storage of cultures for future use

Once a pure culture was obtained a 10 µl loop full of culture was added to 1 ml of 10% sterile Marvel Milk (autoclaved 30 mins at 115°C) in a 1.5 ml Eppendorf tube. This was then vortexed and stored at -20°C.

4.2.4 DNA extraction

Extraction of the DNA from the pure culture obtained was performed using a Qiagen QIAamp DNA mini blood kit. A 10 µl loop of culture (from the PDA plate) was re-suspended into 180 µl of ATL buffer and DNA was extracted using the manufacturer's protocol. DNA samples were stored at -20°C until needed.

4.2.5 PCR

Primers were adapted from those designed by Fraaije et al. (2011) for the *CYP51* gene so that they included certain SNPs at the end of the gene which were not previously recognised SNPs in the literature. The primers (ST51F1- 5' ATGGGTCTCCTCCAGGAACTCCTCC 3', ST51R3- 5' TTGTGAAAGCAGCGTCTCCCTC 3') wereused for PCR (Table 4.1). The following cycling conditions were used: 98°C for 30 seconds followed by 35 cycles of 98°C for 10 seconds, 68°C for 20 seconds and 72°C for 1 min and a final extension step of 72°C for 10 min. PCR products were

separated on 1.2 % agarose gels in TBE (90 mM Tris/borate/EDTA) buffer containing a final concentration of 0.2µg/mL ethidium bromide and visualized under UV light.

Table 4.1 Components used for the PCR reaction to amplify the CYP51 gene of *Zymoseptoria tritici*

Component	50 µl reaction	Final concentration
5X Phusion HF buffer	10 µl	1X
10 mM dNTPs	1 µl	200 µM
10 µM Forward Primer (ST51F1)	2.5 µl	0.5 µM
10 µM Reverse Primer (ST51R3)	2.5 µl	0.5 µM
DMSO	1.5 µl	3%
Phusion Hot Start Flex DNA Polymerase (Biolabs)	0.5 µl	1.0 units/50 µl PCR
Nuclease-free water	31 µl	
Template DNA	1 µl	

4.2.6 Sequencing and analysis

Sequencing primers were designed using Primer3 software (Version 0.4.0) (SF- 5' GCGCAGTTCGACGCGCAATT 3', F3- 5' GCGGACCTCTACCACTACCTCGA 3', SR2- 5'CGCGCTATTCATTAGCATAACATCCACC 3') and DNA samples were sent off for sequencing to Eurofins MWG Operon (Ebersberg, Germany). Sequences were first checked and trimmed using ABI Sequencer Scanner and later aligned and analysed for SNPs using MEGA version 4 (Tamura et al., 2007).

4.2.7 Analysis of the *CYP51* promoter region

Analysis of the *CYP51* promotor region was carried out by amplifying the sections of DNA upstream from the start site of the *CYP51* gene. This was undertaken by Catherine Harrison at FERA Science Ltd. and results were provided for this study in order to look at the distribution of different insertions present in different variant types.

4.2.8 Statistical analysis

Prism 7 and SPSS Statistics were used to initially analyse the data and a chi-square test was used to associate actual frequencies of variants with geographic locations. Further analysis was carried out by Roy Macarthur a statistician at FERA Science Ltd. under the author's direction. A generalised linear mixed model (logistic response, fixed effect: farm, random effects: site nested within field, field nested within farm) was fitted to the proportion of each of the six most common types of *Z. tritici* (1, 2, 3, 4, 6 and 15). The estimated mean prevalence of each of these types was then

calculated. The parameters that describe the expected prevalence such as within-field and between field standard deviation was shown on a logistic transformed scale. The significance of the variation in prevalence of types between farms was assessed by comparing models with a 'farm' fixed effect to null 'intercept only' models. Similarly the significance of the variation in prevalence of types between fields was assessed by comparing models with a 'farm*field' fixed effects to models with farm only. The significance of within-field variation was assessed by comparing the prevalence of types at the two intensively sampled locations. This was done by comparing Bayesian posterior distributions for the proportion of each type at each of the two locations.

4.3 Results

4.3.1 Overall *Zymoseptoria tritici* collection

From the 1620 samples that were collected, isolates were recovered and successfully sequenced from 321 samples. Reasons for this include: some samples did not show evidence of *Z. tritici* and therefore were unlikely to have any present, culturing was unsuccessful (69% unsuccessful) (either over-grown with other organisms or no viable organisms growing), samples failed to show correct size band on gel (1.5% unsuccessful) or sequencing failed (10.1% unsuccessful). The *CYP51* gene (1907 bp) of each isolate was sequenced, three introns were then removed and the consensus sequences were screened for alterations compared to the wild-type (Figure 4.1a). Sixteen alterations at 13 positions throughout the protein were found; these also included a 6 bp deletion leading to the deletion of two amino-acids (ΔY459/G460). There were 24 different combinations of mutations (referred to as variant types throughout this chapter), found and no wild-type sequences were found (Table 4.2).

The most commonly observed alterations were L50S, I381V, V136A and S188N, found in 98%, 98%, 67% and 52% of the isolates respectively with the ΔY459/G460 occurring in 51% of the isolates. The least observed alterations were N284H, Y459D and I377V, all only present in 0.6% of the isolates. The greatest number of alterations seen in a single isolate was 10 as seen in variant Type 21 (Table 4.2).

In addition, 3 different size inserts were found in the collection following PCR amplification of the putative promoter region (Figure 4.1b). A total of 8 isolates had

the expected product size of 334 bp (depicted in this study as zero, i.e. no insert present), 69 isolates had the 120 bp insertion and 244 isolates had an insert of approximately 800 bp. Of the 6 variant types which were the most commonly found (Types 1,2,3,4,6,15), apart from in Type 2, the 800 bp insert was found to be the most common. Type 2 and type 14 both had the 120 bp insertion, though all the isolates of variant type 2 contained this insert (Table 4.3).

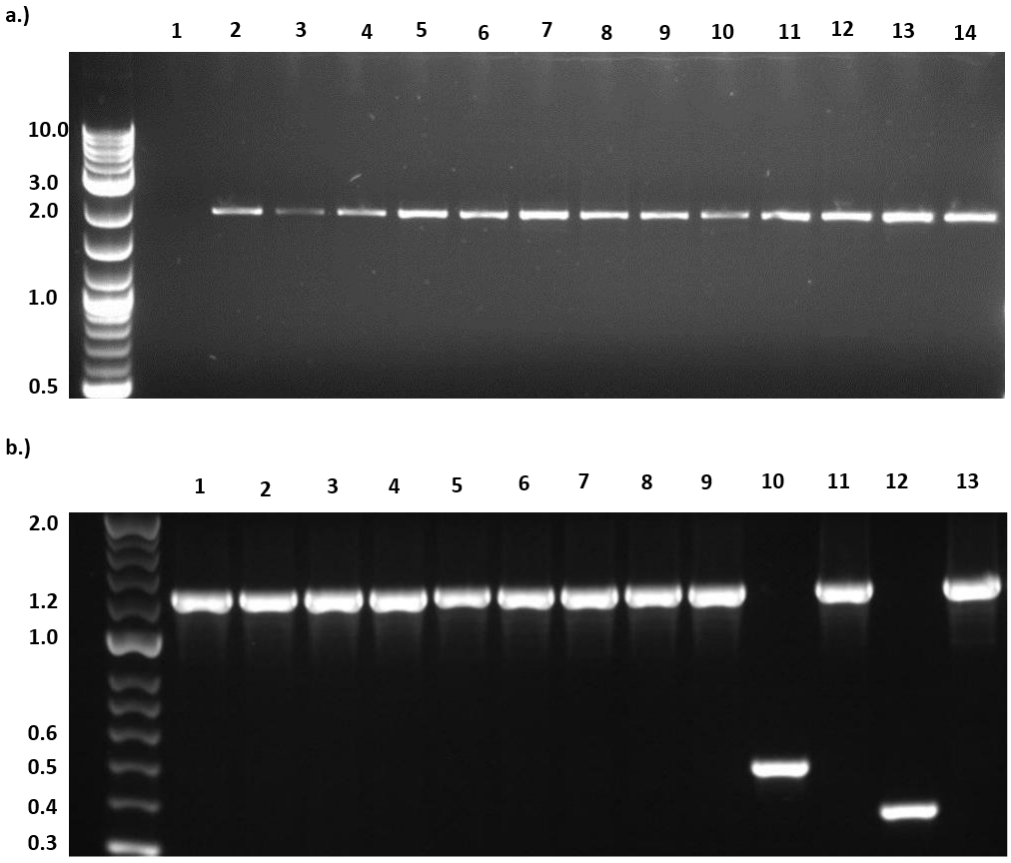


Figure 4.1 PCR amplification of target sequences for *Z. tritici*. a.) The CYP51 gene (1907bp), 1; negative control, 2-14; CYP51 gene target from extractions b.) The putative promoter region, 1-9,11,13; 800bp insertion, 10; 120 bp insertion, 12; no insertion (334 bp).

Table 4.2 The amino acid alterations corresponding to the different *CYP51* variants of *Z. tritici* found in this study

Variant Type	Amino acid alterations													Total
	50 - L	134 - D	136 - V	188 - S	284 - N	379 - A	381 - I	410 - A	459 - Y	460 - G	461 - Y	513 - N	524 - S	
1	S	G	A				V				H			109
2	S			N			V		-	-		K		68
3	S		A	N		G	V		-	-			T	56
4	S	G	A				V				H		T	13
5	S	G	A				V		-	-		K		1
6	S		A				V				H		T	20
7	S		A				V				S		T	1
8	S		A			G	V				S		T	1
9			C				V				H		T	6
10			A			G	V				S		T	1
11	S			N		G	V		-	-		K		6
12	S			N	H	G	V		-	-		K		2
13	S			N		G	V	T	-	-		K		2
14	S		A	N		G	V		-	-		K	T	3
15	S		C	N		G	V		-	-			T	14
16	S		C	N			V		-	-			T	1
17	S			N		G	V		D				T	2
18	S		A	N			V		-	-			T	4
19	S		A	N					-	-			T	5
20	S		A	N					-	-		K	T	1
21	S	G	A	N		G	V	T	-	-		K		1
22	S		C	N			V				H		T	1
23	S		C	N		G	V		-	-		K	T	1
24	S						V				H			2

Table 4.3 The insertions found in the *CYP51* putative promoter regions of *Z. tritici* found in this study

	Variant Type																								Total
Insertion	**1**	**2**	**3**	**4**	**5**	**6**	**7**	**8**	**9**	**10**	**11**	**12**	**13**	**14**	**15**	**16**	**17**	**18**	**19**	**20**	**21**	**22**	**23**	**24**	
0	2	0	0	1	0	1	0	1	1	1	0	1	0	0	0	0	0	0	0	0	0	0	0	0	8
120	0	68	0	0	0	0	0	0	0	0	0	0	0	1	0	0	0	0	0	0	0	0	0	0	69
800	107	0	56	12	1	19	1	0	5	0	6	1	2	2	14	1	2	4	5	1	1	1	1	2	244
Total	109	68	56	13	1	20	1	1	6	1	6	2	2	3	14	1	2	4	5	1	1	1	1	2	321

4.3.2 The geographical distribution of variant types

There were significant associations between the frequency of some variant types (1,2,3 and 15) and location (Table 4.4). Of the 24 types that were found in the whole sample, both SCR and Dorset were found to have the most diversity with 17 different types. Thompson however only had 9 different variant types present, although this may be due to the smaller sample size that was available from this farm. All three farms had different variant types that were the most prevalent. Of the 6 most common variant types found, variant Type 1 was most prevalent on SCF, almost double the numbers found on the other farms, variant Type 2 was most prevalent on Thompson with very low numbers appearing on the Dorset farm and variant Type 3 was found most on Dorset farm. Both Types 4 and 6 were found most frequently at SCF and although Type 15 was less prevalent at SCF and not found at all on the Thompson farm it was the fourth most prevalent on the Dorset farm. There were 7 variant types that were solely found on the Dorset farm, 6 from SCF and only 1 from the Thompson farm. However this again may be due to difference in sample size between the farms (Table 4.4).

Field to field variation was also observed across the three farms. Up to 12 different variant types were found in a single field (Dorset 3). Some variant types such as Type 1 were broadly similarly distributed between fields in the same farm however most variant types differed in their distribution (Table 4.5). A similar trend was observed for intense and normal sampling sites within a field with clustering of different types present in different locations and up to 9 different variant types found within an area of intense sampling (data not shown).

Table 4.4 The number of times variants were found on each farm location represented as percentage of location sample size

Variant Type	Overall frequency (n=321)	Farm			Chi-square	
		Dorset (n=122)	Sutton court Farm (n=168)	Thompson (n=31)	X^2	*P*
1	34.0%	23.8%	43.5%	22.6%	14.2	<0.001
2	21.2%	4.1%	28.6%	48.4%	40.6	<0.001
3	17.4%	39.3%	3.6%	6.5%	65.7	<0.001
4	4.0%	2.5%	5.4%	3.2%		
5	0.3%	0.0%	0.6%	0.0%		
6	6.2%	5.7%	7.1%	3.2%	0.8	0.681
7	0.3%	0.0%	0.6%	0.0%		
8	0.3%	0.0%	0.6%	0.0%		
9	1.9%	0.8%	1.8%	6.5%		
10	0.3%	0.8%	0.0%	0.0%		
11	1.9%	0.8%	2.4%	3.2%		
12	0.6%	0.0%	1.2%	0.0%		
13	0.6%	1.6%	0.0%	0.0%		
14	0.9%	0.8%	0.6%	3.2%		
15	4.4%	9.0%	1.8%	0.0%	10.4	0.005
16	0.3%	0.0%	0.0%	3.2%		
17	0.6%	1.6%	0.0%	0.0%		
18	1.2%	3.3%	0.0%	0.0%		
19	1.6%	2.5%	1.2%	0.0%		
20	0.3%	0.0%	0.6%	0.0%		
21	0.3%	0.0%	0.6%	0.0%		
22	0.3%	0.8%	0.0%	0.0%		
23	0.3%	0.8%	0.0%	0.0%		
24	0.6%	1.6%	0.0%	0.0%		

Table 4.5 The number of times the 6 most common overall variants were found in each field location represented as percentage of location sample size.

Variant Type	Overall frequency (n=321)	Field									Chi-square	
		Dorset 1 (n=43)	Dorset 2 (n=45)	Dorset 3 (n=34)	SCF 1 (n=59)	SCF 2 (n=51)	SCF 3 (n=58)	Thompson 1 (n=4)	Thompson 2 (n=21)	Thompson 3 (n=6)	X2	*P*
1	34.0%	20.9%	22.2%	29.4%	40.7%	43.1%	46.6%	25.0%	23.8%	16.7%	14.3	0.074
2	21.2%	2.3%	6.7%	2.9%	37.3%	23.5%	24.1%	75.0%	47.6%	33.3%	47.5	<0.001
3	17.4%	55.8%	33.3%	26.5%	3.4%	7.8%	0.0%	0.0%	4.8%	16.7%		
4	4.0%	2.3%	0.0%	5.9%	5.1%	0.0%	10.3%	0.0%	0.0%	16.7%		
6	6.2%	4.7%	4.4%	8.8%	5.1%	13.7%	3.4%	0.0%	4.8%	0.0%		
15	4.4%	7.0%	15.6%	2.9%	1.7%	3.9%	0.0%	0.0%	0.0%	0.0%		

4.3.3 Developing future detection sampling strategies

The data collected in this study makes it possible to plan for future detection sampling strategies. As clustering of different variant types of *Z. tritici* was observed, this study shows that it is advisable to take samples from different locations and to increase sample sizes.

A generalised linear mixed model was fitted to the proportion of each of the six most common types of *Z. tritici* (1, 2, 3, 4, 6 and 15). The estimated mean prevalence of each of these types was then calculated to account for the discrepancy between sample sizes. The parameters that describe the expected prevalence such as within-field and between field standard deviation was shown on the linear predictor (logistic transformed) scale. As shown previously in Table 4.4 there was a significant association of the variation in prevalence of Types 1, 2, 3 and 15 found between farms (Table 4.6). When looking at the mean prevalence there was also a significant association of Types 3 and 15 between certain fields and Types 1, 2 and 6 between certain intense sampling locations ($p = <0.025$) (data not shown).

Table 4.6 The mean prevalence of the 6 most common overall *Z. tritici* variant types represented as percentage of location sample size and the estimated parameters that describe the expected prevalence and variation of different variant types.

		Mean prevalence					Estimates on logistic scale			
Variant type	Farm	Estimate	Confidence Interval		'p' varies between farms	'p' varies between fields	Coefficient	Standard error	Between-field s.d.	Within-field s.d.
1	Dorset	23.6	16.1	33.3			-1.173	0.243		
	SCF	43.2	34.2	52.7	0.014	0.979	-0.274	0.195	0	0.33
	Thompson	22	10.3	40.9			-1.267	0.458		
2	Dorset	3.86	1.53	9.39			-3.214	0.483		
	SCF	28.5	20.8	37.6	<0.0001	0.476	-0.922	0.212	0	0.356
	Thompson	47.6	29.4	66.5			-0.096	0.398		
3	Dorset	38.3	25.2	53.4			-0.476	0.311		
	SCF	3.09	1.15	8.04	0.0017	0.0456	-3.446	0.515	0.306	0.483
	Thompson	5.87	1.27	23.2			-2.775	0.804		
4	Dorset	2.17	0.539	8.35			-3.806	0.72		
	SCF	4.52	1.55	12.4	0.7	0.293	-3.051	0.561	0.6	0
	Thompson	3.05	0.357	21.6			-3.459	1.108		
6	Dorset	4.76	1.88	11.6			-2.996	0.49		
	SCF	5.97	2.71	12.6	0.71	0.637	-2.756	0.42	0	0.636
	Thompson	2.65	0.326	18.5			-3.604	1.081		
15	Dorset	8.64	4.21	16.9			-2.359	0.391	0.287	0
	SCF	1.73	0.52	5.57	0.036	0.0236	-4.042	0.618		

This knowledge was then used to predict the limits of detection (95% probability of detection) for the presence of 'rare' types of *Z. tritici* where it is assumed that the variation between fields and between locations within fields is equal to the largest variation estimated for the six more common *Z. tritici* types. This is expressed as the percentage of proportion of a variant type in the population that gives a 95% probability of appearing in the sample. The example highlighted (yellow) in Table 4.7 shows that if 60 lesions in total are assessed, 2 each from each of 10 locations in each of 3 fields, then there is at least a 95% probability of including a lesion in the sample from a variant type that is present at a level of at least 6.1% in the population. Equally if a variant type in the sample of 60 lesions is not found then it may not be present in the population at all, and if it is present then it is only below levels of 6.1% in the population.

If this table is used as a basis for planning an effective detection sampling strategy this can therefore lead to help with planning treatment enabling a more targeted approach. Using the above example, if treatments were available that were known to be effective against just those variant types found in the sample of 60 lesions, then it can be assumed that the treatment is effective against at least 93.9% (100- 6.1%) of lesions in the population from which the sample was taken.

Table 4.7 Limits of detection (95% probability of detection) for the presence of *Z. tritici* variants when different sampling protocols are employed

Number of fields	Locations per field	Total number of lesions tested										
		40	50	60	70	80	90	100	120	150	200	300
1	1	15	13	11	10	8.6	7.8	7.1	6.1	5.0	3.8	2.7
	2	13	11	9.3	8.0	7.1	6.5	5.8	4.9	4.0	3.1	2.1
	5	12	10	8.2	7.2	6.2	5.7	5.2	4.3	3.5	2.7	1.9
	10	11	9.2	7.8	6.9	6.1	5.4	4.9	4.2	3.3	2.6	1.7
	20	11	9.3	7.7	6.8	6.0	5.3	4.8	4.1	3.3	2.5	1.7
2	1	13	11	9.5	8.3	7.3	6.5	5.9	5.1	4.1	3.1	2.2
	2	11	9.1	7.7	6.7	6.0	5.4	4.8	4.1	3.3	2.5	1.7
	5	9.9	8.1	6.8	5.8	5.2	4.6	4.3	3.5	2.8	2.2	1.5
	10	9.4	7.7	6.5	5.6	4.9	4.4	4.1	3.4	2.8	2.1	1.4
	20	9.3	7.6	6.3	5.4	4.8	4.3	3.9	3.3	2.6	2.0	1.3
3	1	13	11	8.9	7.8	7.0	6.3	5.7	4.7	3.9	2.9	2.0
	2	11	8.6	7.4	6.3	5.6	5.0	4.5	3.8	3.1	2.3	1.6
	5	9.2	7.5	6.3	5.5	4.8	4.3	3.9	3.3	2.6	2.0	1.3
	10	8.8	7.2	6.1	5.2	4.6	4.1	3.8	3.1	2.5	1.9	1.3
	20	8.6	7.0	5.8	5.1	4.5	3.9	3.6	3.1	2.5	1.9	1.3
4	1	12	10	8.6	7.5	6.8	6.0	5.4	4.6	3.7	2.9	2.0
	2	10	8.3	7.1	6.1	5.4	4.8	4.3	3.6	3.0	2.3	1.5
	5	8.8	7.2	6.2	5.4	4.6	4.2	3.8	3.1	2.6	1.9	1.3
	10	8.5	6.9	5.8	5.1	4.4	3.9	3.6	3.1	2.4	1.9	1.3
	20	8.3	6.7	5.7	4.9	4.3	3.9	3.5	2.9	2.3	1.8	1.3
5	1	12	10	8.5	7.4	6.5	6.0	5.4	4.5	3.7	2.8	1.9
	2	10	8.1	6.9	6.0	5.3	4.7	4.3	3.6	2.9	2.3	1.5
	5	8.7	7.1	6.0	5.2	4.6	4.1	3.6	3.1	2.5	1.9	1.3
	10	8.4	6.7	5.8	4.8	4.3	3.9	3.5	3.0	2.4	1.8	1.3
	20	8.2	6.6	5.6	4.8	4.2	3.8	3.4	2.8	2.3	1.8	1.2

4.4 Discussion

The *CYP51* protein of *Z. tritici* has rapidly evolved in recent years, with certain combinations of amino acid alterations and insertions in the promoter region causing loss of sensitivity towards azoles. In this study the *Z. tritici* population was very diverse with 16 amino acid alterations at 13 positions throughout the protein found, leading to 24 variant types found in total. As with recent studies, such as that carried out by Dooley (2015), no wildtype was found and only one variant type (Type 24) had less than 5 amino acid alterations, showing the collection to be highly evolved. Although all amino acid alterations were found cited in other literature (Cools and Fraaije, 2013) only 13 of the 24 variant types could be found (Fraaije et al., 2011, Marzani, 2011, Chassot et al., 2008, Leroux et al., 2007, Leroux and Walker, 2011).

Variant types found in this study had up to 10 alterations including certain alterations which are considered rare such as A410T (Stammler and Semar, 2011). The most common alterations were L50S, I381V, V136A and S188N and the double deletion of amino acids Y459 and G460. Some alterations such as the L50S and S188N are believed to have no effect on azole sensitivity (Cools and Fraaije, 2013) however overall it is recognised that a general increase in the number of amino acid alterations in the *CYP51* has been shown to decrease the sensitivity of isolates towards azoles. Certain combinations of alterations increase azole resistance which can be attributed to alterations falling within a key residue or moving a residue out of the reach of an azole thus impacting on the structural changes of the protein which can cause changes in affinity to azoles (Mullins et al., 2011).

The variants found in this collection often included the potent combination of V136A and I381V. These are known to affect azole sensitivity and were not found in populations before 2008 (Cools and Fraaije, 2013). This was due to structural constraints attributed to them both being located within different substrate recognition sites (Cools and Fraaije, 2008). In order to overcome this, modern isolates which have both alterations must have developed additional compensatory mutations to preserve function.

The combined deletion of amino acids Y459 and G460, are known to restore the function of variants that have multiple alterations which can result in a loss of fitness

(Mullins et al., 2011). The combined deletion has been shown to dramatically affect the proximity of other key residues to the azoles when binding occurs as the deletion results in the removal of a whole section of a beta turn of the heme pocket which includes the amino acid at 461 (Mullins et al., 2011). This could account for why the double deletion and an alteration at 461 are never observed together, as there is no need for an alteration at 461 if it is no longer within close proximity to the azole. Another suggested compensatory alteration often found in this population was S524T, which is now common in modern European populations and is also thought to cause reduced azole sensitivity (Cools and Fraaije, 2013).

Of the 6 most prevalent *Z. tritici* variant types in this study all have been shown to be at least moderately resistant to certain azoles. Fraaije et al. (2011) found Type 1, the most prevalent in this study, to be resistant to both epoxiconazole and prochloraz but sensitive to tebuconazole. Dooley (2015) also found it to show signs of resistance towards epoxiconazole; and found it to be sensitive towards metconazole. Type 2 in this study similarly was shown by both Dooley (2015) and Fraaije et al. (2011) to have high to moderate resistance towards epoxiconazole with the former research group also showing it to be resistant towards metconazole. Mullins et al. (2011) also found it to be highly resistant to epoxiconazole and tebuconazole with less resistance to prochloraz. Conversely Marzani (2011) showed this variant type to have sensitivity towards epoxiconazole with a calculated low resistance factor of 4.3 ± 1.9. However, it must be pointed out that these studies (except Dooley (2015)) did not include details of the presence of inserts in the putative *CYP51* promoter region which could have been a possible reason for discrepancies in findings.

When analysing isolates for the presence of inserts in the putative *CYP51* promoter region, most in this study had either the 120 bp insertion (69 in total) or the 800 bp insertion (244 in total). The presence of either insertion has been linked to reduced sensitivity in azoles by many research groups (Chassot et al., 2008, Dooley, 2015) with Cools et al. (2012) even finding an association between the 120 bp insertion and *CYP51* overexpression in isolates with reduced sensitivity. Dooley (2015) reported that the 120 bp insertion is only present in variants with 5 or less amino acid alterations, claiming that it would be of concern if this was combined with more

evolved *CYP51* variants. However, variant Type 14 found in this study has 9 amino acid alterations and although found previously by Dooley (2015) (that study's type 49) has not yet been found with the 120 bp insertion as in this study.

This study illustrates the diversity and spatial distribution of different *Z. tritici* variant types across farms and fields. A clustering effect was observed in this study with certain variant types showing association to certain geographical locations i.e. farm, field, and areas within a field. Knowing the *Z. tritici* population in its entirety allows for better understanding of a farm's individual specific needs and thus helps to establish a more informed approach to fungicide use. For this reason a future sampling plan was suggested with different sampling options in order to optimise the detection of certain variant types that may occur within a population in a specific location. This knowledge combined with continued research into the amino acid alterations, could help with making predictions about how pathogen populations on individual farms will evolve and which isolates are particularly of interest. Two general potential targets for detection that could be found in these isolates can be proposed from this study which may reduce sampling time for detection. This includes the 120 bp insertion in the putative promotor region of the *CYP51* protein as this insertion has, as discussed above, previously been shown to increase overall azole resistance with overexpression of the protein. Other potential targets which could be proposed are compensatory amino acid deletions/alterations within the *CYP51* protein, again as discussed above. Variants that have these usually have accumulated more alterations or have the potential to do so resulting in a corresponding increase in azole resistance.

This study highlights the benefit of creating an approach to a detection system which is tailored to the needs of the end user i.e. the farmer, and the specific location i.e. the farm, which may help individuals with decision making and the ability to futureproof their crop security.

Chapter 5 Assessment of life cycle traits of different *Zymoseptoria tritici* CYP51 variants to understand which variants are of most importance for detection.

5.1 Introduction

DMI fungicides, mostly consisting of the azoles (triazole and imidazole), inhibit fungal growth by interfering with the biosynthesis of ergosterol, the predominant sterol in fungal membranes, by the interaction of the azole ring with the heme iron of the cytochrome P450 sterol 14α-demethylase (CYP51) (Cools et al., 2010). Erosion of azole efficacy has been recorded, with higher doses now being required to achieve effective disease control. The past 10–15 years has seen an increasing number of mutations related to azole resistance emerging in the CYP51 gene (Cools and Fraaije, 2013). These mutations and deletions occur in combinations, creating diverse CYP51 haplotypes with different mutation profiles which impact on particular DMIs in various ways (Wieczorek et al., 2015). The more recent *Z.tritici* CYP51 variants have up to eight amino acid alterations compared to the wild type (Cools and Fraaije, 2013).

To establish models of disease development it is important to determine how mutations impacting fungicide sensitivity may affect aspects of the pathogen, such as latent period and life cycle. From this, specific variants that pose a high risk can be detected early on in the season and fungicide application timing as well as choice of fungicide can then be changed accordingly.

Deconstructing the pathogen cycle into fundamental life traits allows the precise identification and quantification of differences among Zymoseptoria triticiCYP51 variants' phenotypes which can then be attributed to pathogen fitness and epidemic development rates. An approach to measuring the aggressiveness of variants in the field usually combines measuring pycnidial production, number of lesions, and latent period (Suffert et al., 2013, Morais et al., 2015). In a lab setting, EC_{50} values are ascertained to measure how resistant different *Z. tritici* CYP51 variants are to certain fungicides. In order to quantify this, the pathogen is measured against different doses of a fungicide.

This pilot study aims to assess the aggressiveness and resistance to fungicides for different CYP51 variants' using the above measures. EC_{50} values were ascertained

from *in planta* experiments using qPCR detection. Isolates were chosen from chapter 4 based on having similar high resistant EC_{50} values towards epoxiconazole as stated by Dooley (2015). A wild type was used for comparison. Although not a true wild type, IRE-3 (WT) has been shown in studies by Marzani (2011) to have a very low EC_{50} to epoxiconazole and only two SNPs. The aim of this pilot study was to highlight which CPY51 variants of *Z. tritici* are of most importance to farmers due to their resistant profiles and therefore should be a priority for detection.

5.2 Methodology

5.2.1 Experimental design

Three isolates of *Z. tritici*: 14, 15 and WT were chosen (Table 5.1). These were SEPT1287, SEPT0532, and IRE -3 respectively. The 'wild type' which was used was not a true wildtype as stocks of a true wildtype isolate (PO323) were unavailable. Isolate IRE -3 was from stocks at The University of Nottingham and both SEPT1287 and SEPT0532 were isolates from the collection obtained from Chapter 4.

Table 5.1 Isolates used in this study, showing the SNPs present in the CYP51 gene

Isolate type	50 - L	136 - V	188 - S	379 - A	381 - I	459 - Y	460- G	461 - Y	513- N	524 - S
Type 14	S	A	N	G	V	-	-		K	T
Type 15	S	C	N	G	V	-	-			T
IRE -3 (WT)	S							S		

The experimental design is shown in Table 5.2. Each of the isolates were grown on wheat which had been sprayed previously with Opus®125 (epoxiconazole) fungicide at varying concentrations (0%, 10%, 25%, 50%, 75% and 100% Opus). There were five additional pots which were not inoculated or sprayed as a control..

5.2.2 Plant material

Cultivar JB Diego was chosen for this study as it is one of the most popular wheat varieties grown in the UK and considered to be moderately susceptible to *Z. tritici* having a resistance rating of 5.2 on a 1–10 scale of decreasing susceptibility (Senova).

One hundred and eighty 9 cm diameter pots were sown with wheat, with 10 plants per pot. The wheat was grown in a glasshouse with the temperature fixed at of 20°C

and supplemented with sodium lamps to achieve 15 hours of light. When seedlings had reached growth stage 12, fungicide treatment, followed by inoculation with *Z. tritici,* was performed.

5.2.3 Fungicide application

Opus®125 was sprayed at various doses when wheat plants reached growth stage 12. Each isolate had 10 pots at each fungicide dosage, these ranged from 0% to 100% of the maximum recommended dose. Calculations were carried out to ascertain the correct concentration of fungicide for the desired % fungicide concentration needed in 20 ml to cover 1 m^2. Plants were set out in 1 m^2 quadrats and the fungicide was sprayed over the whole 1 m^2 using a trigger sprayer. The Opus®125 fungicide was obtained from Agrii.

5.2.4 Inoculation

PDA plates were used to grow up each isolate and plates were washed with sterile water to collect spores. Inoculation was carried out three days after fungicide had been applied. The spore suspensions were quantified using a haemocytometer and the concentration adjusted to 5×10^5 spores ml^{-1} by dilution, pots were sprayed using a hand-held sprayer for uniformity of droplets. A 50 ml spore suspension was used for each batch of 10 pots (Lovell et al., 2004). After inoculation, each pot was covered in a separate plastic bag and sealed with an elastic band. Distilled water was added in the base of a tray and the covered pots were transferred into this to maintain high humidity. Plastic bags were removed after 72 h (Suffert et al., 2013).

5.2.5 Disease assessment

5.2.5.1 Visual

Disease severity was visually assessed twice a week by observing three inoculated leaves for % of leaf with lesions and % of leaf sporulating area (area showing visible pycnidia). In addition, the number of leaves with lesions was counted and two lesions were assessed for the number of pycnidia present and an average was calculated. Visual averages of % of leaf with lesions and % of leaf sporulating area were estimated at the time of observation and therefore a standard deviation could not be

performed. The % of leaf with lesions and % of leaf sporulating area were assessed to the nearest 5%.

5.2.5.2 qPCR

One leaf was taken at each sampling point from every group to assess for disease progression using real time PCR. Leaves were stored at -20°C and DNA extraction took place within one week of freezing. Frozen leaves were added to a universal tube with a ball bearing and were homogenised using a Geno/Grinder® for 4 min at 1,500 strokes. After homogenisation, 100 mg of sample was weighed and DNA extraction was performed using the DNeasy Plant Mini Kit, using the manufacturers' protocol (Qiagen).

A set of primers and TaqMan probe specific to *Z. tritici* were used (Duvivier et al., 2013). The *Z. tritici* probe was labelled with FAM and contained BHQ-1 as a quencher. The real-time PCR assay was prepared with 12.5 µl of Environmental mastermix (Applied Biosystems™),forward and reverse primers at 500 nM, probe at 500 nM and 1 µl of DNA extract in a total volume of 25 µl. Six standards were used ranging from 25 to 0.00025 ng of purified DNA from *Z. tritici* grown on PDA plates. These were included in all runs as well as negative controls containing nuclease-free water in the place of DNA. All reactions were performed in duplicate. The qPCR was carried out using standard cycling conditions using an Applied Biosystems ABI 7500 instrument and CT values were obtained. For DNA quantification, a standard curve was generated by plotting the log of the DNA concentration of standards against the cycle number of each curve within the log-linear stage of amplification. All analysis was performed using Prism 7.

5.2.5.3 Results Analysis

Percentage disease control of each parameter (no. of leaves with lesions, % lesion area, % sporulating area, no. of pycnidia and CT value from qPCR) was calculated using the control (0% fungicide) as a baseline. EC_{50} values for each isolate were calculated using CT values from 440 dd. The control (0% fungicide) was again used as a baseline. EC_{50} values were found from reading the 50% control on plotted graph of the results. Excel was used for these calculations and graphs were plotted using Prism.

5.3 Results

5.3.1 Visual assessments

Lesion development was observed on many of the samples, with all types of *Z. tritici* successfully growing on the wheat when no fungicide was present (Figure 5.1).

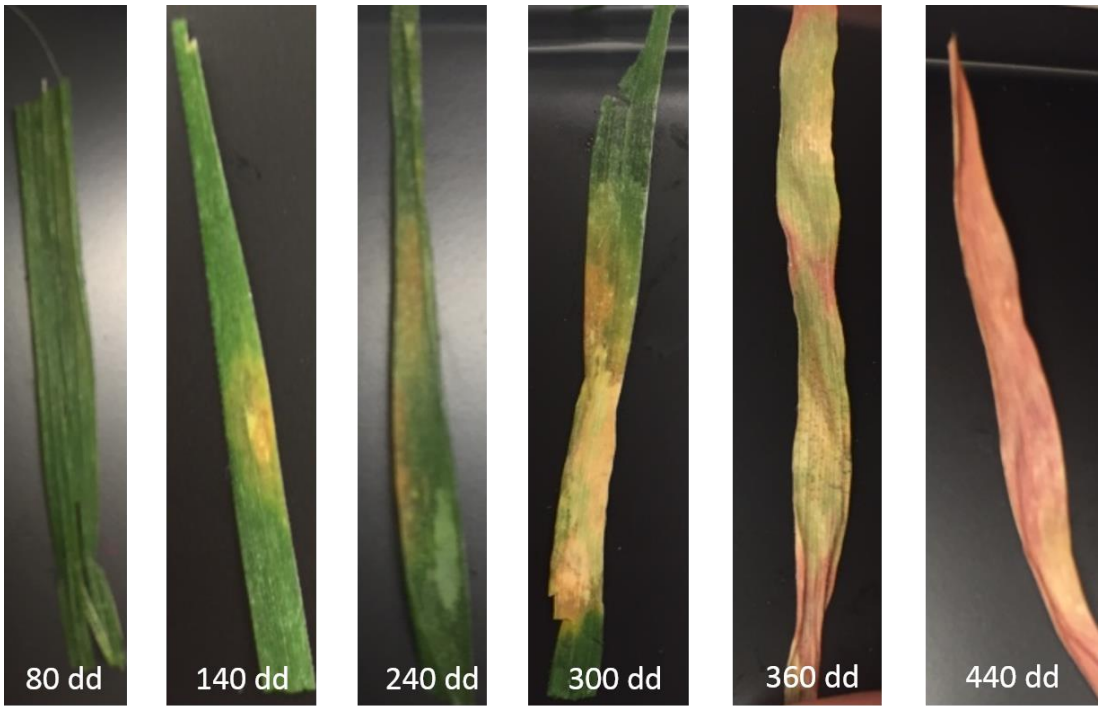


Figure 5.1 Typical *Zymoseptoria tritici* lesion development

5.3.1.1 Isolate traits without fungicide application

The three isolates were compared as a baseline without fungicide application. Both isolate type 14 and 15 infected 100% of the leaves which were inoculated. However, only 70% of the WT inoculated leaves showed signs of infection (Figure 5.2a). The largest increase of lesions for all types was between 300-360 degree-days (dd). If the latent period is taken to be the time interval between inoculation and first symptoms, types 14 and 15 showed a shorter latent period (140 dd) than the WT (240 dd) (Figure 5.2a).

At 440 dd all isolate types showed the same percentage leaf area (90%) covered by lesions with the largest increase being between 330 dd and 360 dd, which was the same amount of increase for all types (Figure 5.2b). However type 14 and 15 overall

showed a faster rate of percentage lesion coverage compared to the WT with type 14 showing colonising faster than the other isolates (Figure 5.2b).

There was no difference between the overall percentages of a leaf covered by a sporulating area at 440 dd, in any of the isolate types. However type 15 had 10% coverage as early as 240 dd, whereas both WT and type 14 did not reach 10% until 360 dd. After reaching 10% dd type 15 seemed to plateau until an eventual increase at 360 dd (Figure 5.2c).

Isolate type 14 produced more pycnidia by the end of the experiment than the other isolate types. Type 15 was shown to have a lower pycnidia density than all isolates. However type 15 produced pycnidia earlier, showing a number of approximately 50 at 240 dd in comparison to both other isolates not showing any signs of sporulation at that time point (Figure 5.2d).

If however the latent period is not taken to be the time taken from inoculation to the first lesion but from inoculation to the first sign of sporulation, the minimum time required for the pathogen to complete its life cycle, type 15 is considered to have a shorter latent period than the others (240 dd), with WT and type 14 having the same

latent period (300 dd).

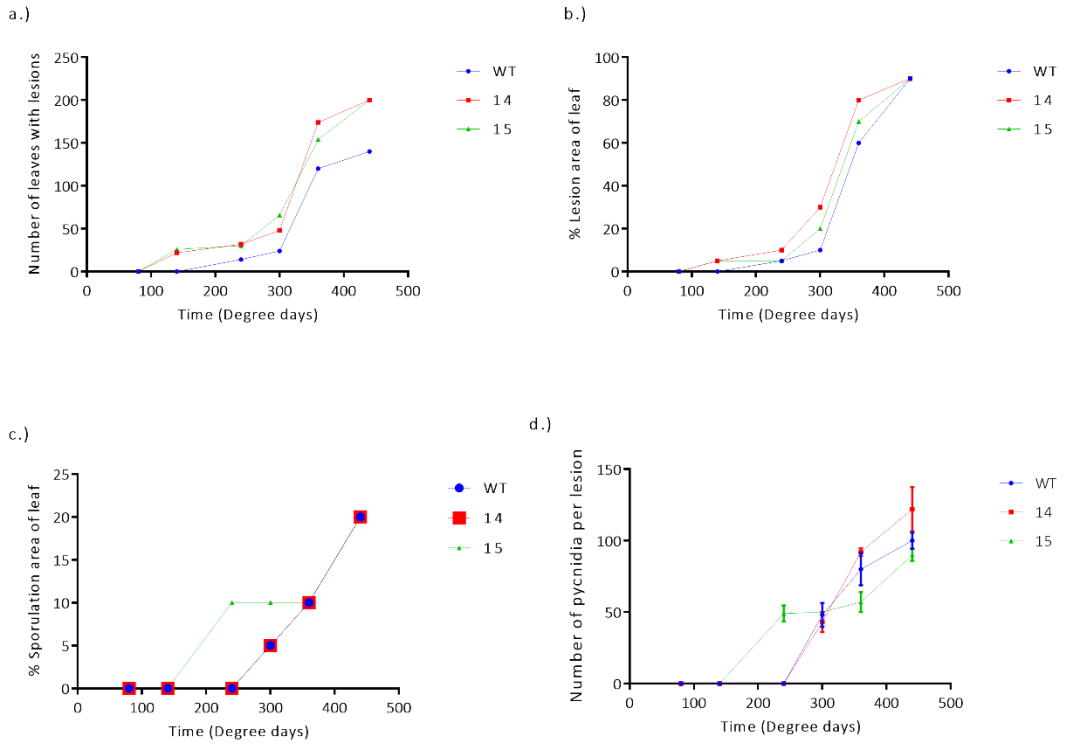


Figure 5.2 Life cycle traits of all isolates without fungicide application. a.) Number of leaves with lesions b.) % lesion area of leaf c.) % sporulation area of leaf d.) Number of pycnidia per lesion.

5.3.1.2 Effect of fungicide

5.3.1.2.1 Wild type

An application of Opus had a significant impact on the numbers of leaves displaying signs of lesions. By 440 dd there was a 38% drop in infection capacity for plants sprayed with 10% Opus, 72% for those sprayed with 25% Opus, and 77% for those sprayed with 50% Opus, with both 75% and 100% Opus concentrations showing complete control compared to untreated plants. This shows a clear dose response to the fungicide (Figure 5.3a). The rate of infection with regards to the number of leaves with lesions also changed with fungicide application. The fastest increase in lesions was seen for most fungicide concentrations between 360-400 dd, whereas those plants not sprayed with fungicide had the largest increase between 300-360 dd. It also had an impact on the latent period, with those plants treated with a concentration of ≥25% fungicide having a longer latent period (Figure 5.3a).

The percentage area of a leaf covered by lesions was also shown to have a clear dose response by 440 dd (Figure 5.3b.) except for plants treated with 10% which showed

the same percentage area covered as those that were not treated. However, at 10% fungicide the rate of lesion coverage was reduced even if it did eventually cover the same area.

As before, if the latent period is taken to be the minimum time required for the pathogen to complete its life cycle, i.e. sporulate, then an application of ≥25% fungicide seems to increase the latent period (Figure 5.3d). However, the percentage of sporulating area on the leaf by 440 dd does not seem to be affected by the concentration of fungicide applied until it reaches 50% concentration where the sporulating area drops to 25% of the capacity reached by lesser concentrations (Figure 5.3c). The number of pycnidia per lesion is higher at a fungicide concentration of 10% compared to the untreated; however, this may be attributed to a small sample size as the standard error suggests. However, by ≥25% fungicide concentration, the number of pycnidia are significantly reduced to just over 50% than that of the numbers found with no fungicide application (Figure 5.3d).

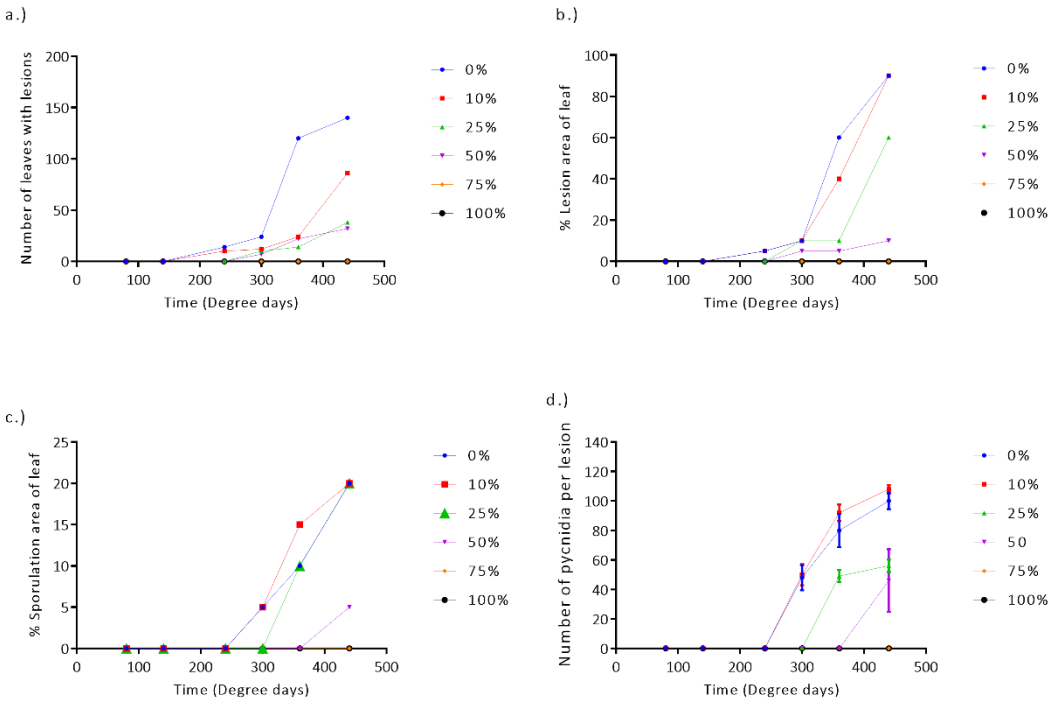


Figure 5.3 Life cycle traits of WT isolate at varying fungicide doses. a.) Number of leaves with lesions b.) % lesion area of leaf c.) % sporulation area of leaf d.) Number of pycnidia per lesion.

5.3.1.2.2 Type 14

Fungicide concentrations of ≤25% by 440 dd were unable to inhibit any of the infections, with 100% of the inoculated leaves showing signs of having lesions (Figure 5.4a). The higher fungicide concentrations appear to reduce the number of lesions on the leaves compared to the lower fungicide concentrations. Although lower fungicide concentrations still have high numbers of lesions, there is a larger reduction in infection capacity shown compared to type 15, with 100% fungicide concentration causing a 26% reduction in infection capacity compared with using no fungicide (Figure 5.4a). The latent period, taken to be the first sign of infection, was also not affected by the fungicide concentration that was applied to the plants (Figure 5.4a).

The area of leaf covered by lesions was again not significantly impacted by the concentration of fungicide applied. Although fungicide concentrations of ≥25% at 440 dd showed a reduction of leaf area covered by lesions, this was again minimal with an 11% decrease compared to that at ≤10% fungicide concentration. There was however a difference in the rate of coverage with higher concentrations showing slower disease coverage on the leaf (Figure 5.4b). The largest increase in area of the leaf covered in lesions for all was between 300 dd and 360 dd.

The concentration of fungicide did not affect the sporulation area of the leaf at all until it reached 100% fungicide application. At this concentration, by 440 dd, the sporulation area was reduced by 50% of that of the other fungicide concentrations (Figure 5.4c). The latent period taken to be the minimum time required for the pathogen to complete its life cycle, i.e. sporulate, was not affected by fungicide concentrations, however the overall numbers of pycnidia produced by a lesion by the end of the time course (440 dd) were generally reduced when higher concentrations of fungicide were applied (Figure 5.4d).

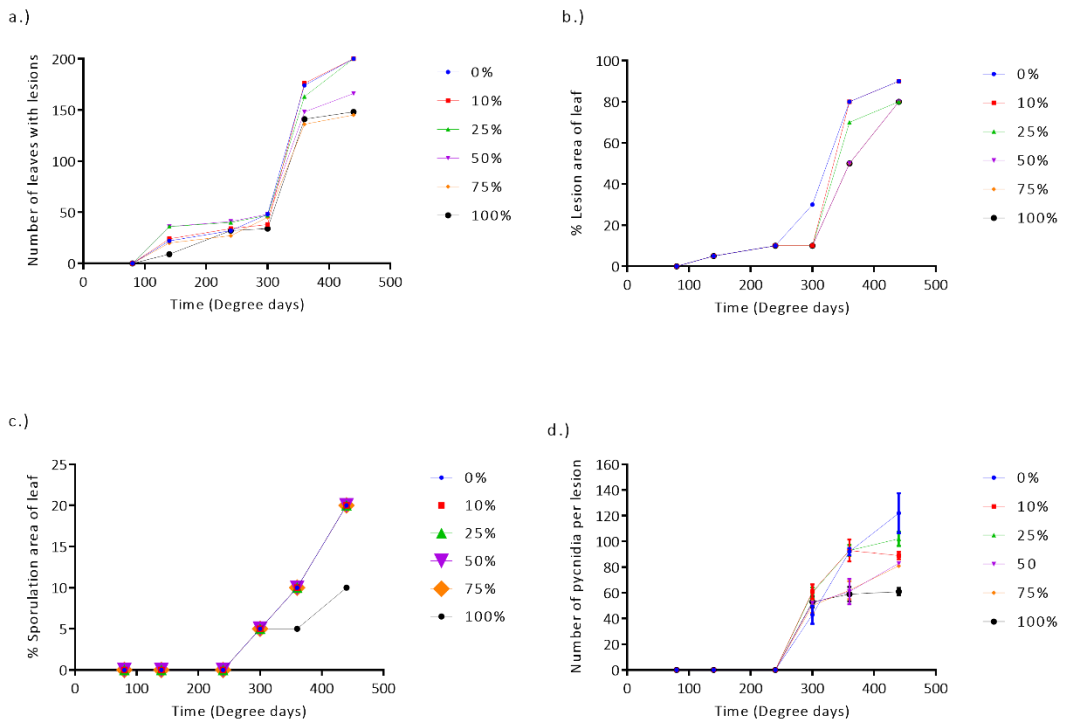


Figure 5.4 Life cycle traits of isolate type 14 at varying fungicide doses. a.) Number of leaves with lesions b.) % lesion area of leaf c.) % sporulation area of leaf d.) Number of pycnidia per lesion.

5.3.1.2.3 Type 15

By 440 dd, fungicide concentrations of ≤25% were unable to suppress the infection, with 100% of the inoculated leaves showing signs of having lesions (Figure 5.5a). The number of lesions on the leaves reduced when using higher fungicide concentrations; however, this is minimal compared to the effect shown on the WT, with only 13% reduction in infection capacity when using 100% concentration of fungicide compared with using no fungicide (Figure 5.5a). The latent period, taken to be the first sign of infection, was also not affected by the fungicide concentration that was applied to the plants (Figure 5.5a).

Although unlike type 14 and WT no difference in leaf area covered by lesions was observed between the different fungicide concentrations until 360 dd, there was a general dose response observed by 440 dd. By 440 dd the fungicide concentration of 100% caused a 44% reduction of leaf area covered by lesions, compared to that at ≤10% fungicide concentration (Figure 5.5b). The largest increase in area of the leaf covered in lesions for all was again between 300 dd and 360 dd (Figure 5.5b).

The concentration of fungicide did seem to affect the sporulation area of the leaf. By 440 dd only at concentrations of ≤10% was the sporulation area seen to be 20% of the leaf area with all other concentrations only allowing 10% sporulation area of the leaf (Figure 5.5c).

The latent period taken to be the minimum time required for the pathogen to complete its life cycle, i.e. sporulate, was not affected by fungicide concentrations, except in the case of 75% fungicide concentration (Figure 5.5c). This did not seem to fit previous trends and may be an anomaly. At 100% fungicide concentration the number of pycnidia and the rate at which they are produced are significantly reduced compared to that of the other concentrations of fungicide. Although with no fungicide treatment type 15 produces less pycnidia than the WT or type 14 by 440 dd, at ≤25% fungicide concentrations the number of pycnida present in a lesion remain unchanged unlike the other types. It is only at very high concentrations of fungicide that the pycnidia numbers are reduced (Figure 5.5d).

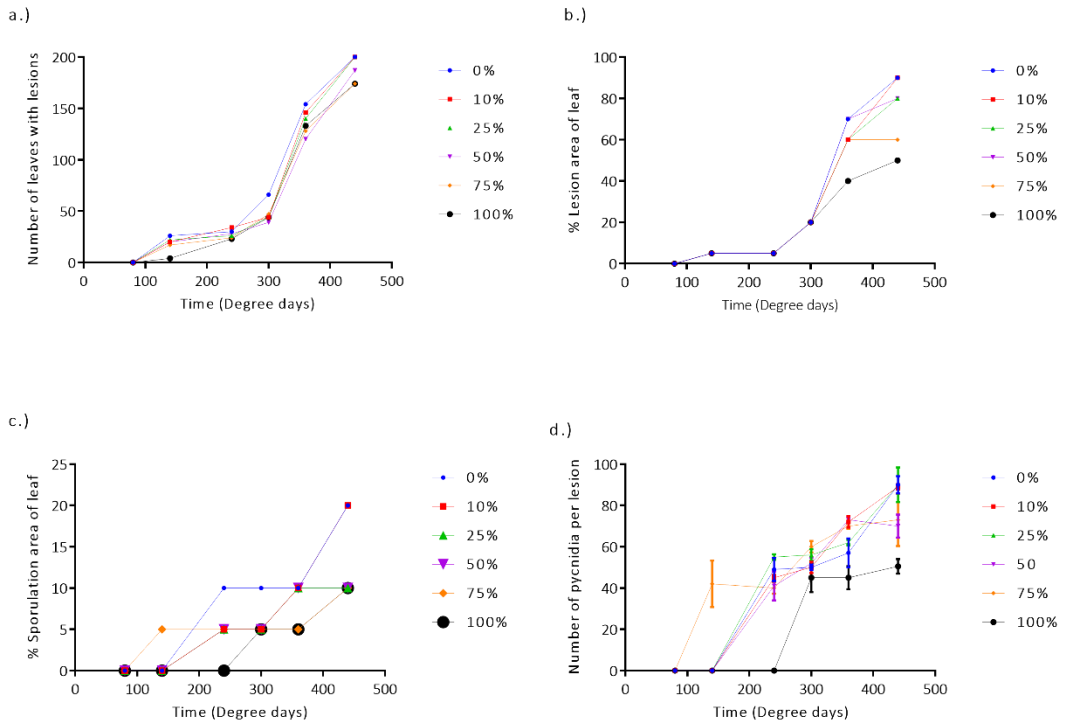


Figure 5.5 Life cycle traits of isolate type 15 at varying fungicide doses. a.) Number of leaves with lesions b.) % lesion area of leaf c.) % sporulation area of leaf d.) Number of pycnidia per lesion.

5.3.2 Fungal quantification using real-time PCR

The WT showed high levels of DNA by 440 dd when fungicide concentrations of ≤50% were used; however, above this concentration no DNA was present in the samples (Figure 5.6a). At concentrations of ≤10% a steady increase in DNA was found with 10% eventually having the most DNA. DNA concentrations when fungicide concentrations of ≤25% were used seem to plateau between 360-440 dd. Both 25% and 50% fungicide concentrations seem to have varying DNA concentrations between samples (finding no DNA present after a previously high concentration were found) however it should be noted the limited sample size (one leaf) (Figure 5.6a).

Type 14 shows a much clearer trend across all fungicide concentrations with a steady overall increase in DNA concentration across the time period with high concentration of DNA reached by 440 dd for all concentrations (Figure 5.6b). The only exception to this is the 100% fungicide concentration sample which depletes to no DNA present in the middle of the time course. Again as stated previously this may be due to the small sample size but it does indicate that not every leaf had *Z. tritici* present at a given time which reflects the findings in section 5.3.1. Like the WT after a steady increase in DNA was shown, at 360 dd this seems to plateau and in most cases decrease (Figure 5.6b).

Although the overall trend of type 15 is that the DNA is increasing over the time course and concentrations of fungicide, by 440 dd it seems to fall into the trend expected (except at 25%).There is however a larger range between the final concentrations compared to that of type 14. Also at concentrations of 50% there is a significant drop to no DNA present halfway through the time course which again may be due to reasons stated above (Figure 5.6c). Again at 360 dd, DNA concentrations seems to plateau compared to previous substantial increases seen at other time points.

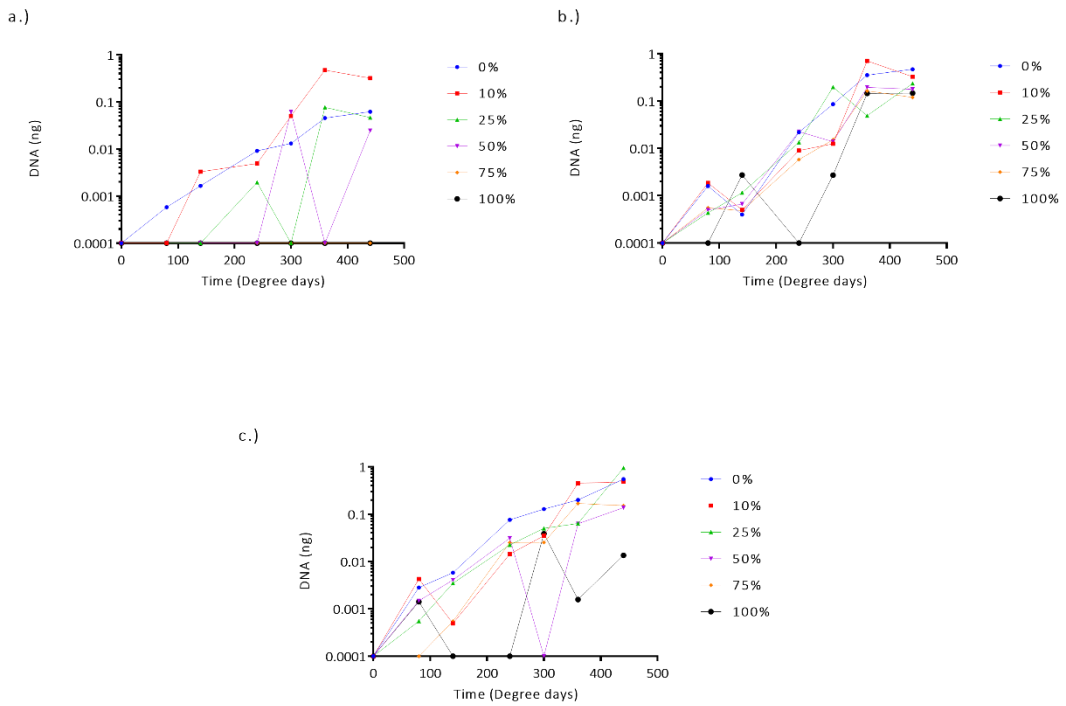


Figure 5.6 Detected DNA of all isolates at varying fungicide doses. a.) Wild Type b.) Type 14 c.) Type 15.

5.3.2.1 Correlation of qPCR to visual assessments

Evaluation of the correlation between the qPCR results and the visual assessments indicated the qPCR correlated with the visual assessments with a positive correlation for all (r = 0.503, 0.683, 0.776, 0.788) (Figure 5.7). However, the strongest positive correlation (r = 0.788) was found to be with the number of pycnidia per lesion. The least significant correlation (r= 0.503) was with the number of leaves with lesions, which was to be expected as it is not a measurement of disease in one given leaf, unlike the other visual assessments, but rather transmission of the disease in the overall leaf population.

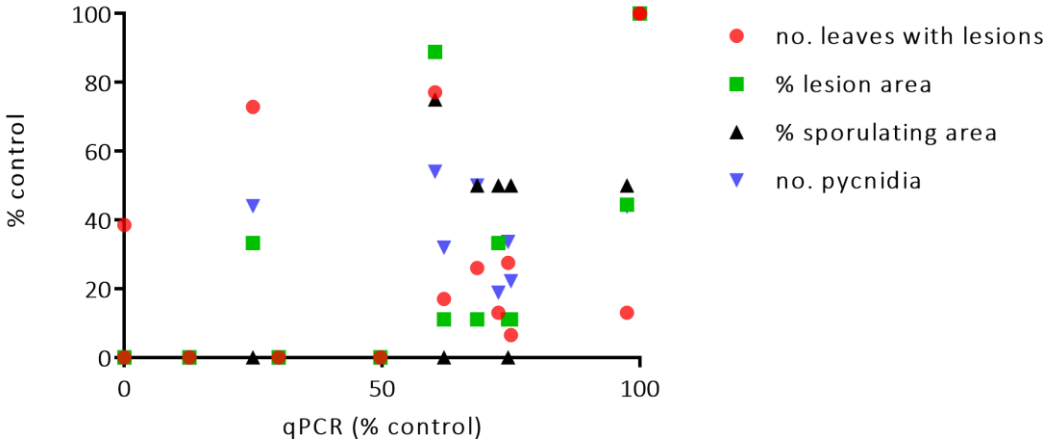


Figure 5.7 The correlation of qPCR % control against % control of the different life cycle traits indicted by graph key.

5.3.2.2 EC_{50}

The EC_{50} was calculated using the % control obtained from the qPCR data (Figure 5.6) using Microsoft Excel. When fitting a line of best fit to calculate the EC_{50} value for type 15 the value at point X=2.2, Y=0 was not included and was seen as an anomaly. This may have been due to problems with fungicide application and watering plants before fungicide uptake could take place. The WT had an EC_{50} value of 251 mg L^{-1} which was considerably more than the 155 mg L^{-1} required to inhibit 50% of isolate type 14's symptoms or the 195 mg L^{-1} required to inhibit 50% of isolate type 15's symptoms. (Figure 5.8). This suggests that the WT needs a higher dosage of fungicide to be inhibited than type 14 and 15 even though both of these types have been shown to be more resistant to the fungicide when the visual symptoms were assessed.

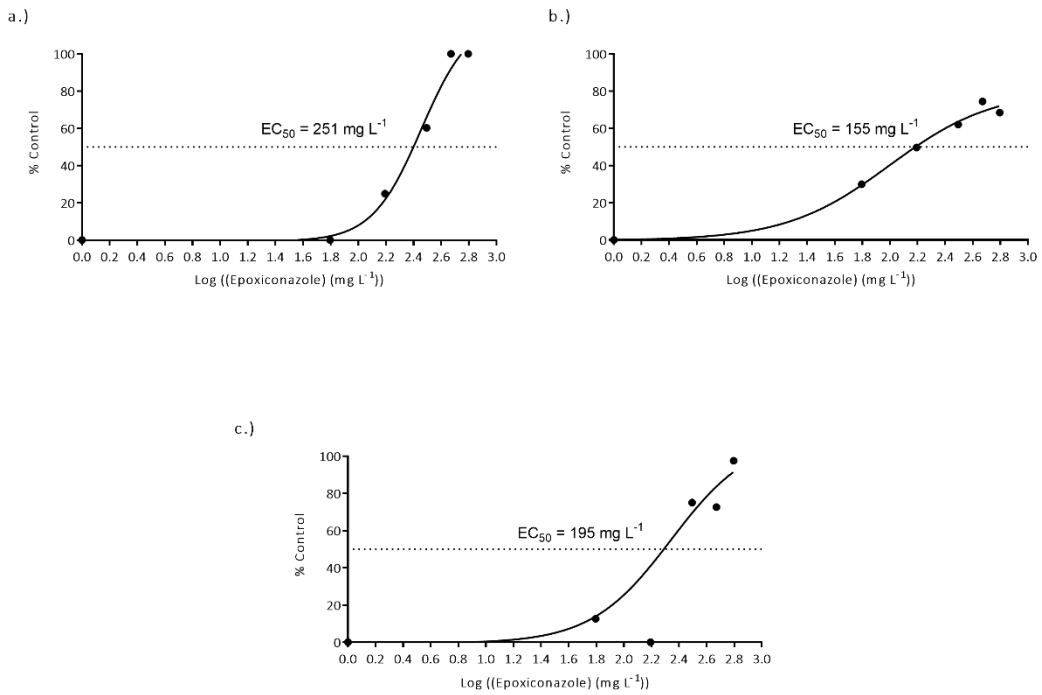


Figure 5.8 The EC_{50}s calculated from qPCR DNA results a.) Wild Type b.) Type 14 c.) Type 15.

5.4 Discussion

The method proposed in this study made it possible to quantitatively characterize the development of *Z. tritici* on wheat plants throughout a complete infection cycle as well as observe differences in the disease progression when different doses of a fungicide were applied.

All isolates showed relatively short latent periods with qPCR detecting *Z. tritici* DNA as early as 80 dd (before visual symptoms). This may be due to the experiment being carried out on seedlings rather than mature plants in the field. Pariaud et al. (2013a) have previously demonstrated an increase in latent period when inoculating mature plants compared to seedlings. One possible reason may be because some resistance genes have been shown to only be expressed by mature plants and not in seedlings (McIntosh et al., 1995). Without fungicide application, type 14 showed a higher percentage area of leaf covered in lesions earlier than other types. There may be a balance in different parts of the life cycle of the pathogen, this isolate spreads readily

on the leaf surface area compared with sporulation area, yet eventually is able to produce high pycnidia density (120) per lesion. Conversely, type 15 generates a larger sporulating area early in the infection cycle and has a reduced lesion coverage. It has less pycnidia-dense lesions but sporulates earlier. This is a trade-off between the two traits and as these are shown to be linked this suggests the fitness cannot be maximised for both traits. This supports findings by Pariaud et al. (2013b) who also found that shorter latent periods were offset by a trade off with spore production capability. This therefore could potentially be seen as the most aggressive type as it has the ability to complete life cycles much earlier than the other types, meaning more life cycles can occur within a season. It has been shown that the length of latent period in this context, and therefore epidemic cycles, has a strong effect on epidemic rate and severity (Lannou, 2012). Type 14 however relies on having the highest spore production capacity overall and whilst the WT has the least efficient rate of lesion coverage it is however able to produce good spore density per lesion, more than type 15. The production of spores can only take place during the necrotrophic phase so type 14, although unable to commence the necrotrophic phase earlier, once started, then catalyses more energy and nutritional uptake from the same given area than type 15 resulting in higher spore production (Lannou, 2012).

The WT was considerably impacted by fungicide application and it was unable to overcome fungicide use and to even emerge at high fungicide doses. The EC_{50} for WT was however relatively high (251 mg L^{-1}) in comparison to the other isolates given its considered sensitivity towards epoxiconazole. Marzani (2011) found the EC_{50} for the same isolate type to be 0.03 mg L^{-1} which is considerably less than the findings in this study. Type 15 was however found to be more resistant to epoxiconazole than type 14 (14.99 mg L^{-1} and 9.68 mg L^{-1} respectively) by research carried out by Dooley (2015), which supports findings in this study. However, the EC_{50} values are considerably higher than those found in the research studies stated above, both of which were conducted *in vitro*. There are several reasons why EC_{50} values may differ between those calculated *in vitro* to those calculated *in planta*, for example the fungicide concentration is diluted in the host tissue during uptake and before full absorption can take place, some may be lost due to environmental breakdown. Reis

et al. (2015) suggests that residual fungicide left on the leaf is reduced by host tissue detoxification activity. Another reason to consider is that there may be other undetected organisms on the leaf surface that interact with the *Z. tritici* and impact the EC_{50}.

Although aggressiveness traits of types 14 and 15 were often reduced with fungicide application, even with a 100% fungicide concentration both isolates were able to colonise the wheat plants. Isolate type 14 displayed high % lesions area and % sporulation area coverage even when fungicides were applied. With fungicide application, type 15 still had the ability to produce high lesion numbers, shorter latent periods (although they did increase with fungicide dose it was still earlier at most concentrations than displayed by other isolate types) and less affected pycnidial numbers.

This is evidence that although both are considered resistant due to their similar high EC_{50} values (Dooley, 2015) these isolates are impacted by the fungicide in different ways showing different pathogenicity profiles. It is therefore important to decide which traits are of most importance to the overall epidemiology and progression of the disease. By knowing more about these differences in profiles these can then be fed into disease epidemiology models such as SIR (S for the number susceptible, I for the number of infections, and R for the number recovered (or resistant) and then predictions made about disease progression in the whole population. From these predictions, traits that are believed to lead to more prolific disease over the season, could then be used as a target for detection.

This pilot study has highlighted that considerable further work is needed to ascertain if these traits are solely quantitative or if they are qualitative. To do this the same experiment should be carried out and isolates should be selected based on having the same SNPs present in the *CYP51* gene rather than having similar EC_{50}s as was done in this study. It would also be wise to highlight that different isolates show variable resistance to different cultivars of wheat. There is therefore a potentially complex genetic determinism of traits involved in host-pathogen interactions which is not shown in the breadth of this study. Another consideration is that other genes other than *CYP51* may be influencing aggressiveness traits, for example *PKS1*, a

polyketide synthase gene known to play a role in the synthesis of melanin which is needed in appressoria to achieve high turgor pressure for penetration of the plants epidermis (Lendenmann et al., 2014). A better understanding of how all these factors affect traits of aggressiveness will allow us in the future to detect isolates that are of importance in specific situations for example when using a specific wheat variety.

Chapter 6 General discussion

6.1 Main conclusions

6.1.1 Specific monoclonal antibody 29.G7.A9 was developed to detect for spores of *Fusarium graminearum*.

In this study a specific monoclonal antibody, 29.G7.A9, that could be used to detect spores of *Fusarium graminearum* was developed. A robust cell line was established and therefore a constant and renewable antibody source can now be generated with batches being identical. Out of 18 antigens tested, the 29.G7.A9 antibody only showed cross reactivity towards one antigen, *Trichothecium roseum*, although different size protein bands were detected compared to the *F. graminearum* antigen. Moreover the negative control (Nosema antibody) also showed reactivity towards *T. roseum*. In addition, the pigmentation from the extracted *T. roseum* could be seen on the PDVF membrane, indicating potential overloading of the proteins onto the gel or presence of contaminating compounds which may exacerbate the cross reaction with IgG antibodies. Immunofluorescence demonstrated the ability of the 29.G7.A9 antibody to bind to the native protein in *F. graminearum* spores. Early detection of *F. graminearum* by detecting spores is now possible with this antibody. Although other antibodies have been produced by other groups for the identification of *F. graminearum* (Ji et al., 2008, Lee et al., 2013, Sanders et al., 2014), these were only developed against DON and not the spore itself, and so unlike the antibody found in this study would not be of use at an early stage of detection. The monoclonal antibody produced within this work was able to be taken forward to be used as a bio-receptor component of an immunosensor.

6.1.2 Production of a recombinant protein of *P. triticina* spores for future antibody development.

A recombinant protein was created from spore cDNA of *P. triticina* which was shown to have good expression. The time taken to screen cell lines can potentially be reduced by immunising mice with recombinant proteins made from target sequences, pre-selected using bioinformatics for unique regions of the pathogen. Unfortunately, the recombinant protein here was unable to be used for monoclonal

antibody production due to ethics approval not being granted. Had it been used for immunisation a more in depth analysis of epitopes could have been undertaken.

6.1.3 Development of an amperometric immunosensor system for onsite detection of *Fusarium graminearum* spores using SPEs

The 29.G7.A9 antibody was incorporated into a hand held immunosensor system for onsite detection of *Fusarium graminearum* spores using SPEs and the HRP/TMB detection system. The system was able to differentiate between positive and negative samples with differences in peak current observed between the 29.G7.A9 and positive control assays compared to the negative control assay. Although more optimisation of the technique is needed to confirm these results, this study provides evidence that this amperometric immunosensor system has the potential to be used out of the lab in a field-based setting operated by non-specialists.

6.1.4 Potential targets identified for detection of azole resistant *Z. tritici* isolates.

The *Z. tritici* population analysed was very diverse with 16 amino acid alterations at 13 positions throughout the *CYP51* protein found, leading to 24 variant types found in total. The prevalence and distribution of these, as well as the presence of inserts in the putative *CYP51* promoter region, 120 bp insertion (69 in total) or the 800 bp insertion (244 in total), was also studied resulting in two general potential targets for detecting azole resistance being proposed.

The first target suggested is the 120 bp insertion in the putative promotor region of the *CYP51* protein; this insertion has previously been shown to increase overall azole resistance with overexpression of the protein (Cools et al., 2012). It has only previously been found in variants with 5 or less amino acid alterations, with concerns if it was combined with more evolved *CYP51* variants (Dooley, 2015). However, variant Type 14 found in this study has 9 amino acid alterations and the 120 bp insertion; highlighting its need to be considered as a target for detection.

The second potential target is the compensatory amino acid deletions/alterations within the *CYP51* protein as variants that have these, have usually accumulated more alterations or have the potential to do so, resulting in a corresponding increase in azole resistance (Mullins et al., 2011).

6.1.5 A future sampling plan was suggested with different sampling options, in order to optimise the detection of certain variant types that may occur within a population of *Z. tritici* in a specific location.

The diversity and spatial distribution of different *Z. tritici* variant types across farms and fields was illustrated. A clustering effect was observed with certain variant types showing association to certain geographical locations i.e. farm, field, and areas within a field. Knowing the *Z. tritici* population in its entirety allows for better understanding of a farm's individual specific needs and thus helps to establish a more informed approach to fungicide use. For this reason a future sampling plan was suggested with different sampling options in order to optimise the detection of certain variant types that may occur within a population in a specific location.

6.1.6 Evidence that life cycle traits of *Z. tritici* resistant variants are impacted differently by fungicide use.

The method proposed in this study made it possible to quantitatively characterize the development of *Z. tritici* on wheat plants throughout a complete infection cycle as well as observe differences in disease progression when different doses of a fungicide (epoxiconazole) were applied. Both isolates used in this study (Type 14 and 15) are considered resistant due to their similar high EC_{50} values (Dooley, 2015); however, in this study these isolates are impacted by the fungicide in different ways, showing different pathogenicity profiles. This highlights the importance of identifying which traits are of the most significance to the overall epidemiology and progression of the disease. Knowledge from these pathogenicity profiles can inform disease epidemiology models and then predictions can be made about disease progression in the whole population. From these predictions, traits that are believed to lead to more prolific disease over the season, could then be used as a target for detection.

6.2 Suggestions for future research

This thesis provides techniques and information for generating further research and contributing new ideas for a more integrated approach for fungal crop pathogen detection research. It is suggested that further research should concentrate on: an interdisciplinary approach to biosensor development for in-field detection, understanding how the presence of different inserts in the putative *CYP51* promoter

region of *Z. tritici* isolates combined with different amino acid alterations in the *CYP51* gene contribute to resistance, and additional fundamental research into life cycle traits of fungicide resistant *Z. tritici* isolates.

A multifaceted approach should be undertaken to be able to detect and monitor fungal crop pathogens. Although in recent years much research has focused on nucleic acid approaches, antibody detection is still a reliable robust method that can be integrated into a range of sensor platforms and is beneficial in the surveillance of plant disease spread (Khater et al., 2017). Although technologies such as next generation sequencing will aid in detecting fungal plant pathogens in the future, currently the technology is not suitable for use in portable devices and complex sample preparation steps are needed (Ray et al., 2017). However some portable sequencing devices have been developed such as the Oxford Nanopore MinION, although only currently used in the medical field, it is able to sequence over 150 kilobases of DNA (Jain et al., 2016). It is therefore suggested that future detection could encompass a multi-level approach using an antibody based detection for initial surveillance followed by a nucleic acid based method with the ability to differentiate between different traits, possibly by probes specific to certain SNPs.

Multiplex technologies will help with the high throughput of samples and multiple detection outcomes. The use of in-lab devices such as the Luminex system have been shown to meet the needs in this area, with not only species specificity but clade or subclade level through target-specific primer extension (TSPE) (van der Vlugt et al., 2015, Kostov et al., 2016). However portable devices with this technology have not yet been developed for in-field detection. Another possible future approach could therefore be the use of loop-mediated isothermal amplification (LAMP) as it can be performed in isothermal conditions, with potential detection carried out in the field. It has been shown to have capabilities for multiplexing (Liu et al., 2017) and the ability to detect SNPs (Nakamura et al., 2007, Ayukawa et al., 2017).

Additionally to this more research in needed to understand specific traits of fungal pathogens, in particular to fungicide resistance. For example, although the 120 bp and 800 bp inserts in the putative *CYP51* promotor region of *Z.tritici* have been linked to reduced sensitivity in azoles by many research groups (Chassot et al., 2008, Dooley,

2015), with an association between the 120 bp insertion and *CYP51* overexpression in isolates with reduced sensitivity (Cools et al., 2012), additional research is needed to ascertain the exact differences in isolates with and without these inserts. Although previous studies have suggested a R-type classification system for categorising *Z.tritici CYP51* variants with reduced sensitivity to azoles; different R-types being associated with SNPs or amino acid deletions in the CYP51 gene (Leroux et al., 2007), it is now suggested that a more complex system needs to be developed with the addition of compiling a database to allow a search for different combinations and insertions with complimentary azole sensitivity results to be identified with ease.

References

ALBERTA AG-INFO CENTRE. 2002. Alberta Fusarium graminearum Management Plan. [Online]. Available: https://www1.agric.gov.ab.ca/$department/deptdocs.nsf/all/agdex5210 [Accessed 1/3/18].

AL MASRI, A., ALISAAC, E., DEHNE, H. W., MAHLEIN, A.-K. & OERKE, E. C. 2016. Simultaneous hyperspectral, fluorescence and thermal imaging for monitoring Fusarium head blight of wheat. [Online]. Available: https://www.researchgate.net/publication/314375887_Simultaneous_hyperspectral_fluorescence_and_thermal_imaging_for_monitoring_Fusarium_head_blight_of_wheat [Accessed 3/6/17].

APS. 2017. *Septoria tritici* blotch (STB) of wheat [Online]. Available: http://www.apsnet.org/edcenter/intropp/lessons/fungi/ascomycetes/Pages/Septoria.aspx [Accessed 4/8/17].

AYUKAWA, Y., HANYUDA, S., FUJITA, N., KOMATSU, K. & ARIE, T. 2017. Novel loop-mediated isothermal amplification (LAMP) assay with a universal QProbe can detect SNPs determining races in plant pathogenic fungi. Scientific Reports, 7, 4253.

BANKS, J. N., RIZVI, R. H., BARKER, I., TURNER, J. A., RAHMAN, S. & NORTHWAY, B. J. 1996. Specific monoclonal antibodies to fusarium species and microdochium nivale. Food and Agricultural Immunology, 8, 249-268.

BECKER, E. M., HERRFURTH, C., IRMISCH, S., KOLLNER, T. G., FEUSSNER, I., KARLOVSKY, P. & SPLIVALLO, R. 2014. Infection of corn ears by *Fusarium spp.* induces the emission of volatile sesquiterpenes. Journal of Agricultural and Food Chemistry, 62, 5226-36.

BEN-ARI, T., ADRIAN, J., KLEIN, T., CALANCA, P., VAN DER VELDE, M. & MAKOWSKI, D. 2016. Identifying indicators for extreme wheat and maize yield losses. Agricultural and Forest Meteorology, 220, 130-140.

BOLTON, M. D., KOLMER, J. A. & GARVIN, D. F. 2008. Wheat leaf rust caused by *Puccinia triticina*. Molecular Plant Pathology, 9, 563-75.

BRACHACZEK, A., KACZMAREK, J. & JEDRYCZKA, M. 2016. Monitoring blackleg (Leptosphaeria spp.) ascospore release timing and quantity enables optimal fungicide application to improved oilseed rape yield and seed quality. European Journal of Plant Pathology, 145, 643-657.

BRAUN-KIEWNICK, A., ALTENBACH, D., OBERHANSLI, T., BITTERLIN, W. & DUFFY, B. 2011. A rapid lateral-flow immunoassay for phytosanitary detection of *Erwinia amylovora* and on-site fire blight diagnosis. Journal of Microbiological Methods, 87, 1-9.

BRAVO, C., MOSHOU, D., OBERTI, R., WEST, J., MCCARTNEY, A., BODRIA, L. & RAMON, H. 2004. Foliar disease detection in the field using optical sensor fusion. Agricultural Engineering International: CIGR Journal, 6, 1-14.

BROWN, J. K. M., CHARTRAIN, L., LASSERRE-ZUBER, P. & SAINTENAC, C. 2015. Genetics of resistance to *Zymoseptoria tritici* and applications to wheat breeding. Fungal Genetics and Biology, 79, 33-41.

BÜRLING, K., HUNSCHE, M. & NOGA, G. 2010. Quantum yield of non-regulated energy dissipation in PSII (Y(NO)) for early detection of leaf rust (*Puccinia triticina*) infection in susceptible and resistant wheat (Triticum aestivum L.) cultivars. Precision Agriculture, 11, 703-716.

BÜRLING, K., HUNSCHE, M. & NOGA, G. 2011. Use of blue–green and chlorophyll fluorescence measurements for differentiation between nitrogen deficiency and pathogen infection in winter wheat. Journal of Plant Physiology, 168, 1641-1648.

BUSHNELL, W., HAZEN, B., PRITSCH, C. & LEONARD, K. 2003. Histology and physiology of Fusarium head blight. Fusarium head blight of wheat and barley, 512, 44-83.

CAHILL, D. & HARDHAM, A. 1994. A dipstick immunoassay for the specific detection of *Phytophthora cinnamomi* in soils. Phytopathology, 84, 1284-1292.

CAO, X., YAO, D., ZHOU, Y., WEST, J. S., XU, X., LUO, Y., DING, K., FAN, J. & DUAN, X. 2016. Detection and quantification of airborne inoculum of Blumeria graminis f. sp. tritici using quantitative PCR. European Journal of Plant Pathology, 146, 225-229.

CHAERLE, L., HAGENBEEK, D., DE BRUYNE, E., VALCKE, R. & VAN DER STRAETEN, D. 2004. Thermal and chlorophyll-fluorescence imaging distinguish plant-pathogen interactions at an early stage. Plant Cell Physiology, 45, 887-96.

CHASSOT, C., HUGELSHOFER, U., SIEROTZKI, H. & GISI, U. Sensitivity of CYP51 genotypes to DMI fungicides in mycosphaerella graminicola. Modern fungicides and antifungal compounds V: 15th International Reinhardsbrunn Symposium, Friedrichroda, Germany, May 6-10, 2007, 2008. Deutsche Phytomedizinische Gesellschaft eV Verlag, 129-136.

CIMMYT. 2010. Rust - Stem: Rust Mapper [Online]. Available: http://apps.cimmyt.org/gis/RustMapper/index.htm [Accessed 3/4/16].

COOLS, H. J., BAYON, C., ATKINS, S., LUCAS, J. A. & FRAAIJE, B. A. 2012. Overexpression of the sterol 14alpha-demethylase gene (MgCYP51) in *Mycosphaerella graminicola* isolates confers a novel azole fungicide sensitivity phenotype. Pest Management Science, 68, 1034-40.

COOLS, H. J. & FRAAIJE, B. A. 2008. Are azole fungicides losing ground against Septoria wheat disease? Resistance mechanisms in *Mycosphaerella graminicola*. Pest Management Science, 64, 681-684.

COOLS, H. J. & FRAAIJE, B. A. 2013. Update on mechanisms of azole resistance in *Mycosphaerella graminicola* and implications for future control. Pest Management Science, 69, 150-5.

COOLS, H. J., PARKER, J. E., KELLY, D. E., LUCAS, J. A., FRAAIJE, B. A. & KELLY, S. L. 2010. Heterologous Expression of Mutated Eburicol 14α-Demethylase (CYP51) Proteins of *Mycosphaerella graminicola* To Assess Effects on Azole Fungicide Sensitivity and Intrinsic Protein Function. Applied and Environmental Microbiology, 76, 2866-2872.

COOPER, M. A. & SINGLETON, V. T. 2007. A survey of the 2001 to 2005 quartz crystal microbalance biosensor literature: applications of acoustic physics to the analysis of biomolecular interactions. Journal of Molecular Recognition, 20, 154-84.

COUSIN, A., MEHRABI, R., GUILLEROUX, M., DUFRESNE, M., T, V. D. L., WAALWIJK, C., LANGIN, T. & KEMA, G. H. 2006. The MAP kinase-encoding gene MgFus3 of the non-appressorium phytopathogen *Mycosphaerella graminicola* is required for penetration and in vitro pycnidia formation. Molecular Plant Pathology, 7, 269-78.

CROPMONITOR. 2017. Defra Winter Wheat Commercial Crops Disease Survey 2017 [Online]. Available: http://www.cropmonitor.co.uk/cmsReport.cfm?id=49 [Accessed 9/2/18].

DANKS, C. & BARKER, I. 2000. On-site detection of plant pathogens using lateral-flow devices. European and Mediterranean Plant Protection Organization (EPPO) Bulletin, 30, 421-426.

DARAIN, F., PARK, S. U. & SHIM, Y. B. 2003. Disposable amperometric immunosensor system for rabbit IgG using a conducting polymer modified screen-printed electrode. Biosensors and Bioelectronics, 18, 773-80.

DENSCHLAG, C., VOGEL, R. F. & NIESSEN, L. 2012. Hyd5 gene-based detection of the major gushing-inducing *Fusarium* spp. in a loop-mediated isothermal amplification (LAMP) assay. International Journal of Food Microbiology, 156, 189-196.

DESJARDINS, A. E. 2006. Fusarium mycotoxins: chemistry, genetics, and biology. American Phytopathological Society, 12, 268.

DOOLEY, H. 2015. Fungicide-resistance management tactics: impacts on *Zymoseptoria tritici* populations. University of Reading.

DUNCAN, K. E. & HOWARD, R. J. 2000. Cytological analysis of wheat infection by the leaf blotch pathogen *Mycosphaerella graminicola*. Mycological Research, 104, 1074-1082.

DUVIVIER, M., DEDEURWAERDER, G., BATAILLE, C., DE PROFT, M. & LEGREVE, A. 2016. Real-time PCR quantification and spatio-temporal distribution of airborne inoculum of *Puccinia triticina* in Belgium. European Journal of Plant Pathology, 145, 405-420.

DUVIVIER, M., DEDEURWAERDER, G., DE PROFT, M., MOREAU, J.-M. & LEGRÈVE, A. 2013. Real-time PCR quantification and spatio-temporal distribution of airborne inoculum of *Mycosphaerella graminicola* in Belgium. European Journal of Plant Pathology, 137, 325-341.

ECPA. 2013. R&D Trends for Chemical Crop Protection Products and the Position of the European Market. Phillips McDougall.

EIBEL, P., WOLF, G. A. & KOCH, E. 2005. Detection of *Tilletia caries*, Causal Agent of Common Bunt of Wheat, by ELISA and PCR. Journal of Phytopathology, 153, 297-306.

ELYASI-GOMARI, S. 2010. Virulence of *Puccinia triticina* on wheat in Iran. African Journal of Plant Science, 4, 026-031.

ERIKSEN, L. & MUNK, L. 2003. The occurrence of *Mycosphaerella graminicola* and its anamorph *Septoria tritici* in winter wheat during the growing season. European Journal of Plant Pathology, 109, 253-259.

EYAL, Z. 1987. The Septoria diseases of wheat: concepts and methods of disease management, Cimmyt.

FANG, Y. & RAMASAMY, R. P. 2015. Current and Prospective Methods for Plant Disease Detection. Biosensors, 5, 537-561.

FANJUL-BOLADO, P., GONZÁLEZ-GARCÍA, M. B. & COSTA-GARCÍA, A. 2005. Amperometric detection in TMB/HRP-based assays. Analytical and Bioanalytical chemistry, 382, 297-302.

FAO. 2017. Crop Prospects and Food Situation No. 2 [Online]. FAO. Available: http://www.fao.org/documents/card/en/c/785da6bc-54db-49ad-9042-ad6041c85dc2/ [Accessed 8/9/17].

FEI, J., DOU, W. & ZHAO, G. 2016. Amperometric immunoassay for the detection of *Salmonella pullorum* using a screen - printed carbon electrode modified with gold nanoparticle-coated reduced graphene oxide and immunomagnetic beads. Microchimica Acta, 183, 757-764.

FERNÁNDEZ-BALDO, M. A., MESSINA, G. A., SANZ, M. I. & RABA, J. 2010. Microfluidic Immunosensor with Micromagnetic Beads Coupled to Carbon-Based Screen-Printed Electrodes (SPCEs) for Determination of *Botrytis cinerea* in Tissue of Fruits. Journal of Agricultural and Food Chemistry, 58, 11201-11206.

FERNÁNDEZ-ORTUÑO, D., LOZA-REYES, E., ATKINS, S. L. & FRAAIJE, B. A. 2010. The CYP51C gene, a reliable marker to resolve interspecific phylogenetic relationships within the Fusarium species complex and a novel target for species-specific PCR. International Journal of Food Microbiology, 144, 301-309.

FIGUEROA, M., HAMMOND-KOSACK, K. E. & SOLOMON, P. S. 2017. A review of wheat diseases-a field perspective. Molecular Plant Pathology.

FONES, H. & GURR, S. 2015. The impact of *Septoria tritici* Blotch disease on wheat: An EU perspective. Fungal Genetics and Biology, 79, 3-7.

FRAAIJE, B., BURNETT, F., COOLS, H., CLARK, W., PAVELEY, N., NORMAN, K. & LUCAS, J. 2011. Understanding evolution and selection of azole resistance mechanisms in UK populations of *Mycosphaerella graminicola*. Project Report No. 475. HGCA.

FRAG-UK 2016. FRAG-UK statement on SDHI fungicides and resistance risk in cereals.

GAO, L., CHEN, W., LIU, T. & LIU, B. 2013. An immunofluorescence assay for the detection of wheat rust species using monoclonal antibody against urediniospores of *Puccinia triticina*. Journal of Applied Microbiology, 115, 1023-8.

GAO, L., YU, H. X., KANG, X. H., SHEN, H. M., LI, C., LIU, T. G., LIU, B. & CHEN, W. Q. 2016. Development of SCAR Markers and an SYBR Green Assay to Detect *Puccinia striiformis* f. sp *tritici* in Infected Wheat Leaves. Plant Disease, 100, 1840-1847.

GARG, S., PANDEY, D., TAJ, G., GOEL, A. & KUMAR, A. 2014. TRIPATH: A Biological Genetic and Genomic Database of Three Economically Important Fungal Pathogen of Wheat – Rust: Smut: Bunt. Bioinformation, 10, 466-468.

GHAFFARI, R., ZHANG, F., ILIESCU, D., HINES, E., LEESON, M. S. & NAPIER, R. 2011. Field asymmetric ion mobility spectrometry based plant disease detection: intelligent systems approach. Applied Signal and Image Processing: Multidisciplinary Advancements, 2, 102-114.

GIESEN, C., JAKUBOWSKI, N., PANNE, U. & WELLER, M. G. 2010. Comparison of ICP-MS and photometric detection of an immunoassay for the determination of ochratoxin A in wine. Journal of Analytical Atomic Spectrometry, 25, 1567-1572.

GOODWIN, S. B., BEN M'BAREK, S., DHILLON, B., WITTENBERG, A. H. J., CRANE, C. F., HANE, J. K., FOSTER, A. J., VAN DER LEE, T. A. J., GRIMWOOD, J., AERTS, A., ANTONIW, J., BAILEY, A., BLUHM, B., BOWLER, J., BRISTOW, J., VAN DER BURGT, A., CANTO-CANCHÉ, B., CHURCHILL, A. C. L., CONDE-FERRÀEZ, L., COOLS, H. J., COUTINHO, P. M., CSUKAI, M., DEHAL, P., DE WIT, P., DONZELLI, B., VAN DE GEEST, H. C., VAN HAM, R. C. H. J., HAMMOND-KOSACK, K. E., HENRISSAT, B., KILIAN, A., KOBAYASHI, A. K., KOOPMANN, E., KOURMPETIS, Y., KUZNIAR, A., LINDQUIST, E., LOMBARD, V., MALIEPAARD, C., MARTINS, N., MEHRABI, R., NAP, J. P. H., PONOMARENKO, A., RUDD, J. J., SALAMOV, A., SCHMUTZ, J., SCHOUTEN, H. J., SHAPIRO, H., STERGIOPOULOS, I., TORRIANI, S. F. F., TU, H., DE VRIES, R. P., WAALWIJK, C., WARE, S. B., WIEBENGA, A., ZWIERS, L.-H., OLIVER, R. P., GRIGORIEV, I. V. & KEMA, G. H. J. 2011. Finished Genome of the Fungal Wheat Pathogen *Mycosphaerella graminicola* reveals dispensome dtructure, chromosome plasticity, and stealth pathogenesis. PLOS Genetics, 7, e1002070.

GOSWAMI, R. S. & KISTLER, H. C. 2004. Heading for disaster: *Fusarium graminearum* on cereal crops. Molecular Plant Pathology, 5, 515-25.

GUO, J.-R., SCHNIEDER, F. & VERREET, J.-A. 2006. Presymptomatic and quantitative detection of *Mycosphaerella graminicola* development in wheat using a real-time PCR assay. FEMS Microbiology Letters, 262, 223-229.

HAWKINS, N. J. & FRAAIJE, B. A. 2016. Predicting Resistance by Mutagenesis: Lessons from 45 Years of MBC Resistance. Frontiers in Microbiology, 7, 1814.

HEITMANN, V., REIß, B. & WEGENER, J. 2007. The Quartz Crystal Microbalance in Cell Biology: Basics and Applications. In: STEINEM, C. & JANSHOFF, A. (eds.) Piezoelectric Sensors. Springer Berlin Heidelberg.

HILL, N., SCHWARZ, P., DAHLEEN, L., NEATE, S., HORSLEY, R., GLENN, A. & O'DONNELL, K. 2006. ELISA Analysis for in Barley. Crop science, 46, 2636-2642.

HU, G., LINNING, R., MCCALLUM, B., BANKS, T., CLOUTIER, S., BUTTERFIELD, Y., LIU, J., KIRKPATRICK, R., STOTT, J., YANG, G., SMAILUS, D., JONES, S., MARRA, M., SCHEIN, J. & BAKKEREN, G. 2007. Generation of a wheat leaf rust, *Puccinia triticina*, EST database from stage-specific cDNA libraries. Molecular Plant Pathology, 8, 451-67.

HUANG, C., SUN, Z., YAN, J., LUO, Y., WANG, H. & MA, Z. 2011. Rapid and Precise Detection of Latent Infections of Wheat Stripe Rust in Wheat Leaves using Loop-Mediated Isothermal Amplification. Journal of Phytopathology, 159, 582-584.

HUNTER, T., COKER, R. & ROYLE, D. 1999. The teleomorph stage, *Mycosphaerella graminicola*, in epidemics of *septoria tritici* blotch on winter wheat in the UK. Plant pathology, 48, 51-57.

JAIN, M., OLSEN, H. E., PATEN, B. & AKESON, M. 2016. The Oxford Nanopore MinION: delivery of nanopore sequencing to the genomics community. Genome Biology, 17, 239.

JANSEN, R. M. C., HOFSTEE, J. W., WILDT, J., VERSTAPPEN, F. W. A., BOUWMEESTER, H. J. & VAN HENTEN, E. J. 2009. Induced plant volatiles allow sensitive monitoring of plant health status in greenhouses. Plant Signaling And Behavior, 4, 824-829.

JAROCKA, U., RADECKA, H., MALINOWSKI, T., MICHALCZUK, L. & RADECKI, J. 2013. Detection of Prunus Necrotic Ringspot Virus in plant extracts with impedimetric immunosensor based on glassy carbon electrode. Electroanalysis, 25, 433-438.

JAROCKA, U., WĄSOWICZ, M., RADECKA, H., MALINOWSKI, T., MICHALCZUK, L. & RADECKI, J. 2011. Impedimetric immunosensor for detection of Plum Pox Virus in plant extracts. Electroanalysis, 23, 2197-2204.

JI, F., CHEN, Z., XU, J., LU, Q. & SHI, J. 2008. Development of the monoclonal antibody to deoxynivalenol. Wei Sheng Wu Xue Bao, 48, 929-34.

JIAO, K., SUN, W. & ZHANG, S.-S. 2000. Sensitive detection of a plant virus by electrochemical enzyme-linked immunoassay. Fresenius' Journal of Analytical Chemistry, 367, 667-671.

JØRGENSEN, L. N., HOVMØLLER, M. S., HANSEN, J. G., LASSEN, P., CLARK, B., BAYLES, R., RODEMANN, B., FLATH, K., JAHN, M. & GORAL, T. 2014. IPM strategies and their dilemmas including an introduction to www. eurowheat. org. Journal of Integrative Agriculture, 13, 265-281.

KEMA, G. H. & VAN SILFHOUT, C. H. 1997. Genetic variation for virulence and resistance in the wheat-Mycosphaerella graminicola pathosystem III. Comparative seedling and adult plant experiments. Phytopathology, 87, 266-272.

KHATER, M., DE LA ESCOSURA-MUÑIZ, A. & MERKOÇI, A. 2017. Biosensors for plant pathogen detection. Biosensors and Bioelectronics, 93, 72-86.

KIKOT, G. E., HOURS, R. A. & ALCONADA, T. M. 2009. Contribution of cell wall degrading enzymes to pathogenesis of *Fusarium graminearum*: a review. Journal of Basic Microbiology, 49, 231-41.

KOLMER, J. 2013. Leaf Rust of Wheat: Pathogen Biology, Variation and Host Resistance. Forests, 4, 70.

KOSTOV, K., VERSTAPPEN, E. C. P., BERGERVOET, J. H. W., DE WEERDT, M., SCHOEN, C. D., SLAVOV, S. & BONANTS, P. J. M. 2016. Multiplex detection and identification of *Phytophthora* spp. using target-specific primer extension and Luminex xTAG technology. Plant Pathology, 65, 1008-1021.

KUTILEK, V., LEE, R. & KITTO, G. B. 2001. Development of Immunochemical Techniques for Detecting Karnal Bunt in Wheat. Food and Agricultural Immunology, 13, 103-114.

LANE, C. R., HOBDEN, E., WALKER, L., BARTON, V. C., INMAN, A. J., HUGHES, K. J. D., SWAN, H., COLYER, A. & BARKER, I. 2007. Evaluation of a rapid diagnostic field test kit for identification of *Phytophthora* species, including *P. ramorum* and *P. kernoviae* at the point of inspection. Plant Pathology, 56, 828-835.

LANNOU, C. 2012. Variation and selection of quantitative traits in plant pathogens. Annual Review of Phytopathology, 50, 319-338.

LEE, G.-Y., PARK, J.-H., CHANG, Y. W., CHO, S., KANG, M.-J. & PYUN, J.-C. 2017. Redox cycling-based immunoassay for detection of carcinogenic embryonic antigen. Analytica Chimica Acta, 971, 33-39.

LEE, H. M., SONG, S. O., CHA, S. H., WEE, S. B., BISCHOFF, K., PARK, S. W., SON, S. W., KANG, H. G. & CHO, M. H. 2013. Development of a monoclonal antibody against deoxynivalenol for magnetic nanoparticle-based extraction and an enzyme-linked immunosorbent assay. Journal of Veterinary Science, 14, 143-50.

LEE, J.-K., PARK, M., JOSE, J., KANG, M.-J. & PYUN, J.-C. 2012. Electrochemical ELISA based on Escherichia coli with autodisplayed Z-domains. Sensors and Actuators B: Chemical, 175, 46-52.

LENDENMANN, M. H., CROLL, D., STEWART, E. L. & MCDONALD, B. A. 2014. Quantitative trait locus mapping of melanization in the plant pathogenic fungus *Zymoseptoria tritici*. G3: Genes, Genomes, Genetics, 4, 2519-2533.

LEROUX, P., ALBERTINI, C., GAUTIER, A., GREDT, M. & WALKER, A.-S. 2007. Mutations in the CYP51 gene correlated with changes in sensitivity to sterol 14α-demethylation inhibitors in field isolates of *Mycosphaerella graminicola*. Pest Management Science, 63, 688-698.

LEROUX, P. & WALKER, A. S. 2011. Multiple mechanisms account for resistance to sterol 14α-demethylation inhibitors in field isolates of *Mycosphaerella graminicola*. Pest management science, 67, 44-59.

LI, Q., LV, S., LU, M., LIN, Z. & TANG, D. 2016. Potentiometric competitive immunoassay for determination of aflatoxin B1 in food by using antibody-labeled gold nanoparticles. Microchimica Acta, 183, 2815-2822.

LIEVENS, B. & THOMMA, B. P. 2005. Recent developments in pathogen detection arrays: implications for fungal plant pathogens and use in practice. Phytopathology, 95, 1374-1380.

LIHUA, C., SHICHANG, X., RUIMING, L., TAIGUO, L. & WANQUAN, C. 2008. Early molecular diagnosis and detection of *Puccinia striiformis* f. sp. *tritici* in China. Letters in Applied Microbiology, 46, 501-6.

LIU, N., ZOU, D., DONG, D., YANG, Z., AO, D., LIU, W. & HUANG, L. 2017. Development of a multiplex loop-mediated isothermal amplification method for the simultaneous detection of *Salmonella* spp. and *Vibrio parahaemolyticus*. Scientific Reports, 7, 45601.

LOVELL, D. J., HUNTER, T., POWERS, S. J., PARKER, S. R. & VAN DEN BOSCH, F. 2004. Effect of temperature on latent period of *septoria* leaf blotch on winter wheat under outdoor conditions. Plant Pathology, 53, 170-181.

LU, P., MARQUARDT, R., FROHLICH, A. & MILLS, J. 1994. Detection of *Penicillium aurantiogriseum* by ELISA utilizing antibodies produced against its exoantigens. Microbiology, 140, 3267-3276.

LUI, L., VIKRAM, A., HAMZEHZARGHANI, H. & KUSHALAPPA, A. C. 2005. Discrimination of three fungal diseases of potato tubers based on volatile metabolic profiles developed using GC/MS. Potato Research, 48, 85-96.

MALDONADO-RAMIREZ, S. L., SCHMALE, D. G., SHIELDS, E. J. & BERGSTROM, G. C. 2005. The relative abundance of viable spores of *Gibberella zeae* in the planetary boundary layer

suggests the role of long-distance transport in regional epidemics of Fusarium head blight. Agricultural and Forest Meteorology, 132, 20-27.

MARKOM, M. A., SHAKAFF, A. Y. M., ADOM, A. H., AHMAD, M. N., HIDAYAT, W., ABDULLAH, A. H. & FIKRI, N. A. 2009. Intelligent electronic nose system for basal stem rot disease detection. Computers and Electronics in Agriculture, 66, 140-146.

MARZANI, Q. A. 2011. Fungicide resistance and efficacy for control of *Pyrenophora teres* and *Mycosphaerella graminicola* on barley and wheat. University of Nottingham.

MATSUDA, R., RODRIGUEZ, E., SURESH, D. & HAGE, D. S. 2015. Chromatographic immunoassays: strategies and recent developments in the analysis of drugs and biological agents.

MCCARTNEY, H. A., FOSTER, S. J., FRAAIJE, B. A. & WARD, E. 2003. Molecular diagnostics for fungal plant pathogens. Pest Management Science, 59, 129-42.

MCINTOSH, R., WELLINGS, C. & PARK, R. 1995. Wheat rusts: an atlas of resistance genes, CSIRO PUBLISHING.

MCMULLEN, M., BERGSTROM, G., DE WOLF, E., DILL-MACKY, R., HERSHMAN, D., SHANER, G. & VAN SANFORD, D. 2012. A unified effort to fight an enemy of wheat and barley: Fusarium Head Blight. Plant Disease, 96, 1712-1728.

MENDES, R. K., FERREIRA, D. C. M., CARVALHAL, R. F., PERONI, L. A., STACH-MACHADO, D. R. & KUBOTA, L. T. 2009. Development of an electrochemical immunosensor for *Phakopsora pachyrhizi* detection in the early diagnosis of soybean rust. Journal of the Brazilian Chemical Society, 20, 795-801.

MENTLAK, T. A., KOMBRINK, A., SHINYA, T., RYDER, L. S., OTOMO, I., SAITOH, H., TERAUCHI, R., NISHIZAWA, Y., SHIBUYA, N., THOMMA, B. P. H. J. & TALBOT, N. J. 2012. Effector-Mediated Suppression of chitin-triggered immunity by *Magnaporthe oryzae* is necessary for rice blast disease. The Plant Cell, 24, 322-335.

MISTRY, K. K., LAYEK, K., CHELL, T. N., CHAUDHURI, C. R. & SAHA, H. 2016. Design and development of an amperometric immunosensor based on screen-printed electrodes. Analytical Methods, 8, 3096-3101.

MORAIS, D., LAVAL, V., SACHE, I. & SUFFERT, F. 2015. Comparative pathogenicity of sexual and asexual spores of *Zymoseptoria tritici* (*Septoria tritici* blotch) on wheat leaves. Plant Pathology, 64, 1429-1439.

MULLINS, J. G., PARKER, J. E., COOLS, H. J., TOGAWA, R. C., LUCAS, J. A., FRAAIJE, B. A., KELLY, D. E. & KELLY, S. L. 2011. Molecular modelling of the emergence of azole resistance in *Mycosphaerella graminicola*. PLoS One, 6, e20973.

NAKAMURA, N., ITO, K., TAKAHASHI, M., HASHIMOTO, K., KAWAMOTO, M., YAMANAKA, M., TANIGUCHI, A., KAMATANI, N. & GEMMA, N. 2007. Detection of six single-nucleotide polymorphisms associated with rheumatoid arthritis by a loop-mediated isothermal amplification method and an electrochemical DNA chip. Analytical Chemistry, 79, 9484-93.

NARVANKAR, D. S., SINGH, C. B., JAYAS, D. S. & WHITE, N. D. G. 2009. Assessment of soft X-ray imaging for detection of fungal infection in wheat. Biosystems Engineering, 103, 49-56.

NIESSEN, L. & VOGEL, R. F. 2010. Detection of *Fusarium graminearum* DNA using a loop-mediated isothermal amplification (LAMP) assay. International Journal of Food Microbiology, 140, 183-191.

NOTOMI, T., OKAYAMA, H., MASUBUCHI, H., YONEKAWA, T., WATANABE, K., AMINO, N. & HASE, T. 2000. Loop-mediated isothermal amplification of DNA. Nucleic Acids Research, 28, e63.

OLMSTEAD, J. W., LANG, G. A. & GROVE, G. G. 2001. Assessment of severity of powdery mildew infection of sweet cherry leaves by digital image analysis. HortScience, 36, 107-111.

OLSSON, C. & HETBERG, N. 1997. Sensitivity of the ELISA test to detect *Phytophthora fragariae* var. *rubi* in raspberry roots. Journal of Phytopathology, 145, 285-288.

PARIAUD, B., BERG, F., BOSCH, F., POWERS, S. J., KALTZ, O. & LANNOU, C. 2013a. Shared influence of pathogen and host genetics on a trade-off between latent period and spore production capacity in the wheat pathogen, *Puccinia triticina*. Evolutionary Applications, 6, 303-12.

PARKASH, O., YEAN, C. & SHUEB, R. 2014. Screen Printed Carbon Electrode Based Electrochemical Immunosensor for the Detection of Dengue NS1 Antigen. Diagnostics, 4, 165.

PRASHAR, A., YILDIZ, J., MCNICOL, J. W., BRYAN, G. J. & JONES, H. G. 2013. Infra-red Thermography for High Throughput Field Phenotyping in *Solanum tuberosum*. PLOS ONE, 8, e65816.

PRIESTLEY, R., MOHAMMED, C. & DEWEY, F. 1994. The development of monoclonal antibody-based ELISA and dipstick assays for the detection and identification of Armillaria species in infected wood. Modem assays for plant pathogenic fungi. CAB International, Oxford, 149-156.

QUAEDVLIEG, W., KEMA, G. H. J., GROENEWALD, J. Z., VERKLEY, G. J. M., SEIFBARGHI, S., RAZAVI, M., MIRZADI GOHARI, A., MEHRABI, R. & CROUS, P. W. 2011. Zymoseptoria gen. nov.: a new genus to accommodate *Septoria*-like species occurring on graminicolous hosts. Persoonia : Molecular Phylogeny and Evolution of Fungi, 26, 57-69.

RASTOGI, S. K., GIBBON, S., BRANEN, J. R. & BRANEN, A. L. Amperometric Detection of Staphylococcal Enterotoxin B in milk using Magnetic Bead-Based Immunoassay on Disposable Screen Printed Carbon Electrode Strip. Nanotech Conference & Expo, 2009.

RAY, M., RAY, A., DASH, S., MISHRA, A., ACHARY, K. G., NAYAK, S. & SINGH, S. 2017. Fungal disease detection in plants: Traditional assays, novel diagnostic techniques and biosensors. Biosensors and Bioelectronics, 87, 708-723.

REIS, E. M., ZANATTA, M., CARMONA, M. & MENTEN, J. O. M. 2015. Relationship between IC50 determined in vitro/in vivo and the fungicide rate used in the Field. Summa Phytopathologica, 41, 49-53.

ROELFS, A. P. 1992. Rust diseases of wheat: concepts and methods of disease management, Cimmyt.

RÖMER, C., BÜRLING, K., HUNSCHE, M., RUMPF, T., NOGA, G. & PLÜMER, L. 2011. Robust fitting of fluorescence spectra for pre-symptomatic wheat leaf rust detection with Support Vector Machines. Computers and Electronics in Agriculture, 79, 180-188.

ROWE, M. & DINH, A. *Fusarium graminearum* spore detection using magnetic resonance force microscopy. 2012 25th IEEE Canadian Conference on Electrical and Computer Engineering (CCECE), April 29 2012-May 2 2012 2012. 1-4.

SANDERS, M., GUO, Y., IYER, A., GARCIA, Y. R., GALVITA, A., HEYERICK, A., DEFORCE, D., RISSEEUW, M. D., VAN CALENBERGH, S., BRACKE, M., EREMIN, S., MADDER, A. & DE SAEGER, S. 2014. An immunogen synthesis strategy for the development of specific anti-deoxynivalenol monoclonal antibodies. Food Additives & Contaminants: Part A: Chemistry, Analysis, Control, Exposure & Risk Assessment, 31, 1751-9.

SCHAAD, N. W. & FREDERICK, R. D. 2002. Real-time PCR and its application for rapid plant disease diagnostics. Canadian journal of plant pathology, 24, 250-258.

SCHMAILE, D. & MUNKVOLD, G. 2009. Mycotoxins in crops: a threat to human and domestic animal health. The Plant Health Instructor. DOI: 10.1094. PHI-I-2009-0715-01.

SENOVA. Available: http://www.senova.uk.com/jb-diego/4592743193 [Accessed 6/7/17].

SHARMA, A., KAUSHAL, A. & KULSHRESTHA, S. 2017. A Nano-Au/C-MWCNT based label free amperometric immunosensor for the detection of capsicum chlorosis virus in bell pepper. Archives of Virology, 162, 2047-2052.

SHETTY, N. P., KRISTENSEN, B., NEWMAN, M.-A., MØLLER, K., GREGERSEN, P. L. & JØRGENSEN, H. L. 2003. Association of hydrogen peroxide with restriction of *Septoria tritici* in resistant wheat. Physiological and Molecular Plant Pathology, 62, 333-346.

SILVA, G. J., ANDRADE, C. A., OLIVEIRA, I. S., DE MELO, C. P. & OLIVEIRA, M. D. 2013. Impedimetric sensor for toxigenic *Penicillium sclerotigenum* detection in yam based on magnetite-poly (allylamine hydrochloride) composite. Journal of Colloid and Interface Science, 396, 258-63.

SINGH, R. P., SINGH, P. K., RUTKOSKI, J., HODSON, D. P., HE, X., JØRGENSEN, L. N., HOVMØLLER, M. S. & HUERTA-ESPINO, J. 2016. Disease impact on wheat yield potential and prospects of genetic control. Annual Review of Phytopathology, 54, 303-322.

SKOTTRUP, P., FROKIAER, H., HEARTY, S., O'KENNEDY, R., HEJGAARD, J., NICOLAISEN, M. & JUSTESEN, A. F. 2007a. Monoclonal antibodies for the detection of *Puccinia striiformis* urediniospores. Mycological Research, 111, 332-8.

SKOTTRUP, P., HEARTY, S., FROKIAER, H., LEONARD, P., HEJGAARD, J., O'KENNEDY, R., NICOLAISEN, M. & JUSTESEN, A. F. 2007b. Detection of fungal spores using a generic surface plasmon resonance immunoassay. Biosensors and Bioelectronics, 22, 2724-9.

SOLEIMAN, N. H., SOLIS, I., SOLIMAN, M. H., SILLERO, J. C., VILLEGAS, D., ALVARO, F., ROYO, C., SERRA, J., AMMAR, K. & MARTÍNEZ-MORENO, F. 2016. Short communication: Emergence of a new race of leaf rust with combined virulence to Lr14a and Lr72 genes on durum wheat. 2016, 14, -7.

SONG, X., RAMPITSCH, C., SOLTANI, B., MAUTHE, W., LINNING, R., BANKS, T., MCCALLUM, B. & BAKKEREN, G. 2011. Proteome analysis of wheat leaf rust fungus, *Puccinia triticina*, infection structures enriched for haustoria. Proteomics, 11, 944-63.

STAMMLER, G. & SEMAR, M. 2011. Sensitivity of *Mycosphaerella graminicola* (anamorph: *Septoria tritici*) to DMI fungicides across Europe and impact on field performance. European and Mediterranean Plant Protection Organization (EPPO) Bulletin, 41, 149-155.

SU, Y., YANG, Y., PENG, Q., ZHOU, D., CHEN, Y., WANG, Z., XU, L. & QUE, Y. 2016. Development and application of a rapid and visual loop-mediated isothermal amplification for the detection of *Sporisorium scitamineum* in sugarcane. Scientific Reports, 6, 23994.

SUFFERT, F., SACHE, I. & LANNOU, C. 2011. Early stages of *septoria tritici* blotch epidemics of winter wheat: build-up, overseasoning, and release of primary inoculum. Plant Pathology, 60, 166-177.

SUFFERT, F., SACHE, I. & LANNOU, C. 2013. Assessment of quantitative traits of aggressiveness in *Mycosphaerella graminicola* on adult wheat plants. Plant Pathology, 62, 1330-1341.

TAMURA, K., DUDLEY, J., NEI, M. & KUMAR, S. 2007. MEGA4: Molecular Evolutionary Genetics Analysis (MEGA) Software Version 4.0. Molecular Biology and Evolution, 24, 1596-1599.

TEAGASC 2017. 2015 - SDHI resistant *Septoria* found in the field - Teagasc | Agriculture and Food Development Authority.

TRAIL, F. 2009. For blighted waves of grain: *Fusarium graminearum* in the postgenomics era. Plant physiology, 149, 103-110.

TURNER, A. P. F., KARUBE, I. & WILSON, G. S. 1987. Biosensors: fundamentals and applications, Oxford University Press.

UAUY, C. 2017. Wheat genomics comes of age. Current Opinion in Plant Biology, 36, 142-148.

VAN DER VLUGT, R. A. A., VAN RAAIJ, H., DE WEERDT, M. & BERGERVOET, J. H. W. 2015. Multiplex detection of plant pathogens through the Luminex Magplex Bead System. In: LACOMME, C. (ed.) Plant Pathology: Techniques and Protocols. New York, NY: Springer New York.

VIKRAM, A., LUI, L. H., HOSSAIN, A. & KUSHALAPPA, A. C. 2006. Metabolic fingerprinting to discriminate diseases of stored carrots. Annals of Applied Biology, 148, 17-26.

VOLPE, G., DRAISCI, R., PALLESCHI, G. & COMPAGNONE, D. 1998. 3, 3', 5, 5'-Tetramethylbenzidine as electrochemical substrate for horseradish peroxidase based enzyme immunoassays. A comparative study. Analyst, 123, 1303-1307.

WEST, J. S., CANNING, G. G. M., PERRYMAN, S. A. & KING, K. 2017. Novel Technologies for the detection of *Fusarium* head blight disease and airborne inoculum. Tropical Plant Pathology, 1-7.

WIECZOREK, T. M., BERG, G., SEMAŠKIENĖ, R., MEHL, A., SIEROTZKI, H., STAMMLER, G., JUSTESEN, A. F. & JØRGENSEN, L. N. 2015. Impact of DMI and SDHI fungicides on disease

control and CYP51 mutations in populations of *Zymoseptoria tritici* from Northern Europe. European Journal of Plant Pathology, 143, 861-871.

WONG, Y. Y., NG, S. P., NG, M. H., SI, S. H., YAO, S. Z. & FUNG, Y. S. 2002. Immunosensor for the differentiation and detection of Salmonella species based on a quartz crystal microbalance. Biosensors and Bioelectronics, 17, 676-84.

XU, J., LINNING, R., FELLERS, J., DICKINSON, M., ZHU, W., ANTONOV, I., JOLY, D. L., DONALDSON, M. E., EILAM, T., ANIKSTER, Y., BANKS, T., MUNRO, S., MAYO, M., WYNHOVEN, B., ALI, J., MOORE, R., MCCALLUM, B., BORODOVSKY, M., SAVILLE, B. & BAKKEREN, G. 2011. Gene discovery in EST sequences from the wheat leaf rust fungus *Puccinia triticina* sexual spores, asexual spores and haustoria, compared to other rust and corn smut fungi. BMC Genomics, 12, 161.

YANG, F., JACOBSEN, S., JØRGENSEN, H. J., COLLINGE, D. B., SVENSSON, B. & FINNIE, C. 2013. *Fusarium graminearum* and its interactions with cereal heads: studies in the proteomics era. Frontiers in plant science, 4, 213-17.

YU, L., GASKELL, S. J. & BROOKMAN, J. L. 1998. Epitope mapping of monoclonal antibodies by mass spectrometry: identification of protein antigens in complex biological systems. Journal of The American Society for Mass Spectrometry, 9, 208-15.

ZEZZA, F., PASCALE, M., MULE, G. & VISCONTI, A. 2006. Detection of *Fusarium culmorum* in wheat by a surface plasmon resonance-based DNA sensor. Journal of Microbiological Methods, 66, 529-37.

ZHANG, J., SU, X. D. & O'SHEA, S. J. 2002. Antibody/antigen affinity behavior in liquid environment with electrical impedance analysis of quartz crystal microbalances. Biophysical Chemistry, 99, 31-41.

ZHAO, Y., LIU, L., KONG, D., KUANG, H., WANG, L. & XU, C. 2014. Dual Amplified Electrochemical Immunosensor for Highly Sensitive Detection of *Pantoea stewartii* sbusp. *stewartii.* ACS Applied Materials and Interfaces, 6, 21178-21183.

ZHENG, M. Z., RICHARD, J. L. & BINDER, J. 2006. A review of rapid methods for the analysis of mycotoxins. Mycopathologia, 161, 261-73.

ZHENG, Y., LUO, Y., ZHOU, Y., ZENG, X., DUAN, X., CAO, X., SONG, Y. & WANG, B. 2013. Real-time PCR quantification of latent infection of wheat powdery mildew in the field. European Journal of Plant Pathology, 136, 565-575.